THE
PHYSICAL REVIEW
A Journal of Experimental and Theoretical Physics
VOL. 44, No. 1 JULY 1, 1933 SECOND SERIES

The Interpretation of the Azimuthal Effect of Cosmic Radiation

M. S. VALLARTA, *Massachusetts Institute of Technology**

(Received April 29, 1933)

IN connection with the directional experiments recently performed in Mexico at 29° geomagnetic latitude by Thomas H. Johnson[1] and by L. Alvarez and A. H. Compton,[2] working independently, showing that the cosmic radiation is predominantly positively charged, the following discussion, based upon the theory of the latitude effect recently developed by Lemaitre and the writer,[3] becomes of interest.

For particles of any given energy we have shown that at any point on the earth there is a cone within which all directions are allowed and the intensity of the cosmic radiation in all allowed directions for each individual energy is the same, and outside of which all directions are forbidden and consequently the intensity is zero. This cone opens from the western horizon if the particles are positively charged (positrons, protons, etc.) and from the eastern horizon if the particles carry a negative charge (electrons, negative ions). The intensity in any direction within the allowed cone is thus the sum of the intensity due to the background radiation (photons, neutrons and charged particles of energy higher than 6×10^{10} electron-volts) plus the intensity in that direction. The angle ψ of opening of this cone, measured from the horizon in the plane through the vertical perpendicular to the geomagnetic meridian plane may be estimated from the calculations already published by Lemaitre and the writer[3] and from certain unpublished results of the writer. This estimate may be in error by as much as 10° either way. The values of ψ at geomagnetic latitudes 0, 10°, 20° and 29° are given as a function of the energy in Table I and plotted in Fig. 1. A table of equivalent energies in electron-volts has been added for convenience. (Table II.)

TABLE I. *Angle of opening of the cone ψ as a function of geomagnetic latitude and energy.*

	x_0	ψ (deg.)		x_0	ψ (deg.)
$\lambda=29°$	0.335	0	$\lambda=20°$	0.372	0
	0.4	70		0.4	20
	0.5	130		0.5	95
	0.6	165		0.6	141
	0.7	176		0.7	165
	0.8	179		0.8	175
	0.825	180		0.9	180 approx.
				0.917	180
$\lambda=10°$	0.405	0	$\lambda=0°$	0.414	0
	0.5	72		0.5	63
	0.6	131		0.6	124
	0.7	157		0.7	153
	0.8	171		0.8	170
	0.9	178		0.9	178
	0.97	180		1.0	180

Examination of these curves shows that at geomagnetic latitude 29° and at an angle of 45° to the vertical in a plane perpendicular to the geomagnetic meridian we may expect all energies greater than $x_0=0.37$ to add to the intensity in

* At present at Mexico City, Mexico.

[1] Thomas H. Johnson, Phys. Rev. **43**, 834 (1933).

[2] L. Alvarez and A. H. Compton, Phys. Rev. **43**, 835 (1933).

[3] G. Lemaitre and M. S. Vallarta, Phys. Rev. **43**, 87 (1933).

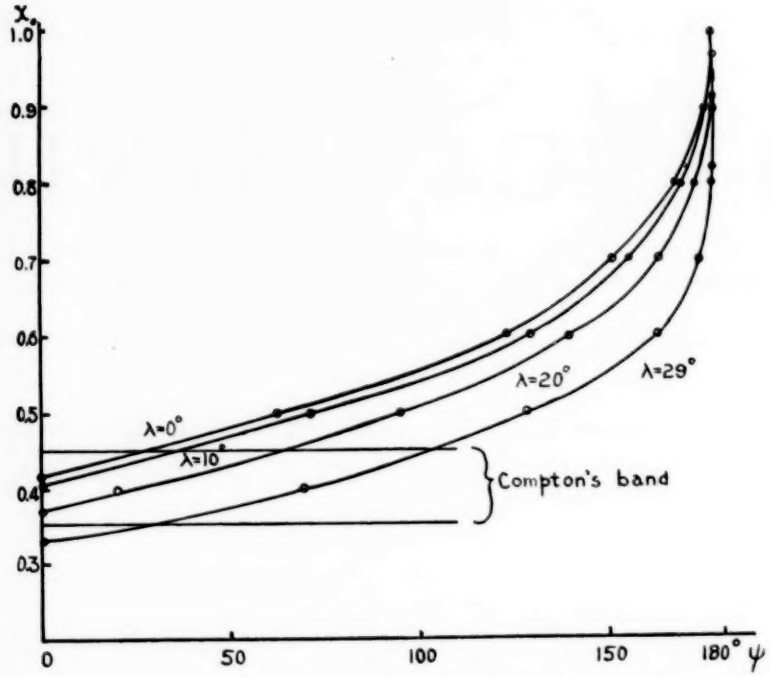

FIG. 1. Angle of opening of cone.

TABLE II. *Equivalent energies in electron-volts.*

x_0	Electrons or positrons (10^{10} volts)	Protons (10^{10} volts)	x_0	Electrons or positrons (10^{10} volts)	Protons (10^{10} volts)
0.335	0.668	0.576	0.7	2.920	2.823
0.372	0.822	0.724	0.8	3.821	3.719
0.4	0.954	0.861	0.825	4.03	3.94
0.405	0.975	0.882	0.9	4.83	4.73
0.414	1.020	1.011	0.917	5.00	4.89
0.5	1.490	1.397	0.97	5.72	5.53
0.6	2.145	2.050	1.0	5.96	5.85

the western direction if the cosmic radiation is predominantly positively charged. At 55° all energies from 0.36 on are available, and at 25° all energies greater than $x_0 = 0.40$. It follows that the east-west intensity difference should increase as the angle with the vertical becomes greater, in agreement with the results of the above-named physicists. However, as the angle becomes larger, atmospheric absorption is so great that only the harder components can reach the observer. If A. H. Compton's[4] estimate of an energy band between 0.35 and 0.45 is correct, the east-west difference should vanish at about 10° to the vertical, also in agreement with the results of the experiments made in Mexico, and it should also vanish at 45° in geomagnetic latitudes less than 10°. Contemplated experiments in Ecuador and Peru should settle this point.[5] On the other hand, the fact that Johnson and Street[6] already obtained an indication of an east-west difference on Mount Washington, N. H., at geomagnetic latitude 55° points out that the band extends on the low energy side at least to $x_0 = 0.2$. Calculation shows that particles (positrons, electrons or protons) of this energy are just able to reach an observer on top of Mount Washington at an elevation of 6280 feet, in the direction in which the experiment was made. The data obtained from such directional experiments, in particular the experimental value of the east-west intensity difference at various angles to the vertical and at different azimuths may thus serve as another basis, in addition to the experimental value of the total intensity at different geomagnetic

[4] A. H. Compton, Phys. Rev. **43**, 399 (1933).

[5] *Added in proof June 13, 1933:* Professor Compton, in a recent letter to the writer, states that, because of late revisions of the value of the total intensity at the geomagnetic equator and at high northern latitudes, his estimate of the energy band may have to be altered.

[6] T. H. Johnson and J. C. Street, Atlantic City Meeting of Physical Society, Phys. Rev. 43, 381A (1933).

latitudes, for the energy analysis of the cosmic radiation.

These results suggest that a predominant part, at least, of the cosmic radiation consists of positive particles (positrons or protons, most likely the former) but it is not excluded that outside the atmosphere there may be a smaller percentage of negative corpuscles. The further analysis of this problem offers fascinating theoretical possibilities.

Since the cone at geomagnetic latitude 29° and for the energy band already named is open at the meridian, it must be expected that the north and south intensities are the same as the west intensity, and in addition that the intensity at intermediate azimuths between the south (or north) and the east must decrease rapidly to the east value. These consequences of the theory seem to be fully confirmed by the above-mentioned experiments.

It is a pleasure to acknowledge the writer's indebtedness to Dr. Johnson, Mr. Alvarez and Professor Compton. In particular he wishes to thank Mr. Jose de la Macorra, manager of the San Rafael paper mill, for his kindness in placing the facilities of the plant at his disposal.

Airplane Cosmic-Ray Intensity Measurements

LEWIS M. MOTT-SMITH AND LYNN G. HOWELL,* *The Rice Institute, Houston, Texas*

(Received May 15, 1933)

With the help of the United States Air Corps and particularly of Captain A. W. Stevens of Wright Field the following cosmic-ray measurements have been made: (1) day-time intensity curve from 1000 to 27,000 feet, (2) night-time intensity curve up to 27,000 feet, (3) absorption in a few cm of lead at various elevations, (4) intensity measurement at 27,000 feet during the solar eclipse of August 31, 1932. A change with altitude in the character of the "uebergangs" effect for cosmic-rays passing from air into lead is shown from the absorption-in-lead curves. Comparison with the earlier high altitude measurements, notably those of Kolhoerster, indicates that the present curve is steeper at 27,000 feet so that the marked decrease in the absorption coefficient above 20,000 feet is not observed. No significant decrease in intensity was observed during the night-time observation even at the highest altitudes. In accord with all previous eclipse measurements, no change in intensity was observed during the solar eclipse. The construction and technique of operation of the high-pressure Wulf-type electroscope used in these measurements are described.

INTRODUCTION

ALTHOUGH accurate measurements of cosmic-ray intensities at altitudes up to 14,000 feet have been made on the ground and in lakes, practically no new observations in the higher region up to 30,000 feet have been made since the 1913–1914 balloon flights of Kolhoerster.[1] He found a very sharp maximum in the values of absorption coefficient as calculated from his intensity curve at a height of about 21,000 feet, which seemed difficult to account for. Under the circumstances, with the lack of new data immediately above 14,000 feet, it seemed desirable to make measurements of cosmic-ray intensities in this region. For obtaining such measurements, the airplane method[2] seemed the best suited. High altitudes can be attained easily and in a short time. Also the altitude of the airplane can be maintained constant while the measurement of the cosmic-ray intensity at any particular altitude is being made. This of course offers a considerable advantage over the free balloon method in which measurements are averaged over a range of altitudes. The weight of the apparatus is not limited to a small value in an airplane, and thus rugged and fairly sensitive instruments can be used for determining both the cosmic-ray intensity and the altitude. Since the work to be presented was begun, Piccard[3] has made intensity measurements up to an altitude of about 50,000 feet in a balloon. Also, Regener[4] has published results obtained with a recording electroscope carried by a pair of small balloons to an altitude corresponding to an atmospheric pressure of about twenty-two millimeters of mercury. His cosmic-ray intensity curve begins approximately where Kolhoerster's ends. Although his results are necessarily rough, they show the important result that the intensity of the cosmic rays increases to extremely high altitudes where the increase with altitude then becomes very small.

EXPERIMENTAL PROCEDURE

A Wulf-type electroscope similar to those used by Millikan[5] has been found to be quite suited for making the measurements. This electroscope has a volume of 500 cc, made small in order that comparatively light lead shields could be provided. It contains argon at a pressure of 75 atmospheres inside a steel case of one-half inch thickness. The high pressure was used to increase

* Geophysics Research Department, Humble Oil and Refining Co.

[1] W. Kolhoerster, Phys. Zeits. **14**, 1153 (1913).

[2] A. Piccard and M. Cosyns, Comptes Rendus **195**, 604 (1932).

[3] E. Regener, Nature **130**, 364 (1932).

[4] K. Buettner, Zeits. f. Geophys. **2**, 254 (1926).

[5] R. A. Millikan and G. H. Cameron, Phys. Rev. **37**, 235 (1931).

the sensitivity (the argon gas[6] was used for the same reason) and to decrease the "zero" of the electroscope, the zero being the rate of discharge due to the radioactivity of the electroscope itself. The zero was also reduced by eliminating some of the α-ray activity of the inside walls with a covering of a film of electrolytic copper.

The zero was determined by measuring the rate of discharge of the electroscope, both unshielded and shielded with lead, in a salt mine 700 feet underground at Grand Saline, Texas. Here the electroscope was shielded from the cosmic rays by the thick layer of earth above. Also, the surrounding salt was found to be surprisingly free from radioactive materials so that it was possible to make a fairly reliable measurement of the zero. Incidentally, in these salt mine measurements it was found that the lead shields are not appreciably radioactive.

Inside the electroscope, the platinized quartz fibers, whose deflection is read, are insulated with quartz and mounted in an invar frame to avoid temperature effects. Tests in the laboratory showed the rate of discharge to be surprisingly free from temperature effect, probably due to accidentally compensating changes of the volt sensitivity with temperature and of the effective ionization. However, it was found that temperature gradients along the steel case set up convection currents of the argon which moved the fibers in an erratic fashion. To avoid sudden changes in temperature, the electroscope was placed inside an insulating wooden case. This wooden case was suspended in the airplane by means of laboratory rubber tubing in order to reduce sufficiently mechanical vibrations transmitted to the fibers.

From discharge curves, a range of about ten divisions on the scale of the reading microscope was found over which the change in deflection of the fibers is linear with time. In practice, thus, the discharge curve is obtained by making a number of observations of the deflection over this range simultaneously with the corresponding values of the time. Sample discharge curves are shown in Fig. 1. It can be seen that the discharge curves taken in the air compare in accuracy quite favorably with those taken on the ground. The various rates of discharge were standardized by comparing the values with the rate of discharge caused by a radium standard of about 0.01 mg which could be clamped at a fixed distance of about 12 cm from the center of the electroscope. When not in use it was removed to a distance of at least 150 cm from the electroscope and placed inside a lead shield 5 cm thick. About half the measurements were made with visual observations of the fibers; the rest, with a simple photographic arrangement which recorded the position of the fibers on a photographic film. Both methods yielded about the same accuracy.

It was of course necessary to know the atmospheric pressure at the altitude at which the measurement was being made with considerable precision on account of the rapid increase in intensity with altitude. (A one percent change in pressure changes the intensity about 2.5 percent at 20,000 feet). After obtaining some widely discordant results with inferior instruments, ordinary aneroid altimeters, recording barographs, etc., a so-called Bureau of Standards-type sensitive altimeter was obtained. In this instrument one of the important sources of error in ordinary aneroids, namely the shift of the zero due to plastic deformation of the soft metal bellows is avoided by use of a bellows made of springy material. It was calibrated with a mercury barometer and also tested for temperature compensation. The errors were not greater than 0.5 percent and it could be read to twenty feet (about one part in a thousand in pressure) so that the atmospheric pressure can be assumed to be known to 0.5 percent.

Some troublesome factors in making measurements in an airplane are: Vibrations set up by the motor, varying tilts of the plane from the level position and the presence of radioactive instrument dials. The disadvantages of vibrations and tilts can be overcome largely by a properly designed suspension and measuring electroscope. It was found necessary to remove the luminous dials from the instrument board. Even with the radium paint removed a small and almost negligible correction for the radioactivity of the plane was made by taking the difference of the rates of discharge of the electroscope in the plane

[6] A. H. Compton and J. J. Hopfield, Phys. Rev. **41**, 539 (1932).

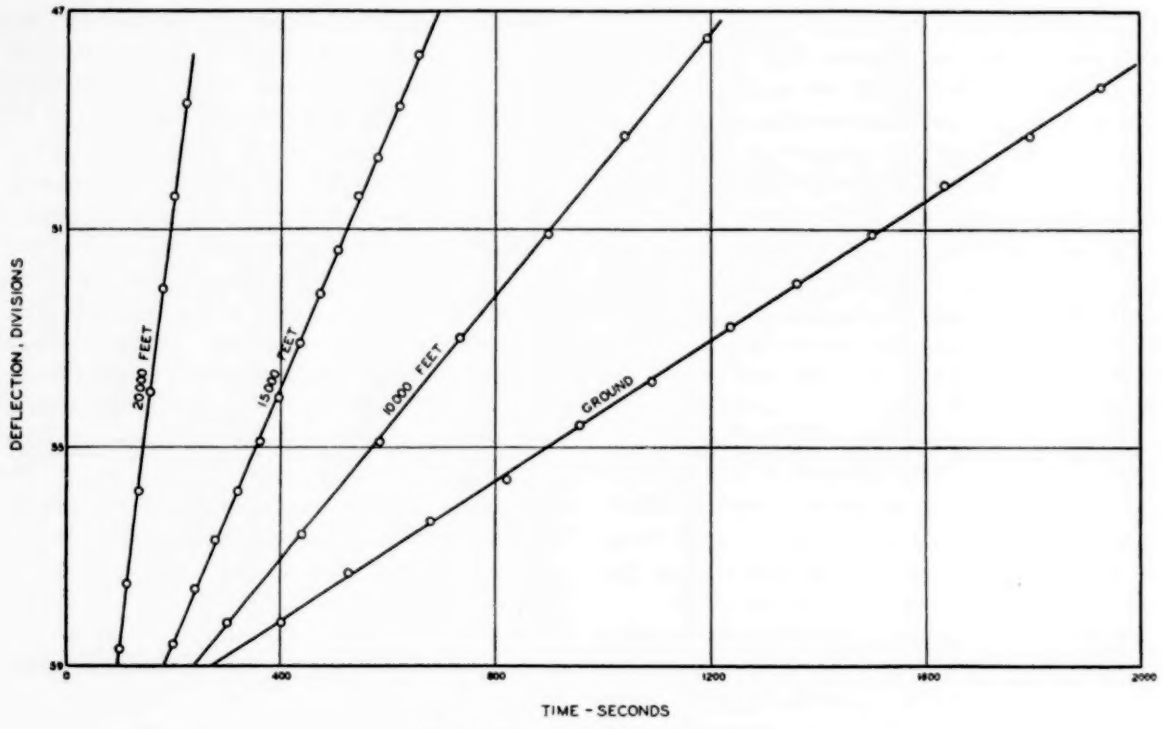

FIG. 1. Sample discharge curves.

on the ground and at the same point with the plane removed.

EXPERIMENTAL RESULTS

The following cosmic-ray measurements have been made: The cosmic-ray intensity curve from 1000 to about 26,000 feet with various thicknesses of lead shielding, taken in the daytime (between 10 A.M. and 2 P.M.: also several points taken around midnight to test for a possible large diurnal effect at very high altitudes. Finally, we had the opportunity of taking a set of readings at an elevation of about 24,000 feet during the recent solar eclipse (that of August 31, 1932).

The altitude curves were taken in the vicinity of Dayton, Ohio, geomagnetic latitude 51°N except the two low-altitude points at 1000 and 3000 feet which were determined enroute from Boston to Washington at an average geomagnetic latitude about the same as that of Dayton. The eclipse observation was made near Biddeford, Maine, at a magnetic latitude of about 54°N.

All the determinations taken with the unshielded electroscope are shown in the curves of Fig. 2 where the abscissas are the atmospheric pressure in cm of mercury and the ordinates the rate of discharge in divisions per second. Values of the intensity taken from a carefully drawn smooth curve through the observed points are presented in Table I. The rate of discharge has not been converted into absolute units, such as ions per cc per second in air under standard conditions, on account of the difficulty in making the conversion. As far as the shape of the curve,

TABLE I. *Cosmic-ray intensities taken from the smooth curve of Fig. 2.*

Values in the third column are determined by using Millikan's value of 2.63 ions/cc per sec. at 74.0 cm pressure.

Barometric pressure, cm Hg	Intensity, division/sec. $\times 10^3$	Intensity, ions/cc/sec.
75	3.76	2.53
70	4.53	3.15
65	5.60	3.77
60	7.12	4.79
55	9.42	6.34
50	12.8	8.62
45	18.4	12.4
40	27.8	18.7
35	42.9	28.8
30	66.3	44.6
25	104.	70.1

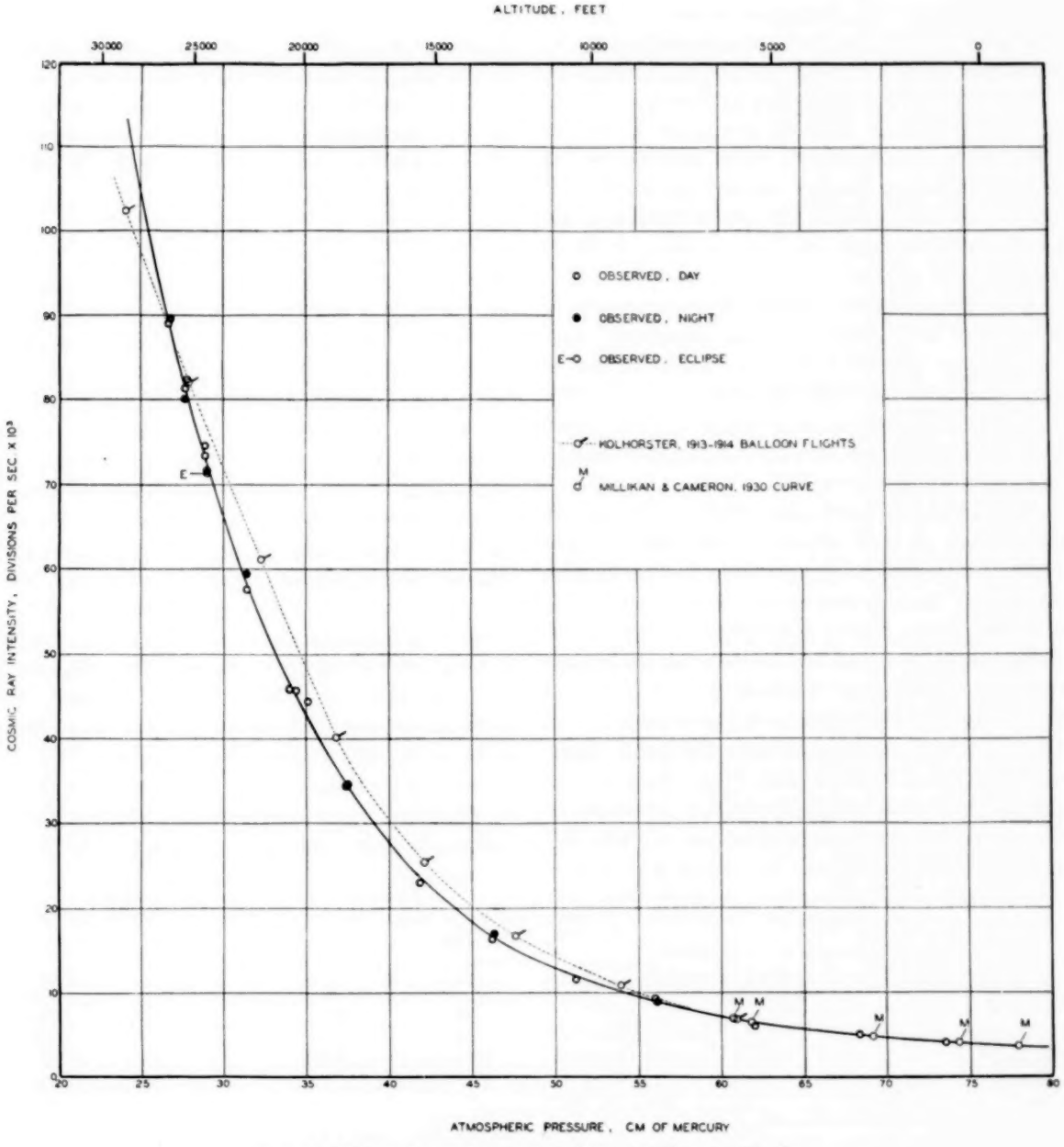

FIG. 2. Observed cosmic-ray intensities at different altitudes.

diurnal changes, etc., are concerned, knowledge of only the rate of discharge is sufficient. However, in order to render the present observations at least roughly comparable with those of other observers we have converted the rate of discharge into ions per cc per second in air by using the value 2.63 ions/cc/second obtained by Millikan[7] at 74.0 cm pressure at Pasadena. These data form column three of the table. From the observed quantities have been subtracted the zero of the electroscope, amounting to 0.00035 divisions per second and the rate of discharge due to the radioactivity of the airplane, 0.00012 divisions per second.

A word must be said about the observations at 1000 and 3000 feet. It was expected that, especially at 1000 feet, an appreciable amount of ground radiation would be picked up. Accordingly these two points were taken over the ocean several miles from shore where the local radiation must be very small.

Measurements were also made with various thicknesses of lead shielding the electroscope. These are shown in Fig. 3, where the unshielded curve has been repeated to allow comparison with the others. Curve one represents the rate of discharge of the unshielded electroscope; curve two, the electroscope shielded with 1.25 cm of lead; curve three, the electroscope shielded with 2.5 cm of lead; and curve four, the electroscope shielded with 4.7 cm of lead. From these curves and the data of Table II showing the fractions of the cosmic-ray intensities absorbed by the different thicknesses of lead at various levels, it is evident that the absorption in lead does not follow an exponential law but represents the type of absorption resulting from the "uebergangs" effect.[8]

TABLE II. *Absorption by the shields.*

I_1 is the intensity with 1.25 cm lead shield, I_2 with 2.5 cm shield, and I_3 with 4.7 cm shield.

Barometric pressure, cm Hg	$\frac{I_0-I_1}{I_0}$	$\frac{I_0-I_2}{I_0}$	$\frac{I_0-I_3}{I_0}$
65	0.15	0.31	——
60	0.17	0.33	0.45
55	0.17	0.35	0.49
50	0.15	0.36	0.51
45	0.14	0.38	0.54
40	0.13	0.40	——
35	0.12	0.41	——
30	0.11	0.40	——

[7] R. A. Millikan, Phys. Rev. **39**, 397 (1932).

It will be noted that the character of this effect changes with altitude. According to Johnson's[9] interpretation this means that the absorption coefficients of the secondary radiation produced in air and in lead and the "production coefficient" of the secondary radiation are undergoing a change. In order to determine the nature of this change we use the relation,

$$I/I_0=[e^{-\mu_1 x}+Ae^{-\nu x}(1-e^{-\mu_2 x})].$$

Here I/I_0, the fractional reduction in ionization produced by a shield of x cm of lead, is the sum of two terms, the first representing the decay in the lead of the secondary radiation accompanying the primary radiation in air, the second giving the growth of the secondary radiation produced in the lead. The factor $e^{-\nu x}$ takes into account the absorption of the primary radiation in passing through the shields. The quantity A determines the relative amounts of ionization produced by the secondary particles from the two media. With this relation, the quantities μ_1, μ_2 and A have been computed from the observed values of the ionization at the altitudes corresponding to atmospheric pressures of 60 and 45 cm of mercury. (The three experimental values of I/I_0 suffice to determine μ_1, μ_2 and A since the value of $e^{-\nu x}$ can be computed by using the air absorption coefficient at the elevation in question.) The computed values of these constants are shown in Table III

TABLE III. *Uebergangs effect constants.*

Barometric pressure, cm Hg	μ_1	μ_2	A
76	0.50	0.98	0.65
60	0.70	1.2	0.54
45	0.66	2.	0.45

where the values at 76 cm have been taken from Johnson's paper.[9] The absorption curves calculated with these constants are shown in Fig. 4 together with the observed points. The observed ionizations at 30 cm are also shown, the dotted curve being sketched in to show the probable be-

[8] Heinz Schindler, Zeits. f. Physik **72**, 625 (1931).

[9] Thomas H. Johnson, Phys. Rev. **41**, 545 (1932).

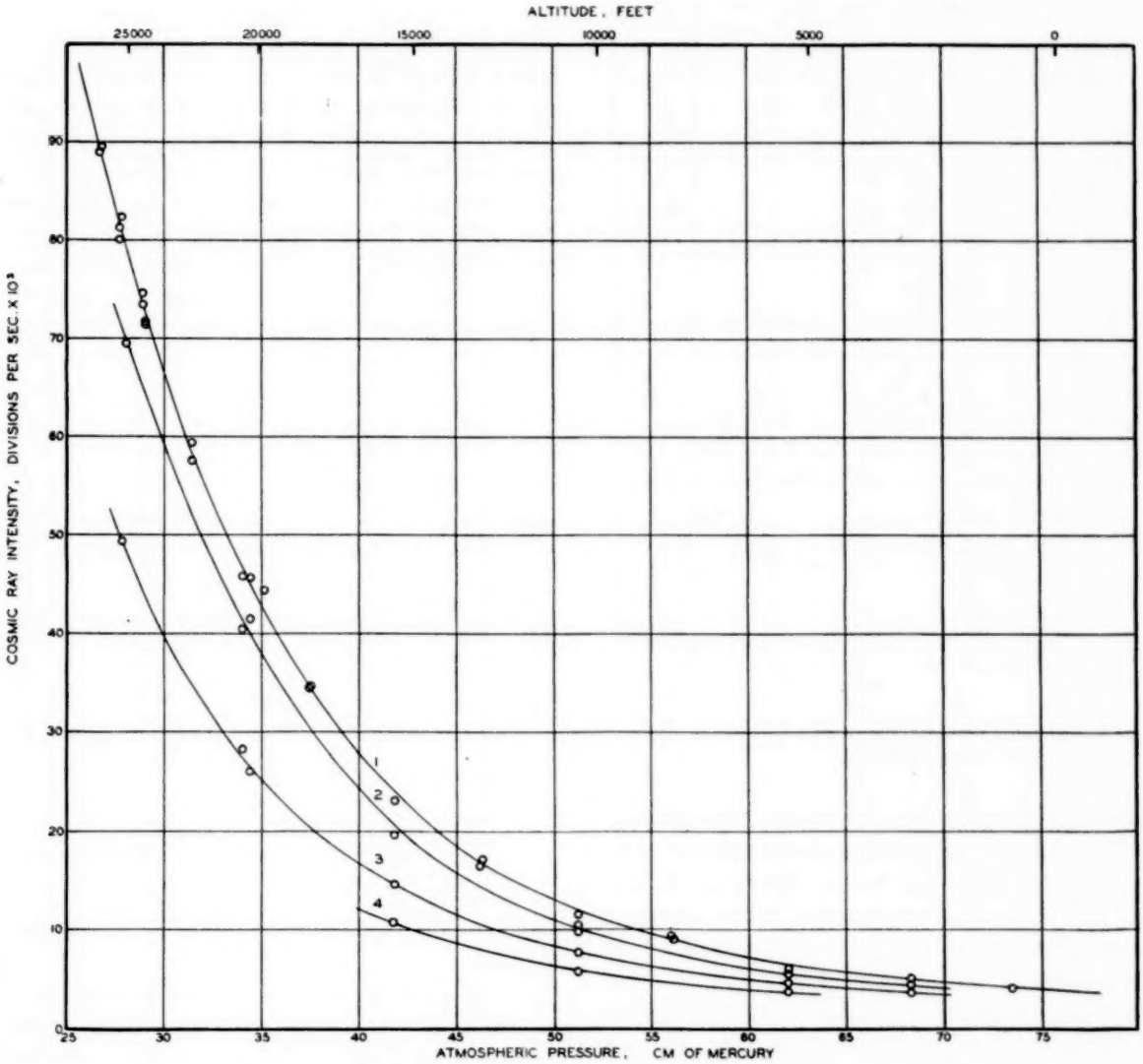

FIG. 3. Effect of various thicknesses of lead shielding on the cosmic-ray ionization at different altitudes.

havior of the curve at this elevation. (Here the computation of the constants was not possible since the datum at 4.7 cm shielding is lacking.) These calculations are necessarily very rough, not only on account of the limited amount of data but also since the uebergangs effect in the walls of the electroscope has not been taken into account. They do, however, seem to indicate that the penetrating power of the secondary radiation, particularly that produced in lead, decreases with increasing altitude. They also show that the amount of secondary radiation in lead becomes less relative to that in air. One conclusion which may be drawn from these observations is that the ionization at different altitudes in any electroscope except one with extremely thin walls will not be proportional to the intensity of the radiation, though the deviation from proportionality does not appear to be very large with any reasonable wall thickness.

Concerning the night observations, it was felt that there might be an appreciable diurnal effect at 25,000 feet since there is some evidence for the existence of a small diurnal effect at low elevations. It will be noted that any diurnal change existing is less than the errors of observation.

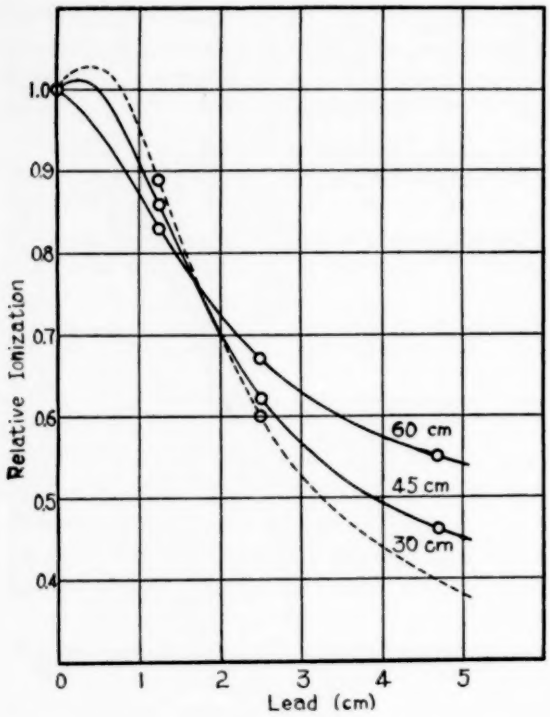

FIG. 4. Calculated absorption curves in lead at different altitudes.

These are estimated to be about three percent.

With regard to the eclipse measurement, since Captain Stevens was to be flying at a high altitude in the path of totality, it was thought worth while again to test whether there is a solar component of the cosmic radiation (coming in rectilinear paths from the sun). Eight discharges of fibers were recorded, just before, during, and just after totality, during which time at least 80 percent of the disk of the sun was obscured by the moon. The result is to be compared with the other points obtained at about the same elevation. It will be noted that no effect was found, again outside of a probable uncertainty of about 3 percent. This is in accord with the result of eclipse measurements made at lower altitudes by other observers, none of whom have found a diminution in intensity during a solar eclipse.

We have compared our results with Kolhoerster's balloon flight data recently recomputed by him and Tuwim (the dotted curve of Fig. 2). There is rough agreement between the two curves, probably within the observational errors of the two sets of observations, for Kolhoerster gives his accuracy as about 10 percent. The difference in the slopes at the top, however, causes a large difference in the computed values of the absorption coefficients. Kolhoerster and Tuwim[10] computed the average absorption coefficient over one kilometer stretches of Kolhoerster's curve from 2 to 9 kilometers and found a sharp maximum at 6 kilometers. We have computed absorption coefficients[11] for our curve in the same manner, and with the same intervals. The two sets of values are compared in the curves of Fig. 5

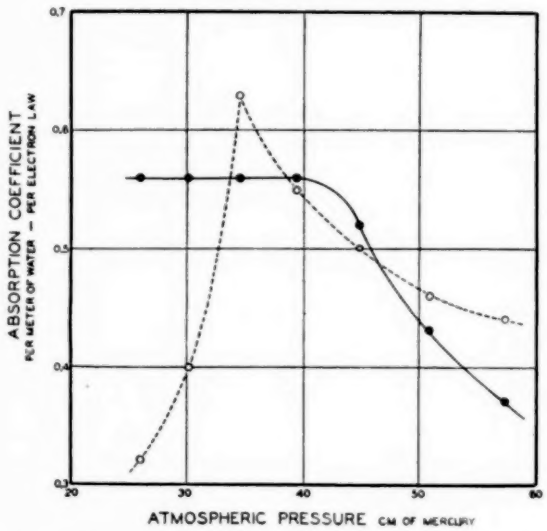

FIG. 5. Variation of absorption coefficients with altitude.

where the dotted curve represents Kolhoerster's values. We find, instead of a sharp maximum, that the absorption coefficient reaches a constant value of 0.56 per meter of water above 17,000 feet. This behavior seems to us to be the more reasonable since it is difficult to see how to account for such a sudden change. It must however be borne in mind that absorption coefficients computed in this manner are purely formal quantities since they are derived by assuming that the elementary rays are exponentially absorbed, a very questionable procedure on account of the complex nature of the radiation.

---

[10] W. Kolhoerster, Naturwiss. **19**, 574 (1931).

[11] The coefficients have been computed under the assumption that the absorption is proportional to the number of extranuclear electrons per cc.

Acknowledgments

This work would not have been possible without the cooperation of Captain Albert W. Stevens of the United States Air Corps, who was responsible for making the arrangements for the flights and who assisted in making many of the observations. We are also indebted to the authorities at Wright Field for their cooperation in the project and to Lieutenants Phillips and MacCallister and to Captain Moffat, who served as pilots. We wish to thank Major T. W. Blackburn of the Texas National Guard and his men for the opportunity of making several preliminary flights, and also Mr. J. E. Hanes of the Morton Salt Company for permission to make the measurements in the salt-mine.

A General Derivation of the Formula for the Diffraction by a Perfect Grating

CARL ECKART, *University of Chicago*

(Received April 29, 1933)

I. INTRODUCTION AND ABSTRACT

The present use of ruled gratings for the absolute measurement of x-ray wave-lengths makes it necessary to investigate the possibility of systematic deviations from the simple formula for the diffraction from a perfect grating. A perfect grating is understood to have the following properties: (1) It is ruled on a continuum—its material has no atomic properties. (2) The optical properties of its material are completely determined by a refractive index (which may be complex). (3) It is ruled on a perfectly plane surface. (4) Its lines are truly parallel, identical, and uniformly spaced. (5) It is infinite in extent. (6) It is so oriented that the plane of incidence and diffraction is perpendicular to the rulings (this makes the problem two-dimensional). Of these properties, only (6) is non-essential and could be eliminated at the expense of a slight complication. The property (5) results in an infinite resolving power: theoretically, the resolving power of a finite portion of a perfect grating may be calculated in a manner which is discussed. It might seem that any derivation based on the foregoing simplifications could be no more general than the usual elementary derivation. However, the latter neglects the following factors: (a) The influence of multiple scattering; (b) Refraction, if the material of the grating is transparent. (This is really a particular case of (a)); (c) Shadows cast by one ruling on its neighbors; (d) Surface waves, similar to those arising on total reflection at a plane surface. In this case, these are the high order spectra for which $\sin\theta_n > 1$. A. H. Compton[1] has given an elementary derivation which takes account of the factors (a), (b) and (c). The present calculation confirms his result that these factors do not influence the calculation of the wave-length, and extends it to include the factor (d).

II. THE CALCULATION

BECAUSE of the properties (1), (2), and (6), the basis of the discussion may be taken to be the wave equation

$$(\partial^2 u/\partial x^2)+(\partial^2 u/\partial y^2)+k^2 u=0, \tag{1}$$

where u is the wave function and

$$k=2\pi\mu/\lambda, \tag{2}$$

λ being the wave-length in vacuo and μ the refractive index. The refractive index may vary from point to point, and may or may not be continuous. It may also be complex (opaque medium) at some points and real (transparent medium) at others. The rulings are taken to be parallel to the z-axis, and x-z is the plane of the grating.

Because of the properties (3), (4) and (5), the function μ will be periodic in x, with the period a = grating space:

$$\mu(x+a, y)=\mu(x, y). \tag{3.1}$$

The dependence on y may be supposed such that

$$\mu(x, +\infty)=\mu', \quad k=k', \tag{3.2}$$

$$\mu(x, -\infty)=\mu'', \quad k=k'', \tag{3.3}$$

where μ' and μ'' are real constants.

The boundary conditions subject to which Eq. (1) is to be solved are, firstly, those of finiteness, continuousness, and single-valuedness. Secondly, it may be supposed that there is a single plane wave incident on the grating (coming from $y=+\infty$) and an infinite number of reflected and transmitted waves. Taking Eqs. (3.2) and (3.3) into account, this means that when $y \gg 0$

$$u(x, y)=\exp\left[ik'(x\sin\varphi-y\cos\varphi)\right] + \sum A_n \exp\left[ik'(x\sin\theta_n+y\cos\theta_n)\right], \tag{4.1}$$

and when $y \ll 0$

$$u(x, y)=\sum B_n \exp\left[ik''(x\sin\varphi_n-y\cos\varphi_n)\right]. \tag{4.2}$$

In Eq. (4.1), the first term is the incident wave and the others are the reflected waves; Eq. (4.2) contains the transmitted waves. Hence all angles are to be taken between $-\pi/2$ and $+\pi/2$ if they are real; however $\sin\theta_n$ and $\sin\varphi_n$ may be greater than unity if, as is to be expected, they are

[1] A. H. Compton, J. Frank. Inst. **208**, 605 (1929).

related to sin φ by the simple grating formulae. In this case, the definition

$$\cos\theta = +i(\sin^2\theta - 1)^{\frac{1}{2}}, \quad \sin\theta > 1, \qquad (5)$$

is to be used. The choice of the sign for this radical is such that u remains finite for large values of y.

The periodicity of the refractive index, expressed by Eq. (3.1) has the following consequence: if $u = f(x, y)$ be a solution of Eq. (1), so is $u = f(x+a, y)$. From this it follows that for certain real constants α, it is possible to find solutions satisfying the equation

$$u(x+a, y) = u(x, y)\exp(i\alpha). \qquad (6)$$

For, let $f(x, y)$ be a solution which does not satisfy this equation; then

$$v(x, y) = (1/N)\sum_{m=0}^{N-1} f(x+ma, y)\exp(-im\alpha)$$

is also a solution and satisfies the equation

$$v(x+a, y) = v(x, y)\exp(i\alpha) + (1/N)[f(x+Na, y)\exp(-iN\alpha) - f(x, y)].$$

Hence

$$u(x, y) = \lim_{N=\infty} v(x, y)$$

is a solution which satisfies Eq. (6). It would seem that this process can be carried out for every value of α; this is true, but the resulting u may be the trivial solution $u \equiv 0$.

It therefore remains to determine the values of α which are consistent with Eqs. (4). From these it is found that when $y \gg 0$:

$$u(x+a, y) = \exp[ik'a\sin\varphi]\{\exp[ik'(x\sin\varphi - y\cos\varphi)] + \sum A_n \exp[ik'a(\sin\theta_n - \sin\varphi)]\exp[ik'(x\sin\theta_n + y\cos\theta_n)]\},$$

and when $y \ll 0$:

$$u(x+a, y) = \exp[ik'a\sin\varphi]\{\sum B_n \exp[ik''a\sin\varphi_n - ik'a\sin\varphi]\exp[ik''(x\sin\varphi_n - y\cos\varphi_n)]\}.$$

When these are compared with the original Eqs. (4), it is seen that Eq. (6) can be satisfied only if

$$\alpha = k'a\sin\varphi \pmod{2\pi}, \qquad (7.1)$$

$$ak'(\sin\theta_n - \sin\varphi) = 2\pi n, \qquad (7.2)$$

$$ak''\sin\varphi_n - ak'\sin\varphi = 2\pi n, \qquad (7.3)$$

where n is an integer which may be identified with the index on the angles.

III. Discussion of the Significance of Eq. (6)

The last two equations above are the ordinary grating formulae. They are seen to follow directly from the requirement that Eq. (6) be satisfied by the solution of the wave equation. The question of the necessity of this requirement arises immediately.

Its physical significance may be seen from the fact that Eq. (6) implies that the intensity $|u|^2$ is periodic in x, with the same period as the grating itself. But this should be a result of the calculation and not a condition to be imposed *a priori*. Also, the requirement of a periodic intensity distribution does not in turn imply the Eq. (6). The latter can not therefore be a consequence of physical considerations. Nor is it a mathematical necessity. The difficulty is the same one which arises each time Fourier's solution of the problem of the stretched string is explained to a beginner. It is not possible to prove that *every* solution of this problem *must* have the form

$$\sin(nx)\sin(nct + \text{const.}).$$

But the need to prove the impossible vanishes when Fourier's theorem shows that it is possible to express the general solution as a series of *particular* solutions which *do* have this form.

In the present case, the solutions u form a complete orthogonal set in terms of which every solution of Eq. (1) can be expressed as a generalized Fourier integral.[2] The orthogonality is readily proved from Eq. (6) and the completeness may be inferred from the fact that the set reduces to a known complete set when the index of refraction has the special form $\mu = \text{constant}$.

As a particular case, it would be possible to

[2] This is strictly true only when another set of functions representing waves incident from $y = -\infty$ is included.

build up a solution representing a finite beam of radiation incident on the infinite grating. This would be the physical equivalent of the omission of property (5) from the definition of the perfect grating. I believe that it would be feasible to make this calculation but that the result would very likely be the same formulae for the resolving power, etc., of a plane grating (used without collimator and telescope) which Stauss and Porter have already obtained by simpler methods.[3]

[3] A. W. Porter, Phil. Mag. **5**, 1067 (1928). H. E. Stauss, Phys. Rev **34**, 1601 (1929).

Radiation From Canal Ray Impact

F. L. VERWIEBE, *Ryerson Physical Laboratory, University of Chicago*
(Received April 24, 1933)

Hydrogen canal rays accelerated in fields up to 40 kv were allowed to impinge on a metal target and the beam of particles and radiation emitted from the target were investigated. Pinhole images of the focal spot were obtained on Schumann plates and plates coated with molybdenum trioxide. The presence of atomic hydrogen was shown by a characteristic light blue color produced on molybdenum trioxide plates. By means of a deflecting magnetic field it was found that the beam from the target consisted mainly of neutral particles (or of radiation) but contained a smaller number of protons whose velocity was practically equal to that of the protons incident on the target. The neutral particles by virtue of their ability to affect a photographic plate could suggest the presence of electromagnetic radiation. A grating was used to detect such radiation. Radiation of wave-length 1216A was excited in the residual gas by the canal ray beam when the pressure was as low as 10^{-4} mm of Hg. Any characteristic radiation from the target excited by canal ray impact is too small to be measured.

THE excitation of radiation by the impact of rapidly moving positive particles on metals has formed the subject of several investigations. On the one hand, there has been the search for a penetrating radiation similar to x-rays that might be expected from the impact of protons. Of such a nature were the experiment of Barton[1] in 1930, and the recent experiments of Cockcroft and Walton.[2] They attempted to determine whether gamma-radiation or x-radiation of sufficiently short wave-length to pass through a thin mica window was produced by the impact of positive ions on matter with accelerating potentials up to 700 kv. These workers report that, if any such radiation is produced, its intensity was inappreciable. According to Cockcroft and Walton its intensity was certainly not greater than 10^{-6} of the intensity of the continuous x-radiation which would have been produced by an electron stream of the same energy.

On the other hand, there is undoubtedly excited an easily observable nonpenetrating radiation that can penetrate only the thinnest celluloid windows. This radiation has been studied by Thomson,[3] Wien,[4] Gerthsen,[5] and others, but the experiments have not as yet conclusively decided whether the effects observed are predominantly due to soft x-rays excited in the target, or to scattered positive or neutral atoms, and furthermore, no determinations have been made of the wave-length of the radiation, if electromagnetic radiation is excited in appreciable intensity.

J. J. Thomson[3] in his 1914 paper concluded that he had found an electromagnetic radiation excited by the impact of canal rays on a target. He seems not to have considered, however, that neutral particles would pass through a deflecting field and affect a photographic plate. In 1926 Thomson[6] studied this radiation by means of the photoelectric effect in a second chamber separated by a celluloid window. Radiation seemed to come from the target but also from the gas in the discharge tube when the target was removed.

In 1927 Wien[4] reported an unexpected fogging of Schumann plates when they were in a gas at a pressure of 0.001 mm of Hg through which canal rays were passing. This occurred even when they were shielded from any direct action from the rays and the metal struck by the rays. A deflecting magnetic field or electrostatic field which would eliminate secondary electrons produced no change. While Wien did not attempt a definite explanation, he did suggest that, rather than electromagnetic radiation, the cause might be a chemical action of atomic hydrogen and oxygen on the silver of the Schumann plates. Ordinary plates protected by the layer of

[1] Barton, J. Frank. Inst. **1**, 209 (1930).
[2] Cockcroft and Walton, Proc. Roy. Soc. **A136**, 619 (1932).
[3] J. J. Thomson, Phil. Mag. **28**, 620 (1914).
[4] Wien, Ann. d. Physik **83**, 1, 19 (1927).
[5] Gerthsen, Ann. d. Physik **85**, 881 (1928).

gelatine did not show the fogging. The degree of fogging increased with increasing pressure and was less with nitrogen in the tube than with hydrogen or oxygen.

In 1928 Gerthsen[5] investigated the radiation caused by the impact of canal rays on metals. He used the photoelectric effect and an experimental arrangement which allowed him to repeat all the observations reported by Thomson[6] in 1926. He concluded that the beam of particles reflected from the target consisted mainly of neutral particles of high velocity and that they could produce all the effects ascribed to electromagnetic radiation, *viz.*, secondary electron emission, ionization of gases, and the blackening of a photographic plate. He found, furthermore, that the absorption of these reflected beams in thin celluloid windows was of the same order of magnitude as the absorption of soft x-rays. To get a separation, therefore, of particles and electromagnetic radiation, an effect purely optical in its nature would have to be utilized, such as reflection from a mirror or diffraction by a grating. Gerthsen accordingly attempted to use such an optical effect and set up sputtered concave mirrors to focus any electromagnetic radiation coming from the target. He did find a slight increase of photoelectric current for the proper angular setting of the mirrors but was unable to decide whether the radiation observed was due to radiation from the beam or to characteristic radiation excited in the target.

The present experiment was undertaken to attempt to determine by means of a diffraction grating whether soft electromagnetic radiation is excited by the impact of canal rays on a target and its wave-length, if any is excited. It was also hoped that the experiment would aid in deciding whether the effects described by other observers were due to electromagnetic radiation or to reflected neutral particles.

Apparatus

The experimental arrangement used is sketched diagrammatically in Fig. 1. A hydrogen discharge tube (120 cm×4 cm) was mounted over a slit system leading to a photographic chamber. An electrically heated palladium tube was joined to the system to control the influx of hydrogen from a reservoir, and a transformer in conjunction with a kenotron provided the potential difference. The cathode consists of the cylindrical block B, on top of which is a slightly concave piece of aluminum A. The slits S_1 and S_2 are each a fine pinhole punched in foil. With this arrangement it was possible by means of two diffusion pumps to maintain the proper discharge pressure in the tube and at the same time keep the pressure in the photographic chamber below 10^{-4} mm of Hg. Below the block B is a carriage, arranged to slide out for loading purposes, on which are mounted the target T, the slit S_3, the grating, and the plateholder. The block C was inserted in some experiments to prevent radiation from the incident beam reaching the plate. The upper edge of the target is in line with the adjustable, rectangular slit S_3, through which the rays from the target pass to the grating and thence to the sensitive plate. The top view of the target and grating shows the mounting of the latter which permits part of the emergent beam to fall directly on the sensitive plate. The grating was ruled with 600 lines to the millimeter.

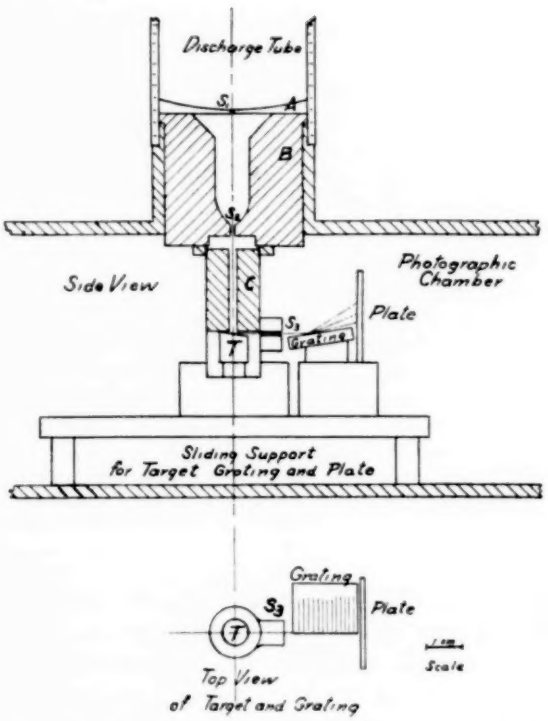

FIG. 1. Experimental arrangement for diffraction patterns.

[6] J. J. Thomson, Phil. Mag. **2**, 674 (1926).

To detect radiation and fast moving particles Schumann plates were used. In addition, pieces of glass smoked with molybdenum trioxide vapor were also utilized. These have a fine whitish surface which is insensitive to radiation but which becomes blue when bombarded by atomic hydrogen.

In some of the tests, moving charged particles were deflected by a magnetic field applied normally to the direction of the beam coming from the target and parallel to the direction of the slit S_3 as shown in the figure.

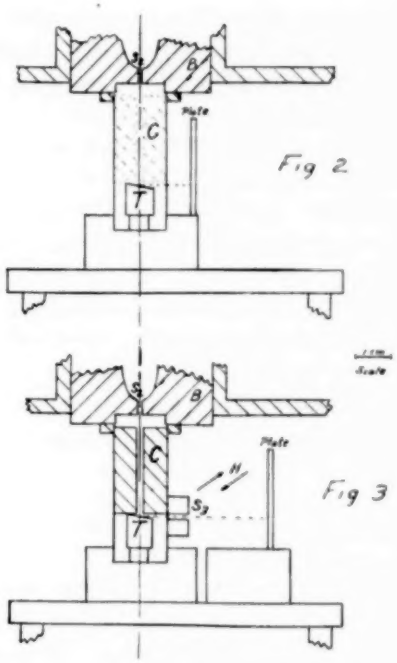

FIG. 2. Arrangement for pinhole images.
FIG. 3. Arrangement with deflecting magnetic field.

EXPERIMENTAL PROCEDURE

The experimental procedure was as follows. The voltage across the discharge tube was maintained between 35 and 40 kv. The amount of hydrogen flowing through the tube was such that a pressure of approximately 0.02 mm of Hg was established in the tube, and a beam of canal rays about 1 mm in diameter was visible in front of the cathode.

With canal rays impinging on the target a study was made of the composite beam of radiation emerging from the target through the slit S_3. In studying the nature and characteristics of the corpuscular beam as well as the electromagnetic radiation coming from the target, the following experiments were carried out.

1. Pinhole images

Pinhole images to determine the position and area of the source of the radiation were taken with the arrangement shown in Fig. 2. The block, C, here drawn with dotted lines, was removed. A pinhole punched in a piece of foil was opposite the target. The photographic plate was placed so that the pinhole was midway between the point of impact on the target and the photographic plate in order that full size images would be obtained. Fig. 4a is a drawing of a typical Schumann plate photograph obtained in this manner. It shows an intense beam coming from the spot on the target struck by canal rays. The elliptical shape is a projection of the circular focal spot on the target. There is also visible on the plate a fainter image of a portion of the canal ray beam itself. When a molybdenum trioxide plate was exposed in this manner this faint vertical line did not appear, indicating that probably electromagnetic radiation was the cause of this faint line image.

When the block C was inserted, this radiation coming from the canal ray beam itself was prevented from reaching the sensitive plate. Fig. 4b represents photographs obtained with this arrangement. Both Schumann plates and molybdenum trioxide plates were exposed and both show the same type of image, the latter

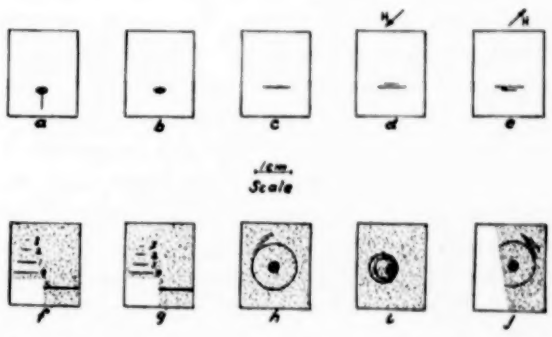

FIG. 4a. Pinhole image of beam and target. b. Pinhole image of focal spot only. c. Rays from target through slit. d. Magnetic deflection of rays from target. e. Image with magnetic field reversed. f. Diffraction pattern of rays from canal ray impact. g. Diffraction pattern from ultraviolet spark. h. Rings due to rays reflected from brass opening. i. Rings from displaced opening. j. Plate partly covered with cellophane.

plates, however, requiring considerably longer time of exposure to obtain a clear image. The characteristic blue color of the images on the molybdenum trioxide plates shows conclusively that the beam coming from the target contains atomic hydrogen, since the molybdenum trioxide is not sensitive to radiation. The general appearance of these images bears a very close resemblance to the pinhole images taken with an ordinary x-ray tube. It was found that a thin piece of cellophane completely absorbed all the radiation coming from the target.

2. Magnetic deflection of the beam from the target

The beam of particles and radiation coming from the target was next studied to see if it contained charged particles which would be deflected by a magnetic field. When the beam was allowed to fall on a plate through the rectangular slit, S_3, as shown in Fig. 3, a horizontal image of the slit was obtained as indicated by Fig. 4c. As before, the molybdenum trioxide plates showed the same images as the Schumann plates.

When a magnetic field of a few hundred gauss was applied normal to the direction of the beam, a deflected image appeared as indicated by Figs. 4d and 4e. The molybdenum trioxide did not show the deflected image probably because of lack of intensity in the deflected beam. The Schumann plate photographs reveal several interesting facts. First of all, most of the beam is undeflected and therefore the beam consists mainly of neutral particles with the possible addition of radiation. Only one displaced line is visible and this is very probably due to protons. Any H_2 or H_3 charged particles can be present in only very small amounts. Assuming that the displaced line is due to protons, an approximate calculation from the amount of the deflection and the strength of the magnetic field shows them to have a velocity practically equal to that of the protons incident on the target. This experimental arrangement is practically that of Thomson's 1914 experiment. Instead of a magnetic field he used an electrostatic field, which deflected the charged particles and allowed the neutral particles to reach the photographic plate.

3. Grating diffraction patterns

The undeflected images on the photographic plates as shown by Figs. 4d and 4e might be due to radiation as well as to neutral particles coming from the target. In order to determine if any radiation was also present, a diffraction grating was interposed between the slit S_3 and the photographic plate, as shown in Fig. 1. Canal rays were allowed to fall on the various targets, brass, calcite, and magnesium, and exposures were taken to obtain the spectrum of any possible electromagnetic radiation. Fig. 4f is a drawing of a typical Schumann plate photograph obtained in this manner. The line in the lower right-hand corner of the plate is due to the unreflected beam coming from that part of the slit which was not covered by the grating, as indicated in the top-view shown in Fig. 1. The clear rectangle in the lower left-hand corner is the shadow cast by the grating. Above the upper edge of the grating shadow there can be seen the directly reflected beam, the zero order of diffraction, and above it several higher orders of diffraction images. Except for the portion of the plate protected by the grating, there is a general fogging over the plate which makes the original unsuitable for reproduction. The line in the lower right-hand corner, due to the unreflected beam, is much more intense than any of the reflected images, the latter requiring as much as six to ten hours' exposure for the higher orders, whereas the former is visible after a few minutes exposure and often showed reversal for the longer exposures. Furthermore, the general fogging was visible on exposures which were not long enough to bring out the diffraction pattern. This indicates that the energy emerging from the slit is predominantly in the form of particles and that these particles can blacken the photographic plate.

Since the distance between the point of incidence on the grating and the plate was only a little over 1 cm, the accuracy of the wave-length determination could not be very great. As computed, however, the value of the wave-length of this radiation was found to agree within the limit of the accuracy of the measurements with that of the first Lyman line, 1216A. The shortest wave-length for which a diffraction pattern could have been distinguished is about

100A. No wave-lengths between this value and 1216A were found. This radiation may have been present in Thomson's experiments and Gerthsen suspected his results to be due partly, at least, to radiation of this wave-length. The molybdenum trioxide plate in this position showed only the unreflected image on the portion not covered by the grating.

This electromagnetic radiation comes from the gas just in front of the inclined target and these experiments show no reason to assume that an electromagnetic radiation is excited in the target itself.

4. Diffraction patterns from an ultraviolet spark

In order to make certain that the experimental arrangement was capable of indicating the presence of wave-lengths shorter than 1216A, an ultraviolet spark was placed opposite the grating. An intermittent discharge from a condenser connected in parallel across a gap of about 1 mm was allowed to pass between the two carbon electrodes mounted in Bakelite. The pressure in the photographic chamber was kept below 10^{-4} mm of Hg. About 50 kv were applied to the condenser so that a very intense spark was obtained. Fig. 4g is a drawing of the diffraction pattern obtained. The value of the strongest line obtained with the particular angle of grating used was found to lie between 500 and 600A. Precision spectrographs show two fairly strong lines at 500 and 538A, respectively, due to C III.

5. Incidental effects

In the preliminary steps of getting the two upper slits and the target into proper alignment, exposures were made with plates in the position of the target, T, as shown in Fig. 1. Sketches of the photographs obtained in this manner are shown in Figs. 4h and 4i. They show a large central spot, at least one fairly prominent ring around it, and several fainter rings of larger diameters. Exactly the same patterns were obtained with molybdenum trioxide plates as with Schumann plates. The diameter of the rings was found to be independent of wide variations in voltage, pressure, and the size of the pinhole at the bottom of slit S_2. The first ring in Fig. 4h was traced geometrically to the upper edge of the slit S_2. When a smaller tube was placed above the pinhole the pattern shown by Fig. 4i was obtained, and, as before, the first ring around the central spot could be traced to the upper edge of the tube. The larger rings in both plates seem to be due to scorings on the inner surfaces of the cylindrical chambers above the slit S_2. Since these rings appear also on the molybdenum trioxide plates they must be caused by atomic hydrogen. They may be due to a charging up of the metal surface and a consequent deflection of charged particles from the discharge tube. This deflection may be through a large angle when the charged particles pass close to the scoring in the metal surfaces, so that the rays can pass through the slit S_2, and cause a circular trace on the photographic plate.

Reference was made at the beginning of this article to the anomalous fogging observed by Wien. In the present experiment all the plates show some fogging and this seems to be the result of scattered charged and uncharged particles. Both Schumann plates and molybdenum trioxide plates show the same effect. Fig. 4j is a drawing of a Schumann plate put in the position of the target T, as shown in Fig. 1, with about one-half of the plate covered by a thin piece of cellophane placed 1 mm above it. The part of the plate protected by the cellophane is completely clear. The general blackening is caused predominantly by charged or uncharged ions, as in these experiments we have seen that both will blacken a Schumann plate.

The writer wishes to take this occasion to express his indebtedness to Professor Dempster for his suggestion of the problem and for his advice and helpful criticism throughout the course of the experiment.

Inelastic Electron Scattering by Helium Atoms

A. L. HUGHES* AND J. H. MCMILLEN, *Washington University, St. Louis*

(Received April 24, 1933)

The angular distribution of electrons scattered by helium atoms when the electrons have lost 21.12 volts energy, thereby exciting the atom to the 2^1P state, has been studied for energies between 27.5 and 400 volts and over an angular range from 6° to 150° in most cases. For the higher energies the angular range over which measurements could be made was less, e.g., for 400 volt-electrons measurements could not be made beyond 22°. The higher the original energy of the electrons, the less the number of electrons scattered with a 21.12 volt energy loss, and the steeper the angular distribution curve. For the lower energies (below about 100 volts) the curves fall gently to about 60° and then become practically flat up to 150°. One curve is given for the distribution of 42 volt-electrons which have lost 22.97 volts energy (excitation to the 3^1P state) and another for 400 volt-electrons which have lost 25 volts energy (thereby ionizing the atom). Comparisons are made between the experimental results and theories proposed by Morse and by Massey and Mohr. A very direct comparison is possible with the theory of Massey and Mohr and a very satisfactory agreement is found.

INTRODUCTION

THE electrons scattered by atoms fall into two classes: Those which are scattered elastically and those which are scattered inelastically. The former all have one and the same energy, equal to that which they had before collision; the latter have lower energies distributed over a wide range. For each possible excited state of the atom there will be a correspondingly discrete energy loss; in addition there will be, in those cases where ionization occurs, a continuous distribution of energy losses depending on the way the energy left over after ionizing the atom is shared between the ionizing electron and the ejected electron. The four lowest energy losses occurring in collisions between electrons and helium atoms are the 19.77, 20.55, 21.12 and 22.97 volt losses, corresponding to excitation of the atom to the 2^3S, 2^1S, 2^1P and 3^1P states, respectively. These have been discovered in experiments designed specially to detect their existence. They are of course given by the spectral terms as well. Theoretical investigations have been made to predict the angular distribution of the electrons which have given rise to any one excited state. It is desirable to check such predictions by experiment. In experiments made to study the angular distribution of electrons after exciting the atom to one particular state, the electron thereby losing a definite amount of energy, certain factors unfortunately hamper the carrying out of systematic measurements on more than a very few energy losses. One factor is the difficulty of resolving energy losses which are separated by less than about 0.5 volt; another is the lack of intensity in the inelastically scattered electron beams. Thus even with the most probable energy loss, 21.12 volts, the number of 200 volt-electrons scattered through an angle greater than about 30° becomes too small to be measured.

Little work has been done in the field of inelastic scattering. McMillen[1] found that when 100 volt-electrons collide with helium atoms, the number of those which lost 21.12 volts energy diminished with extraordinary rapidity with increasing angle from 10° to 30°, beyond which it was too small to measure. Mohr and Nicoll[2] studied the angular distribution of 54 to 196 volt-electrons over the range 15° to 150°, after they had lost 21.12 volts energy in collision with helium atoms, thus leaving them in the 2^1P state. For those electrons which left the helium atom in the 3^1P state (energy loss, 22.97 volts) they gave

* The senior author was aided in part by a grant from the Rockefeller Foundation to Washington University for research in science.

[1] J. H. McMillen, Phys. Rev. **36**, 1034 (1930).

[2] C. B. O. Mohr and F. H. Nicoll, Proc. Roy. Soc. **A138**, 469 (1932).

the distribution between 20° and 50°, for one primary energy, 83 volts. Van Voorhis[3] has published a preliminary abstract describing results of scattering experiments in the small angle region 0° to 15°. The primary electrons had energies varying from 100 to 300 volts, and the scattered electrons selected for study were those which had lost 21.12 volts.

Apparatus and Method

The apparatus used in this investigation was that used by us[4] in a recently published article on *Elastic Scattering in Neon*. For a description of the apparatus the reader is referred to that article. The only difference was that the slit S_2 was absent, and in front of the slit S_1 there was a grid of fine wires. By placing a retarding field between the grid and S_1 it was possible to slow down the electrons passing into the analyzer and simultaneously to decrease the angle within which the scattered electrons had to be to enter the analyzing chamber. Further details concerning the use of such a field will be found in our paper on argon.[5] When the primary energies were 400 and 200 volts, the electrons were slowed down to 50 volts energy in the analyzer. For lower primary energies, this was unnecessary, as sufficient intensity could be obtained without any retarding field between the grid and analyzer.

Results and Discussion

The number of electrons scattered per unit solid angle, after losing 21.12 volts in collisions with helium atoms, is given in Table I as a function of the angle and the primary electron energy. The values are all in terms of the same arbitrary unit. It should be stated that this unit is identical with the one used in our paper on the elastic electron scattering in helium[6] and therefore it is possible to effect a quantitative comparison between the elastic and the inelastic scattering. The angular distributions of electrons which have lost 21.12 volts energy in collisions with helium atoms are shown in Figs. 1 and 2, the different curves corresponding to the various electron energies before collision. It is very evident how the scattering, especially at medium and large angles, falls off very rapidly with increasing primary energies when these exceed 50 or 100 volts. For lower energies, it is noteworthy

[3] C. C. Van Voorhis, Phys. Rev. **43**, 777 (1933).

[4] A. L. Hughes and J. H. McMillen, Phys. Rev. **43**, 875 (1933).

[5] A. L. Hughes and J. H. McMillen, Phys. Rev. **39**, 585 (1932).

[6] A. L. Hughes, J. H. McMillen and G. M. Webb, Phys. Rev. **41**, 154 (1932).

Table I. *Angular distribution of scattered electrons which have lost 21.12 volts energy.*

θ° \ V	27.5	30	35	42	50	θ° \ V	100	200	400
6°	....	(129.0)	(140.0)	....	....	6°	238.0	140.5	40.00
8°	204.0	113.8	128.5	131.0	222.0	8°	164.0	100.0	25.6
10°	183.2	105.2	118.0	122.0	195.8	10°	107.5	58.5	15.4
12.5°	150.1	97.5	105.0	109.0	162.8	12°	71.2	29.9	9.50
15°	127.0	89.0	92.2	96.2	126.5	14°	51.9	16.4	5.08
20°	106.0	77.0	73.2	67.9	79.0	16°	35.7	8.97	2.68
25°	95.5	66.8	53.3	48.2	48.9	18°	27.8	5.46	1.60
30°	87.0	55.7	41.2	32.8	32.0	20°	21.1	3.43	0.80
35°	79.0	46.5	33.5	26.0	22.6	22°	....	2.21	0.28
40°	72.7	40.5	28.2	21.1	16.2	24°	....	1.30	
45°	66.3	37.1	24.2	17.8	13.4	25°	8.45		
50°	63.2	35.3	20.9	15.7	11.7	30°	4.57		
60°	56.8	33.8	17.7	13.1	9.6	35°	3.17		
70°	56.3	33.0	15.6	11.2	7.8	40°	2.36		
80°	56.2	32.5	15.0	10.2	6.4	45°	1.76		
90°	56.2	31.4	14.9	9.72	5.83	50°	1.41		
100°	55.3	30.7	14.5	9.48	5.83	55°	1.21		
110°	55.3	30.7	14.1	9.40	5.83				
120°	55.3	30.7	13.6	9.37	5.83				
130°	55.3	30.0	13.1	9.13	6.02				
140°	55.3	28.0	12.1	9.02	6.12				
150°	55.3	24.6	11.6	8.90	5.64				

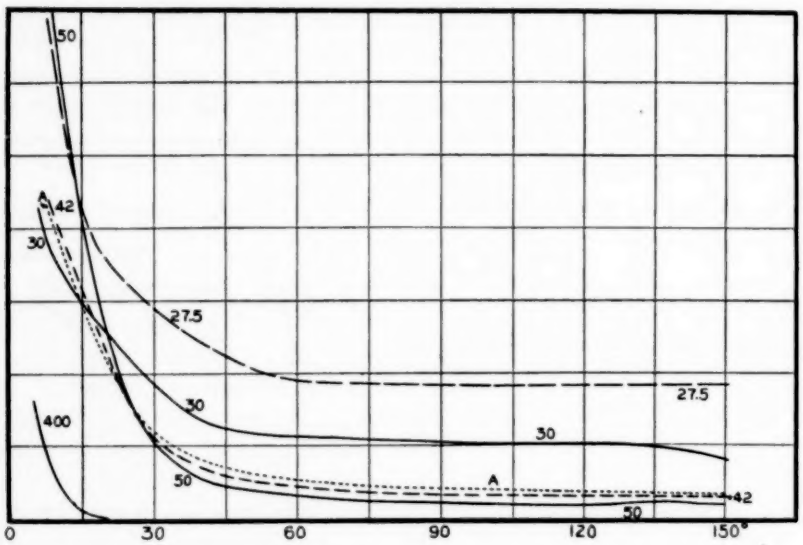

FIG. 1. Angular distribution curves for electrons losing 21.12 volts energy. Electron energy (before collision) indicated on each curve. Curve A is for 42 volt-electrons losing 22.94 volts at collision. Scale for ordinates of curve A is $\frac{1}{3}$ that of other curves.

that the scattering becomes almost independent of the angle in the middle range, 50° to 150°. In Fig. 1, curve A is the angular distribution curve for 42 volt-electrons, which, on colliding with the helium atoms, excite them to the 3^1P state, (thereby losing 22.94 volts energy). It should be noted that the units for the ordinates for curve A are three times smaller than those for the other curves. In Fig. 2 we have plotted as a dotted line the angular distribution of 400 volt-electrons which have lost 25 volts energy in collisions with atoms, thereby ionizing them. It will be noticed that this angular distribution curve is considerably less steep than the corresponding one for the 21.12 volt loss. This characteristic is in agreement with that found under similar circumstances in argon.

Mohr and Nicoll[2] find a maximum at 60° for 54 volt-electrons. There is no indication of a maximum in our corresponding curve. There is fair agreement between their curves and ours for electrons of higher energies, except at small angles where the differences between the curves become larger.

Morse[7] has studied electron scattering from a theoretical standpoint, and has obtained an expression

$$\alpha_i(\mu)=\frac{e^4m}{4h^2}\left[\frac{1}{Z}\left(1-\frac{F^2}{Z^2}\right)\right]\frac{Z^2}{\mu^4} \qquad (1)$$

for the *total* inelastic electron scattering, where e

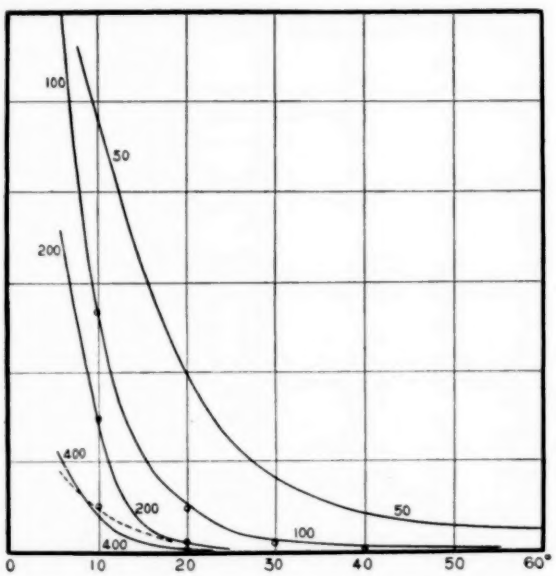

FIG. 2. Angular distribution curves for electrons losing 21.12 volts energy. Electron energy (before collision) indicated on each curve. Dotted curve is for 400 volt-electrons which have ionized the atom. Circles denote Massey and Mohr's computed values for the 400, 200 and 100 volt curves.

[7] P. M. Morse, Phys. Zeits. **33**, 443 (1932); Rev. Mod. Phys. **4**, 610 (1932).

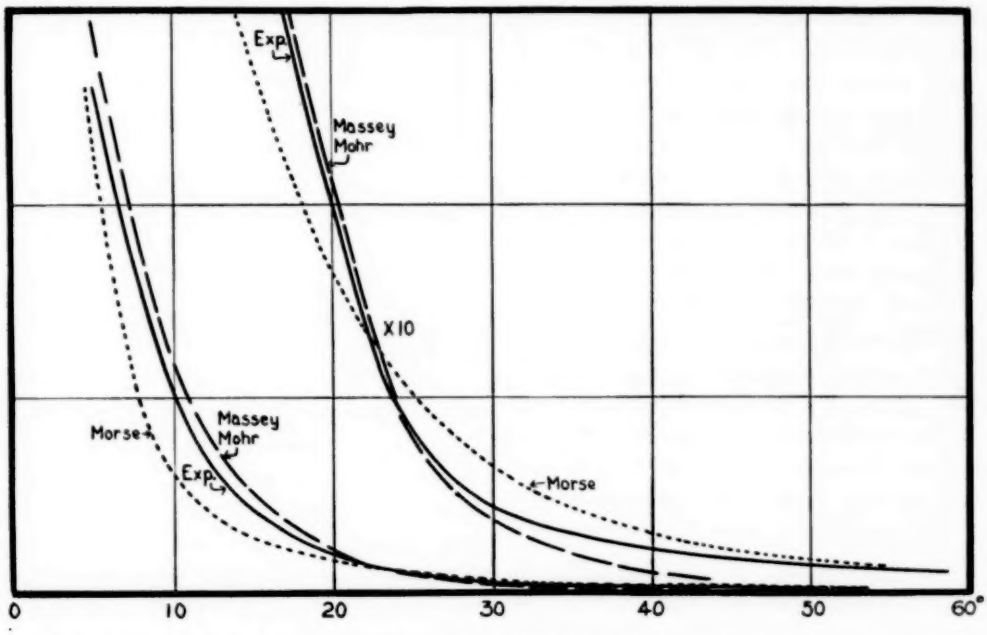

FIG. 3. Comparison of experimental and theoretical scattering curves. Unbroken line, experimental curve. Dotted line, Morse's theory. Broken line, Massey and Mohr's theory. Energy before collision, 100 volts. Energy lost at collision, 21.12 volts.

and m refer to the electron, h is Planck's constant, $Z=2$ for helium, F the form factor for helium and $\mu = \sin(\theta/2)/\lambda$ where λ is equal to the electron wave-length. The approximations made in deriving this equation are such that it is expected to hold only when the electron energy exceeds $50Z^2$ ($= 200$ volts for helium). Although the electrons losing 21.12 volts energy form only a part of all the electrons scattered inelastically, it may be instructive to compare our experimental results with Morse's formula. In Fig. 3, the theoretical $\alpha_i(\mu)$ and the experimental $\alpha_i'(\mu)$ for 100 volt-electrons are plotted together. A more stringent test of Eq. (1) is afforded by plotting $\alpha_i'(\mu)\cdot\mu^4$ against μ, which should give a curve proportional to $(1-F^2/Z^2)$. This is done in Fig. 4. It is clear that, even at 400 volts, there is no approach to agreement.

In a recent paper Massey and Mohr[8] have developed a theory which takes into account the effect of distortion of both the incident and scattered electron waves by the static field of the atom, together with the effect of electron exchange. They publish angular distribution curves for electrons which have excited the 2^1P state (21.12 volts energy loss). The computed curve for 33 volt-electrons may be described as a curve which falls off steeply all the way from 0° to 180° on which is superposed a pronounced hump between 60° and 120°. Our experimental curve for 30 volt-electrons (Fig. 1) has quite different characteristics. In a more recent unpublished investigation,[9] Massey and Mohr, following the

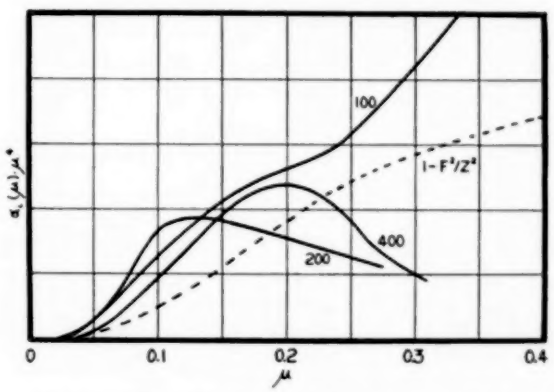

FIG. 4. Experimental and theoretical graphs for $\alpha_i(\mu)\cdot\mu^4$. Unbroken lines, experimental curves. Dotted line, theoretical curve.

[8] H. S. W. Massey and C. B. O. Mohr, Proc. Roy. Soc. **A139**, 187 (1933).

[9] We are glad to thank Messrs. Massey and Mohr for sending us a copy of the unpublished paper.

same methods, extend their computations to the case of electrons having 100, 200 and 400 volt energies and cover the range 0° to 40°. A comparison of their results with ours is shown in Fig. 3. It will be seen that the agreement is quite satisfactory except possibly in the vicinity of 40°. In Fig. 2 we have denoted Massey and Mohr's values by circles. It will be seen that they fit our curves remarkably well. (It is unfortunate that the intensities of the 200 and 400 volt-electrons scattered in our experiments were so small, that we could not make measurements at angles greater than about 20°.) It should be pointed out that the circles representing Massey and Mohr's results were not fitted arbitrarily to *each* of our curves; their results were fitted to ours at *one* voltage and at *one* angle only. The agreement shown is therefore a much more stringent test of their theory than it would have been had the check been made for each voltage independently of the others.

It is possible to calculate the cross section of the helium atom for electron collisions which have led to excitation to the 2^1P state, or alternatively to a 21.12 volt energy loss, by multiplying each scattering coefficient given in Table I by $\sin\theta$ and then integrating from 0° to 180°. Some extrapolation is necessary at the small angle end as the smallest angle at which we could take observations was about 6°. The scattering at the larger angles is so small that no appreciable error is introduced by the absence of data above 150° for the slow electron, or even above 25° for 400 volt-electrons. The 2^1P cross sections, as they may be conveniently designated, are plotted in Fig. 5 as a function of the energy of the electrons before collision. The dotted curve is the 2^1P cross section computed by Massey and Mohr.[10] It will be seen that the agreement is poor.

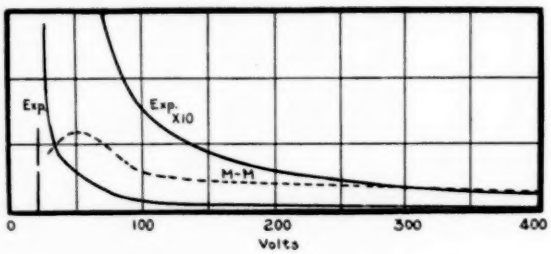

FIG. 5. The 2^1P atomic cross section. Unbroken line, experimental values. Dotted line, Massey and Mohr's theory. Broken line, conjectured course just above threshold, 21.12 volts.

[10] H. S. W. Massey and C. B. O. Mohr, Proc. Roy. Soc. **A33**, 198 (1933). We fitted the data given here over the range 30 to 100 volts, to the data given in the unpublished paper, already referred to, over the range of 100 to 400 volts.

The Quantum Mechanical Cross Section for Ionization of Helium by Electron Impact

W. W. WETZEL, *University of Minnesota*

(Received May 12, 1933)

By using Born's collision theory without exchange the effective ionization cross section is calculated for helium when the resulting ion is left in the normal state. A plane wave is used as a mathematically manageable substitute for the hyperbolic functions previously employed to represent the ejected electron. A comparison is made of the calculated cross section with the experimental values obtained by P. T. Smith. The maximum of the calculated curve falls at approximately three times the ionization potential. The calculation predicts that the maximum probability of ionization occurs when the energy transfer is about 3.5 volts greater than the ionization potential.

INTRODUCTION

ALTHOUGH a number of papers on the probability of elastic and inelastic scattering of electrons by atoms have appeared in the literature,[1] only one attempt has been made to evaluate a cross section for ionization. This is the work of Ochiai[2] who made certain calculations on the effective cross section for ionization of atomic hydrogen. Ochiai used the hyperbolic solutions for hydrogen to represent the ejected electron but was unable, because of their complexity, to bring his calculations to a satisfactory conclusion. Because of the difficulties involved, no experimental measurements have as yet been made on the probability for ionization of atomic hydrogen and therefore no check on the values obtained by Ochiai is possible.

It is the purpose of this paper to apply Born's theory (neglecting exchange) to calculate the cross section of helium for the case when the ion is left in an unexcited state. In order to avoid the difficulties encountered by Ochiai a plane wave is used to represent the electron ejected from the atom. That this method of attack leads to reasonable results will be shown by a comparison of the calculated cross section with the experimental measurements of P. T. Smith.[3]

PROCEDURE

If we represent the ejected atomic electron by a plane wave Born's formula for the ionization cross section becomes

$$\sigma(k) = (m^2/2\pi h^4 k) \int k' \mid U \mid^2 k''^2 dk'' d\Omega'' d\Omega', \tag{1}$$

where

$$U = \int \psi_a e^{i\mathbf{k}\cdot\mathbf{r}_1} \bar{V} \psi_i^* e^{-i\mathbf{k}'\cdot\mathbf{r}_1} e^{-i\mathbf{k}''\cdot\mathbf{r}_2} dv. \tag{2}$$

Here m is the mass of an electron. k, k' and k'' are equal respectively to $2\pi m/h$ times the velocity of the colliding, deflected and ejected electrons. ψ_a is the wave function of the normal atom and ψ_i that for the ionized atom. $d\Omega' = \sin\theta' d\theta' d\phi'$ and $d\Omega'' = \sin\theta'' d\theta'' d\phi''$ where θ' and ϕ', and θ'' and ϕ'' are the direction angles of the vectors k' and k'', respectively, in a fixed set of cartesian axes to be specified later. The origin for all coordinate systems is chosen at the atomic nucleus.

In the particular problem we are considering where the ion is left in the state of lowest potential energy, ψ_i will be given by the solution for the ground state of the hydrogenic atom of double nuclear charge. Thus

[1] For references, see P. M. Morse, Rev. Mod. Phys. **4**, 577 (1932).

[2] K. Ochiai, Proc. Phys.-math. Soc. Japan **11**, 43 (1929).

[3] P. T. Smith, Phys. Rev. **36**, 1293 (1930).

$$\psi_i = (\beta^3/\pi)^{\frac{1}{2}} e^{-\beta r_2},$$

where $\beta = 2/a_0$, a_0 being the radius of the first Bohr orbit in hydrogen. Hylleraas'[4] first approximation representing the ground state of helium is chosen for ψ_a. This is

$$\psi_a = (\alpha^3/\pi) e^{-\alpha(r_2+r_3)},$$

where $\alpha = 27/16a_0$.

The perturbation energy is[5]

$$\bar{V} = e^2(2/r_1 - 1/r_{21} - 1/r_{31}).$$

On substituting these values into Eq. (2) we may integrate over the coordinates of the colliding electron by using Bethe's[6] formula

$$\int (e^{i\mathbf{q}\cdot\mathbf{r}_1}/r_{n1}) dv_1 = (4\pi/q^2) e^{-i\mathbf{q}\cdot\mathbf{r}_n},$$

where, in this problem, $\mathbf{q} = \mathbf{k} - \mathbf{k}'$.

This gives

$$U = (4e^2\alpha^3\beta^3/\pi^{\frac{1}{2}}q^2)(2I_a - I_b - I_c),$$

where

$$I_a = \int e^{-\gamma r_3} dv_3 \int e^{-\alpha r_2} e^{-i\mathbf{k}''\cdot\mathbf{r}_2} dv_2,$$

$$I_b = \int e^{-\gamma r_3} dv_3 \int e^{-\alpha r_2} e^{i(\mathbf{q}-\mathbf{k}'')\cdot\mathbf{r}_2} dv_2,$$

$$I_c = \int e^{-\gamma r_3} e^{i\mathbf{q}\cdot\mathbf{r}_3} dv_3 \int e^{-\alpha r_2} e^{-i\mathbf{k}''\cdot\mathbf{r}_2} dv_2,$$

and $\gamma = \alpha + \beta$.

Let us choose the polar axis to which r_2 is referred to be in the direction of $\mathbf{k}''$ in the cases of integrals I_a and I_c. For the evaluation of I_b choose the polar axis to be in the direction of the vector $\mathbf{l} = \mathbf{q} - \mathbf{k}''$. The exponents containing the scalar product $\mathbf{k}''\cdot\mathbf{r}_2$ and $\mathbf{l}\cdot\mathbf{r}_2$ may then be written as $ik''r_2 \cos\theta_2$ and $ilr_2 \cos\Theta_2$ and dv_2 is replaced by $r_2^2 \sin\theta_2 dr_2 d\theta_2 d\phi_2$ and $r_2^2 \sin\Theta_2 dr_2 d\Theta_2 d\Phi_2$, respectively. The integrals are then easily evaluated to give

$$U = (A/q^2)\{[2/(\alpha^2+k''^2)^2] - [\gamma^4/(\alpha^2+k''^2)^2(\gamma^2+q^2)^2] - [1/(\alpha^2+l^2)^2]\},$$

where $A = 256e^2\alpha^4\beta^{\frac{1}{2}}\pi^{\frac{1}{2}}/\gamma^3$.

A choice of $\mathbf{k}$ as the polar axis from which θ' is measured allows us to write $q^2 = k^2 + k'^2 - 2kk' \cos\theta'$.

This choice of axis defines θ' as the usual scattering angle for the deflected electron. Similarly, taking $\mathbf{q}$ as the polar axis for θ'' permits us to write $l^2 = q^2 + k''^2 - 2qk'' \cos\theta''$, which on differentiation gives

$$\sin\theta''\, d\theta'' = l dl/qk''. \tag{3}$$

Since, with this definition of polar axes, the integrand of Eq. (1) is independent of ϕ' and ϕ'' we may integrate over these two coordinates and on substituting Eq. (3) obtain

$$\sigma(k) = (2\pi m^2/h^4 k) \int (k'k''/q) |U|^2 dk'' \sin\theta'\, d\theta'\, dl.\tag{4}$$

[4] E. Hylleraas, Zeits. f. Physik **54**, 347 (1929).

[5] It should be noted that if our wave functions really satisfied the proper orthogonality relations the first term in $\bar{V}$, representing the contribution of the nucleus to the inelastic scattering would vanish on integrating Eq. (2). That we must retain it in the following can be made plausible by interpreting Eq. (2) as the result of the interaction of the colliding electron with a system of generalized electrical moments representing the atom as a whole. Actually this term is partially cancelled in the integration by other terms which also arise from the lack of orthogonality of the wave function.

[6] H. Bethe, Ann. d. Physik **5**, 325 (1930).

Integrating over l from $l_{\min}=q-k''$ to $l_{\max}=q+k''$ the above expression becomes

$$\sigma(k)=\frac{B}{h}\int_0^{k''_{\max}}\int_0^{\pi}\frac{k'k''}{q^5}\left\{2qk''\left(\frac{4}{(\alpha^2+k''^2)^4}+\frac{\gamma^8}{(\gamma^2+q^2)^4(\alpha^2+k''^2)^4}-\frac{4\gamma^4}{(\gamma^2+q^2)^2(\alpha^2+k''^2)^4}\right)\right.$$
$$+\left(\frac{\gamma^4}{(\alpha^2+k''^2)^2(\gamma^2+q^2)^2}-\frac{2}{(\alpha^2+k''^2)^2}\right)\cdot\left(\frac{1}{\alpha^2+(q-k'')^2}-\frac{1}{\alpha^2+(q+k'')^2}\right)$$
$$\left.+\frac{1}{6}\left(\frac{1}{[\alpha^2+(q-k'')^2]^3}-\frac{1}{[\alpha^2+(q+k'')^2]^3}\right)\right\}dk''\sin\theta'\,d\theta'. \qquad (5)$$

Here $B=(27/2\gamma)^6(\alpha^2/4a_0^{11})$.

Numerical Computations and Comparison with Experiment

Although it is possible to carry the analytical integration further, the expression becomes unwieldy and since a numerical evaluation at this point yields interesting information, that method of procedure was adopted. In order that the calculations may be compared directly with experiment, it is convenient to make a change of variables given by

$$k^2=CV_c;\quad k'^2=CV \quad\text{and}\quad k''^2=CV_e,$$

where $C=8\pi^2me/300h^2$. Also let $\theta'=2\pi\theta/360$. Now θ is measured in degrees, and V_c, V and V_e in volts (i.e., not electron volts, as they are no longer expressed in energy units). From the energy relation we have $dV=dV_e$.

Eq. (5) may be written as

$$\sigma(V_c)=\int_0^{V_{\max}}\int_{0^\circ}^{180^\circ}f(\theta,\,V,\,V_c)\,dV\,d\theta, \qquad (6)$$

where $f(\theta,\,V,\,V_c)$ is equal to the integrand of Eq. (5) multiplied by $2\pi eB/300\times360$.

Let us define $F(V,\,V_c)$ by the relation

$$F(V,\,V_c)=\int_{0^\circ}^{180^\circ}f(\theta,\,V,\,V_c)\,d\theta. \qquad (7)$$

$f(\theta,\,V,\,V_c)$ was evaluated for $V_c=50$, 75, 100, 200, 350 and 500 volts. In each case several values of θ were used. Figs. 1 and 2 give the result for $V_c=75$ and $V_c=200$ volts, respectively. $f(\theta,\,V,\,V_c)$ is proportional to the probability of an electron which has fallen through a potential of V_c volts, striking an atom of helium, ionizing it and coming away from the ion with an energy in electron volts numerically equal to V at an angle θ measured from the original direction of travel. The ejected electron comes away from the ion at an unspecified angle but with an energy in electron volts equal numerically to V, which, in accordance with the law of conservation of energy, satisfies the equation

$$V_e=V_c-V_i-V,$$

where V_i is the ionization potential of helium.

Having plotted the function $f(\theta,\,V,\,V_c)$ the integration indicated in Eq. (7) was carried out by use of a planimeter to evaluate $F(V,\,V_c)$. Fig. 3 shows the complete set of points obtained in this manner. $F(V,\,V_c)$ is proportional to the probability of an electron, which has fallen through a potential of V_c volts, colliding with an atom of helium, ionizing it and coming away from the ion at an unspecified angle with an energy in electron-volts numerically equal to V. The area under a curve of Fig. 3 when multiplied by (V_c-V_i) gives a final value for $\sigma(V_c)$. These values are plotted on Fig. 4.

For purposes of comparison, Smith's values[3] for the experimental total cross section, together with values calculated from Thomson's formula[7] are also plotted on Fig. 4. The experimental values include all possible types of ionization while Thomson's curve and the curve obtained with the present theory include only ionization without excitation. One should expect therefore, that the calculated will fall below the experimental values although just how much below it is impossible to state. Bleakney[8] has found that, up to several hundred volts, the contribution to the total cross section due to double ionization is less

[7] J. J. Thomson, Phil. Mag. **23**, 449 (1912).
[8] Walker Bleakney, Phys. Rev. **36**, 1303 (1930).

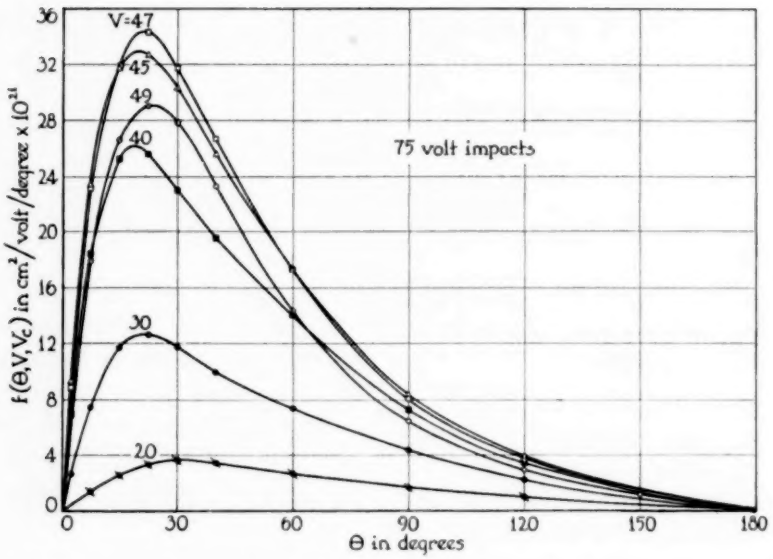

FIG. 1. Angular scattering of the deflected electron for 75-volt collisions in helium which result in simple ionization. V is the potential fall in volts necessary to stop the deflected electron.

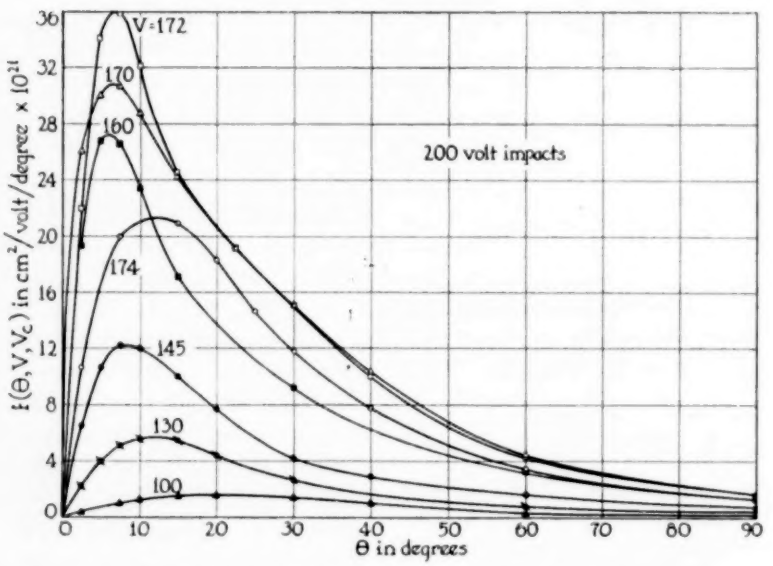

FIG. 2. Angular scattering of the deflected electron for 200-volt collisions in helium which result in simple ionization. V is the potential fall in volts necessary to stop the deflected electron.

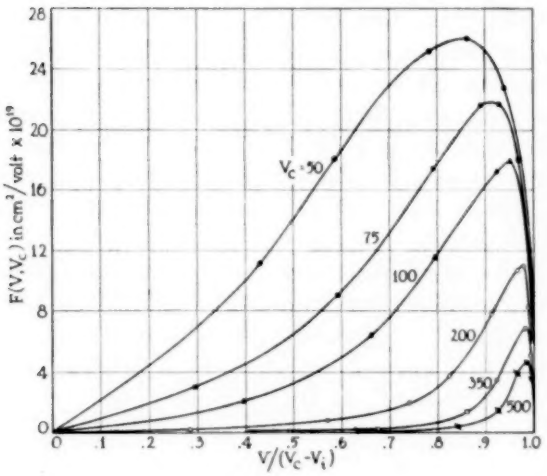

FIG. 3. Total probability of ionization for collisions of V_c volts. V is the potential fall in volts necessary to stop the deflected electron and V_i is the ionization potential.

than one percent of the total experimental cross section. No data are available on the contribution due to ionization plus excitation. As an estimation we may say that the calculated $\sigma(V_c)$ is too great by a factor somewhat less than two.

The experimental curve in Fig. 4 has a maximum at 110 volts while the calculated maximum falls at approximately 75 volts. The addition of contributions due to ionization plus excitation would probably increase the voltage at which the calculated maximum falls and bring it to a better agreement with experiment.

When $F(V, V_c)$ is plotted against V instead of $V/V_c - V_i$ it is seen that, within the accuracy of the calculation, the maximum probability of ionization occurs when the energy transfer is 3.5 volts more than the ionization potential. At impacts of 200 volts or more it should be possible to separate experimentally two groups of electrons coming from the ion. One group should consist of slow electrons whose maximum distribution in energy comes at about 3.5 volts and the other of fast electrons whose volt energy V is given by $V \cong V_c - V_i - 3.5$. This value for the maximum is independent of V_c within the range of 50 to 500 volts.

Figs. 1 and 2 show a series of curves similar to those obtained in angular scattering measurements. For 75 volt collisions the average maximum of the high energy group occurs at about twenty degrees. For 200 volt collisions it has decreased to about ten degrees. This decrease in scattering angle with increased energy of the

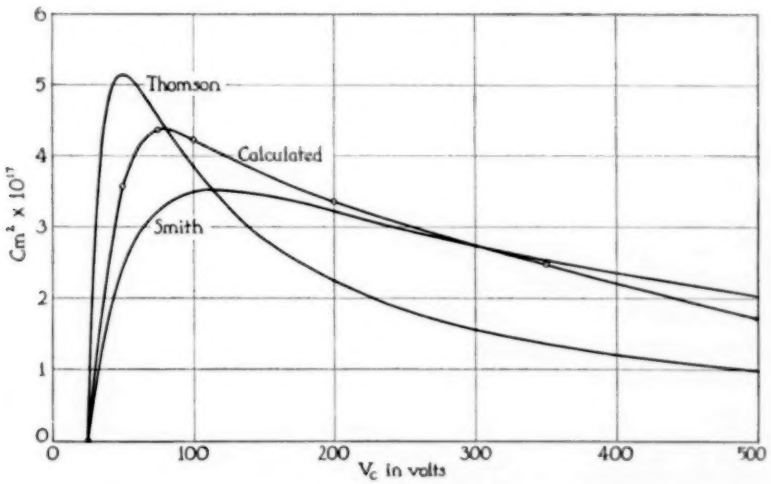

FIG. 4. The calculated cross section for simple ionization as a function of the accelerating potential applied to the colliding electron. Thomson's theoretical and Smith's experimental curves are plotted here for comparison.

colliding electron is in qualitative agreement with Tate and Palmer's work on mercury vapor.[9] The curves illustrated in the first two figures lead to the prediction that for any particular value of V_c, the maximum of the probability for scattering changes as V decreases, first occurring at de-

[9] J. T. Tate and R. R. Palmer, Phys. Rev. **40**, 731 (1932).

creasing values of θ then at increasing values of θ. The smallest angle at which the maximum falls for any particular value of V_e corresponds to an energy transfer of about five volts more than the ionization energy of helium.

One may ask what influence the inclusion of "electron interchange" between the colliding and atomic electrons would have on our results. As we have not yet actually calculated this factor, we cannot be absolutely sure of the effect but it seems reasonable to expect that it would be small, except perhaps for energies of the colliding electron in the neighborhood of the ionization energy of the atom. Qualitatively we may expect this since, in our calculations, the probability that the deflected and ejected electrons leave the atom in nearly the same direction with nearly the same velocity is very small as soon as the energy of the impacting electron is more than 10–20 volts above the ionization potential. However, even though there should be no large change in the numerical results, the inclusion of exchange would completely eliminate any possible identification of the deflected and the impacting electrons such as we have employed in our integrations.

The results obtained seem to justify further calculations and it is intended to correct the present values for exchange effect as well as to extend the work to include some of the lower excited levels of the ion.

In conclusion the author wishes to express his gratitude to Professor John T. Tate who suggested the problem and to Professor E. L. Hill for his continued interest and assistance in its solution.

Quantum Statistics of Almost Classical Assemblies

JOHN G. KIRKWOOD, *Research Laboratory of Physical Chemistry, Massachusetts Institute of Technology*

(Received March 25, 1933)

The sum of states of an assembly in statistical equilibrium may be transformed into an integral in phase space, which is analogous to the classical Gibbs phase integral. With the use of an equation obtained by Bloch it is possible to expand the quantum phase integral in powers of Planck's constant h. The present method of treating the problem supplements that of Wigner and of Uhlenbeck and Gropper by furnishing a more convenient means of obtaining the h-expansion.

INTRODUCTION

IT is generally assumed that an assembly, consisting of a large number of mechanical systems in statistical equilibrium, has the properties of a Gibbs canonical ensemble in respect to its probability distribution in energy. The thermodynamic properties of such an assembly may be calculated from the sum of states

$$\sigma = \sum_n e^{-\beta E_n}, \tag{1}$$

where β is the reciprocal of the product of Boltzmann's constant k and the absolute temperature T. The sum is extended over all accessible energy states E_n. When σ is known, the energy, entropy and thermodynamic potential of the assembly may be obtained from the following relations:[1]

$$\bar{E} = -d \ln \sigma/d\beta; \quad S = k(\ln \sigma - \beta(d \ln \sigma/d\beta)) \tag{1a}$$

$$A = \bar{E} - TS = -(1/\beta) \ln \sigma.$$

If the laws of classical mechanics are assumed to be valid, which would be true if Planck's constant h were allowed to approach zero, the sum of states may be conveniently transformed into an integral over the phase space of the assembly.

$$\lim_{h=0} h^N \sigma = z = \int\int e^{-\beta H(p,q)} dp\, dq, \tag{2}$$

where $H(p, q)$ is the classical Hamiltonian function of the momenta p and the configuration coordinates q, and N is the number of degrees of freedom of the system. The integral is extended over all of momentum and configuration space. From the Gibbs phase integral z, the energy, entropy, and thermodynamic potentials of the classical assembly may be determined except for additive constants.

For systems governed by quantum mechanics, the evaluation of σ is usually more complicated. The direct procedure would consist in determining the allowed energies of the system by means of the Schrödinger equation together with certain restrictions on the symmetry character of the wave functions, and then carrying out the summation. However, in many cases this method requires a prohibitive amount of mathematical labor. The question arises whether one could transform the sum of states into an integral in phase space analogous to the Gibbs integral z, without explicitly solving the dynamical problem. The basis for such a transformation is furnished by work of von Neumann.[2] It has been used by Bloch[3] and by Wigner[4] in the treatment of certain problems. The phase integral which is thus obtained is considerably more difficult to evaluate than the corresponding classical one. However, for systems nearly classical in their behavior, Wigner has shown that it may be expanded in powers of h, the first term of which is the Gibbs integral z.

It is the aim in the present article to carry out an expansion of σ in powers of h similar to that of

[1] J. W. Gibbs, *Elementary Principles in Statistical Mechanics*, Yale University Press.

[2] von Neumann, Gött. Nachr. 273 (1927).

[3] Bloch, Zeits. f. Physik **74**, 295 (1932).

[4] Wigner, Phys. Rev. **40**, 749 (1932).

Wigner. By starting from an equation obtained by Bloch, it is possible to obtain for the coefficients in this expansion a recursion formula which permits a simpler calculation of the higher approximations than the method employed by Wigner. In addition, the correction to σ required by the symmetry restrictions to be placed on the wave functions in accordance with the Fermi-Dirac or the Bose-Einstein statistics is obtained. This correction, neglected by Wigner, has been calculated by Uhlenbeck and Gropper.[5] It is included here, since it seems desirable to give a general formulation of the problem yielding all of the quantum corrections which must be applied to the Gibbs phase integral for systems deviating but little from classical behavior.

Transformation of the Sum of States

We take for consideration an assembly consisting of N similar particles of mass m, moving in a conservative field of force. The potential function of the system $V(q_1 \cdots q_{3N})$ will be determined by the $3N$ coordinates $q_1 \cdots q_{3N}$, specifying position in configuration space. The Schrödinger equation for such a system is

$$(H-E)\psi=0, \quad H=H_0+V(q_1 \cdots q_3), \quad H_0=-h^2\sum_{k=1}^{N}\frac{1}{2m}\Delta_k, \tag{3}$$

where h is Planck's constant divided by 2π, and Δ_k is the Laplacian operator in the configuration space of the particle k. The normalized wave functions will be denoted by ψ_n and the corresponding energy levels by E_n.

The sum of states may be expressed as an integral in configuration space, in the following manner.

$$\sigma=\sum_n e^{-\beta E_n}=\sum_n \int \cdots \int \psi_n^* e^{-\beta H}\psi_n dq_1 \cdots dq_{3N}, \tag{4}$$

where the operator $e^{-\beta H}$ is defined by the series[6]

$$e^{-\beta H}=\sum_{l=0}^{\infty}\frac{(-\beta)^l}{l!}H^l. \tag{5}$$

Eq. (4) follows simply from the relation, $H^l\psi_n=E_n{}^l\psi_n$, and from the fact that the functions ψ_n are normalized. The integral (4) has much in common with the Gibbs phase integral z. Thus it will be remembered that the transformation determinant of the volume element $dp_1 \cdots dp_{3N}, dq_1 \cdots dq_{3N}$ in the classical integral (2) is unity for any canonical transformation of the momentum and configuration coordinates. The quantum mechanical analogue of the classical canonical transformation consists in a transformation of the orthogonal function set ψ_n. From (4) it is seen that σ is the diagonal sum of the matrix $[e^{-\beta H}]$, the elements of which are given by

$$[e^{-\beta H}]_{n'n}=\int \psi_{n'}^* e^{-\beta H}\psi_n dq. \tag{6}$$

Since the diagonal sum of such a matrix is invariant under a transformation of the ψ's, one may employ not only the characteristic functions ψ_n of the operator H in its evaluation, but any other convenient set of orthogonal functions having the same symmetry properties as the ψ_n's. This corresponds to the fact that one may employ any convenient canonically conjugate set of momentum and space coordinates in the evaluation of the classical Gibbs phase integral.

[5] Uhlenbeck and Gropper, Phys. Rev. **41**, 79 (1932).

[6] One may write $e^{-\beta H}$ as $e^{-\beta(H_0+V)}$ where H_0 is the kinetic energy operator. However, since H_0 and V do not commute, $e^{-\beta H}$ is not equal to $e^{-\beta H_0}e^{-\beta V}$ or $e^{-\beta V}e^{-\beta H_0}$.

We wish to replace the energy summation in the integral (4) by an integration in momentum space. For this purpose we choose the characteristic functions $\varphi(p, q)$ of the kinetic energy operator H_0.[7] These functions together with the corresponding continuous energy levels are easily found to be

$$\varphi(p, q) = \exp\left[\frac{i}{h}\sum_{k=1}^{N}\mathbf{p}_k\cdot\mathbf{r}_k\right], \quad T(p) = \sum_{k=1}^{N}\mathbf{p}_k^2/2m, \tag{7}$$

where $\mathbf{p}_k$ is the momentum vector and $\mathbf{r}_k$ is the radius vector in the phase space of the particle k. It will be assumed that the characteristic functions ψ_n of the operator H are either symmetric or antisymmetric in the coordinates of the N particles. The first assumption corresponds to the Bose-Einstein and the second to the Fermi-Dirac statistics. Linear combinations of the functions $\varphi(p, q)$, which are symmetric or antisymmetric must be constructed before they are suitable for an expansion of the functions ψ_n. The required linear combinations are the following:

$$\Phi(p, q) = \frac{1}{(N!)^{\frac{1}{2}}}\sum_{P}(\pm 1)^{(P)}\exp\left[\frac{i}{h}P\sum_{k=1}^{N}\mathbf{p}_k\cdot\mathbf{r}_k\right]. \tag{8}$$

The summation is extended over the $N!$ functions generated by allowing the permutation operator P to redistribute the $\mathbf{r}_k$'s among the $\mathbf{p}_k$'s in the sum $\sum_{k=1}^{N}\mathbf{p}_k\cdot\mathbf{r}_k$. The order of the permutation is denoted by (P). When it is even the factor $(\pm 1)^{(P)}$ has the value $+1$, and when odd the value ± 1. The functions ψ_n are then expanded in terms of the orthogonal set $\Phi(p, q)$ by means of Fourier integrals, and the sum over the index n carried out by means of the completeness relation

$$\sum_{n}\psi_n^*(q')\psi_n(q) = \delta(q'-q), \tag{9}$$

where $\delta(q'-q)$ is the Dirac delta-function. Eq. (4) then becomes

$$\sigma = \frac{1}{(2\pi h)^{3N}N!}\sum_{P'P}(\pm 1)^{(P'+P)}\int_{-\infty}^{+\infty}\cdots\int_{-\infty}^{+\infty}\exp\left[-\frac{i}{h}P'\sum_{k=1}^{N}\mathbf{p}_k\cdot\mathbf{r}_k\right]e^{-\beta H}\exp\left[\frac{i}{h}P\sum_{k=1}^{N}\mathbf{p}_k\cdot\mathbf{r}_k\right]dp_1\cdots dq_{3N}. \tag{10}$$

This integral is the quantum mechanical analogue of the Gibbs phase integral.

The evaluation of the quantum phase integral (10) depends upon a determination of the following functions

$$u(P) = e^{-\beta H}\varphi(P); \quad \varphi(P) = \exp\left[\frac{i}{h}P\sum_{k=1}^{N}\mathbf{p}_k\cdot\mathbf{r}_k\right]. \tag{11}$$

One notes that as β approaches zero, u must approach φ. Moreover differentiation of both sides of Eq. (11) with respect to β leads to the Bloch equation

$$Hu + \partial u/\partial\beta = 0, \quad \lim_{\beta=0} u = \varphi. \tag{12}$$

This equation, which may be regarded as a fundamental equation of quantum statistics, is identical in form with the Schrödinger equation containing the time, differing from it only in the appearance of β instead of it/h. Bloch[3] noting that its solutions may be obtained from the Kennard transformation functions by replacing it/h by β, has obtained exact solutions of Eq. (12) for certain special problems. We will attempt here an approximate solution of Eq. (12), which depends upon an expansion in powers of Planck's constant h. While the method resembles in principle the Wentzel-Brillouin-Kramers solution of the wave equation, its details are quite different. Let us suppose that

[7] The quantities $\mathbf{p}_k$ and $\mathbf{r}_k$ in the wave function are to be regarded as vectors in ordinary three-dimensional space. The components of $\mathbf{p}_k$ are of course numbers, not operators.

$$u = w\varphi(P)e^{-\beta H(p,\,q)}, \tag{13}$$

where $H(p, q)$ is the ordinary classical Hamiltonian function, $T+V$. With the aid of Eq. (12) and the relations $H_0\varphi(P) = T\varphi(P)$ and

$$-ih\sum_{k=1}^{N}\nabla_k\varphi(P)\cdot\nabla_k = \varphi(P)\left(P\sum_{k=1}^{N}\mathbf{p}_k\cdot\nabla_k\right)$$

one finds that w must satisfy the following equation:

$$\frac{\partial w}{\partial\beta} - e^{+\beta V}\left\{\frac{ih}{m}\left(P\sum_{k=1}^{N}\mathbf{p}_k\cdot\nabla_k e^{-\beta V}w\right)+\frac{h^2}{2m}\sum_{k=1}^{N}\Delta_k e^{-\beta V}w\right\} = 0; \quad \lim_{\beta=0} w = 1. \tag{14}$$

Because of the boundary condition at $\beta = 0$, Eq. (14) may be conveniently written as an integral equation

$$w = 1+\frac{ih}{m}\int_0^{\beta} e^{Vt}\left[P\sum_{k=1}^{N}\mathbf{p}_k\cdot\nabla_k e^{-Vt}w\right]dt+\frac{h^2}{2m}\int_0^{\beta} e^{Vt}\sum_{k=1}^{N}\Delta_k(e^{-Vt}w)dt. \tag{15}$$

Solution of Eq. (15) by successive approximations yields

$$w = \sum_{l=0}^{\infty} h^l w_l,$$

$$w_0 = 1, \quad w_1 = -\frac{i\beta^2}{2m}\left(P\sum_{k=1}^{N}\mathbf{p}_k\cdot\nabla_k V\right),$$

$$w_2 = -\frac{1}{2m}\left\{\frac{\beta^2}{2}\sum_{k=1}^{N}\Delta_k V-\frac{\beta^3}{3}\left[\sum_{k=1}^{N}(\nabla_k V)^2+\frac{1}{m}\left(P\sum_{k=1}^{N}\mathbf{p}_k\cdot\nabla_k\right)^2 V\right]+\frac{\beta^4}{4m}\left(P\sum_{k=1}^{N}\mathbf{p}_k\cdot\nabla_k V\right)^2\right\}. \tag{16}$$

The general term w_l may be calculated by means of the following formula

$$w_l = \frac{1}{m}\int_0^{\beta} e^{Vt}\left\{\frac{1}{2}\sum_{k=1}^{N}\Delta_k(e^{-Vt}w_{l-2})+i\left(P\sum_{k=1}^{N}\mathbf{p}_k\cdot\nabla_k e^{-Vt}w_{l-1}\right)\right\}dt. \tag{17}$$

This recursion formula permits a calculation of any term in the series (16) by simple operations of differentiation and integration on the two preceding terms.

The functions $u(P)$ may now be written

$$u(P) = \varphi(P)e^{-\beta H(p,\,q)}\sum_{l=0}^{\infty} h^l w_l(P) \tag{18}$$

and the quantum phase integral becomes

$$\sigma = \frac{1}{(2\pi h)^{3N}N!}\int\cdots\int e^{-\beta H(p,\,q)}\sum_{P',\,P}(\pm 1)^{(P'+P)}\exp\left[\frac{i}{h}(P-P')\sum_{k=1}^{N}\mathbf{p}_k\cdot\mathbf{r}_k\right]\sum_{l=0}^{\infty}h^l w_l(P)dp_1\cdots dq_{3N}. \tag{19}$$

For convenience, the sum over P and P' may be arranged so that the first member contains all terms in which P' and P are the same permutation, the second those in which P' and P differ only with respect to a single pair of particles, etc. Certain simplifications are then possible. Each of the $N!$ terms in which $P' = P$, when integrated over the p's, gives the same result, since $H(p, q)$ is symmetrical in the p's and it cannot matter which p is associated with a given q. One may therefore replace the function $w_l(P)$ by its value w_l for the identity permutation. For terms in which P' and P

differ by the permutation of two particles similar simplifications may be made, and it is only necessary to use two functions $w_l(jk)$ and $w_l(kj)$, corresponding to the two permutations of the pair jk, regardless of what pair of momentum coordinates happens to be involved. The integral (19) then becomes

$$\sigma=\frac{1}{(2\pi h)^{3N}}\int\cdots\int e^{-\beta H(p,\,q)}\left\{\sum_{l=0}^{\infty}w_l h^l \pm\frac{1}{2}\sum_{k\neq j}^{N}\left[\exp\left[\frac{i}{h}(\mathbf{p}_j-\mathbf{p}_k)\cdot(\mathbf{r}_j-\mathbf{r}_k)\right]\sum_{l=0}^{\infty}h^l w_l(jk)+\exp\left[-\frac{i}{h}(\mathbf{p}_j-\mathbf{p}_k)\cdot(\mathbf{r}_j-\mathbf{r}_k)\right]\sum_{l=0}^{\infty}h^l w_l(kj)\right] +\cdots\right\}dp_1\cdots dp_{3N}\cdots dq_{3N}. \quad (20)$$

When the values of w_l calculated with the aid of Eq. (17) are inserted in Eq. (20) and the integration over the momentum coordinates is carried out, there results

$$\sigma=\frac{(2\pi mkT)^{3N/2}}{(2\pi h)^{3N}}\int_{-\infty}^{+\infty}\cdots\int_{-\infty}^{+\infty}e^{-\beta V}\left\{\left[1-\frac{h^2\beta^2}{12m}\sum_{k=1}^{N}\left(\Delta_k V-\frac{\beta}{2}(\nabla_k V)^2\right)+\cdots\right] \pm\sum_{j\neq k}e^{-mr_{jk}^2/\beta h^2}\left[1+\frac{\beta}{2}\mathbf{r}_{jk}\cdot(\nabla_j V-\nabla_k V)+\cdots\right]+\cdots\right\}dq_1\cdots dq_{3N};\quad \mathbf{r}_{jk}=\mathbf{r}_j-\mathbf{r}_k. \quad (21)$$

The first three terms of the series $\sum_{l=0}^{\infty}h^l w_l$ have been retained in the part of σ involving identical permutations, and the first two terms in the part involving permutations differing with respect to two particles. The first part agrees with the result obtained by Wigner and the second with that obtained by Uhlenbeck and Gropper.[5a] Since they become rather cumbersome, the higher approximations are not written down. They may, however, be calculated by simple processes of differentiation and integration with the aid of the recursion formula (17). In an actual problem, their form may usually be kept simpler by inserting an explicit expression for the potential V at the beginning.

In the case of relatively weak coupling between the particles as between the molecules of a gas at low pressures, the arrangement of terms in the sum over permutations in Eq. (19) actually corresponds to their order of magnitude. Because of the factors $e^{-mr_{jk}^2/\beta h^2}$, the ratio of each member to the preceding one will be v/V, where v is of the order of magnitude of the second virial coefficient of the gas and V the total volume of the vessel in which it is confined. The walls of the vessel may be represented by means of high potential barriers which cause $e^{-\beta V}$ to vanish in regions of configuration space outside the vessel. In practice, if one neglects small wall corrections, this is equivalent to restricting the integrations in configuration space to regions inside the vessel.

Probability Distribution in Phase Space

In the preceding section, the sum of states has been transformed into the phase integral of a function $F(p, q)$ having the form $e^{-ipq/h}e^{-\beta H}e^{ipq/h}$. The relation which this function bears to the probability distribution in phase space has not yet been investigated, and indeed from a purely thermodynamic point of view is unessential. It may be shown, however, that $F(p, q)$, when integrated over momenta, yields a probability in configuration, and when integrated over configuration space, a probability in momentum, consistent both with a canonical distribution in energy and with the Schrödinger equation.

A discussion of the probability distribution in phase space is facilitated by the use of the

[5a] A trivial oversight of making the derivative of x^2 equal to x instead of $2x$, causes the coefficient of $r_{jk}\cdot(\nabla_j V-\nabla_k V)$ in their formula to be $\beta/4$ instead of $\beta/2$.

following function, which differs but little from Wigner's[8] $P(x, p)$

$$P(p, q) = (2\pi h)^{-1} \int_{-\infty}^{\infty +} e^{ip(q'-q)/h} \psi^*(q') \psi(q) dq', \quad (22)$$

where ψ satisfies the Schrödinger equation

$$H\psi - ih(\partial\psi/\partial t) = 0. \quad (23)$$

When $P(p, q)$ is integrated with respect to p, it yields the probability in configuration space $\psi^*(q)\psi(q)$ and when integrated with respect to q the corresponding probability in momentum space $(2\pi h)^{-1}\Phi^*(p)\Phi(p)$ where

$$\Phi(p) = \int_{-\infty}^{+\infty} e^{-ipq/h} \psi(q) dq. \quad (24)$$

The above relations are equally valid whether the system is made up of a pure state or of a mixture of states.

For an arbitrary distribution in energy

$$\psi = \sum_n C_n \psi_n e^{2\pi i \nu_n t + i\varphi_n}, \quad (25)$$

where Ψ_n satisfies the Schrödinger equation $(H - E_n)\psi_n = 0$; $\nu_n = -E_n/2\pi h$, and φ_n is an arbitrary phase angle. The probability in configuration space is

$$P(q) = \psi^*\psi = \sum_{n', n} C_{n'}^* C_n \psi_{n'}^* \psi_n e^{2\pi i \nu_{n'n} t + i(\varphi_n - \varphi_{n'})} \quad (26)$$

To give this probability a physical meaning it is necessary to form an average over the arbitrary phases φ_n,[9] and one finds

$$\overline{P(q)} = \sum_n C_n^* C_n \psi_n^* \psi_n \quad (27)$$

with a similar expression for $\overline{P(p)}$, the probability in momentum space

$$\overline{P(p)} = \sum_n C_n^* C_n \Phi_n^* \Phi_n, \quad (28)$$

where Φ_n may be calculated with the aid of Eq. (24). The probability distribution function in energy is

$$P(E_n) = C_n^* C_n / \sum_n C_n^* C_n. \quad (29)$$

For a canonical distribution $P(E_n) = e^{\beta(A - E_n)}$ where A is the thermodynamic potential $E - TS$. Thus one may write

$$C_n^* C_n = e^{-\beta E_n}$$

$$\sigma = e^{-\beta A} = \sum_n C_n^* C_n = \sum_n e^{-\beta E_n}. \quad (30)$$

The probability functions $\overline{P(q)}$ and $\overline{P(p)}$ become for a canonical distribution

$$\overline{P(q)} = \sigma^{-1} \sum_n \psi_n^* e^{-\beta E_n} \psi_n,$$

$$\overline{P(p)} = \sigma^{-1} \sum_n \Phi_n^* e^{-\beta E_n} \Phi_n. \quad (31)$$

They may be obtained by integration from the function

$$\overline{P(p, q)} = (2\pi h\sigma)^{-1} \int_{-\infty}^{+\infty} \sum_n e^{ip(q'-q)/h} \psi_n^*(q') e^{-\beta E_n} \psi_n(q) dq'. \quad (32)$$

When integrated with respect to p, $\overline{P(p, q)}$ gives the probability in configuration $\overline{P(q)}$, and when integrated with respect to q, the probability in momentum $\overline{P(p)}$. If one remembers that $e^{-\beta E_n}\psi_n = e^{-\beta H}\psi_n$ and expands ψ_n in the functions $e^{ipq/h}$ by means of a Fourier integral, there is obtained

$$\overline{P(p, q)} = (2\pi h\sigma)^{-1} \int\int_{-\infty}^{+\infty} \int \left\{ \left[\sum_n \psi_n^*(q') \psi_n(q'') \right] e^{i(pq' - p'q'')/h} e^{-ipq/h} e^{-\beta H} e^{ip'q/h} \right\} dp' dq'' dq'. \quad (33)$$

When the sum over n is carried out by means of the completeness relation (9) and the indicated integrations are performed, Eq. (33) reduces to

$$\overline{P(p, q)} = (2\pi h\sigma)^{-1} e^{-ipq/h} e^{-\beta H} e^{ipq/h}. \quad (34)$$

Thus the normalized probability function $\overline{P(p, q)}$ is proportional to the integrand $e^{-ipq/h} e^{-\beta H} e^{ipq/h}$ employed in the representation of the sum of states.

[8] Wigner, reference 4, Eq. (5).

[9] For a discussion of this point see J. C. Slater, Phys. Rev. **38**, 237 (1931).

The expansion of $\overline{P(p, q)}$ in powers of h does not agree exactly with Wigner's expansion of $P(p, x)$. Thus his expansion contains no odd powers of h, while the expansion of $\overline{P(p, q)}$ does. However, when integrated over momenta, the two functions appear to lead to the same result for the probability in configuration. They also give the same result for the probability in momentum space, when the potential function V becomes positive and infinite on the boundary of a finite region in configuration space. The difference between $\overline{P(p, q)}$ and $P(p, x)$ may possibly be connected with the average over the arbitrary phases of the wave functions, which seems physically necessary. However, it should be remembered that because of the uncertainty principle, neither function has a physical meaning until it is integrated either over momentum space or over configuration space. Thus, it would not be surprising if one could construct a number of different functions of p and q, all of which would give the correct results for the momentum and configuration probabilities after integration over p or q.

The practical value of the method outlined in this article depends of course on the convergence of the expansion of $e^{-ipq/h}e^{-\beta H}e^{ipq/h}$ in powers of h. Its convergence will depend upon the properties of the integral Eq. (15). A detailed investigation of this equation would be desirable, but will not be undertaken here. However, from a physical standpoint, it seems likely that the expansion may be employed with confidence when kT is large relative to the spacing of the energy levels of the assembly, provided that the term system coalesces into a continuous spectrum as the potential function V approaches zero.

In conclusion, the writer wishes to express his indebtedness to Dr. F. London, Dr. F. Bloch, and to Dr. E. Wigner for the opportunity to discuss with them some of the questions treated here.

Magnetic Quadrupole Field and Energy in Cubic and Hexagonal Crystals

L. W. McKeehan, *Sloane Physics Laboratory, Yale University*

(Received May 15, 1933)

In crystalline arrays of equal and co-directed ideal bar magnets or circular Amperian current loops the magnetic field at certain important points and the magnetic potential energy of the array depend, if the linear dimensions of the magnetic elements are small in comparison with the shortest distance between elements, upon a series of terms, the first of which would be due to a similar array of dipoles. The second term, which, by analogy, has been styled the quadrupole term, depends upon a sum, over all points of the array except the origin, of the fourth-order zonal harmonic of a certain angle, divided by the fifth power of the radius to the point. This sum is evaluated by a precise method for several cubic and hexagonal arrays, and the results are compared with such published values as are available.

Introduction

NUMEROUS investigators have attempted to explain the existence of easy directions of magnetization in ferromagnetic crystals by the interaction of magnetic elements more complicated than dipoles. Ewing's theories of 1890[1] and 1922[2] are of this type, though the necessary crystalline symmetry of the model appears by implication rather than explicitly. In them Ewing sought to confer particular stability upon co-directed bar magnets (with point poles) or upon Amperian currents in parallel planes, by magnetic forces alone. He did not do much quantitative work with this model because it appeared, by approximate methods, that even in a single row of elements the magnetic potential energy minimum for the saturated state was not deep enough to explain the observed stability with respect to heat or other disorganizing agents, nor shallow enough to allow the observed easy transition from one direction of saturation to another under the control of magnetic forces. In other words the molecular field is not wholly, nor even principally, magnetic.

Ewing limited his analysis to the effect of adjacent bar magnets so that his theory is essentially that of a one-dimensional crystal. The two-dimensional crystal, for adjacent magnets only, has been treated by Honda and Okubo[3] who calculated the equilibrium orientation of a centrally pivoted bar magnet under the simultaneous action of an applied magnetic field and the magnetic fields of eight similar bar magnets centrally pivoted in a plane containing the applied field, at the adjacent points of a square net, and constrained to be parallel to the magnet under investigation. In the absence of an applied field this model is magnetically stable for magnetization parallel to the edges of the square meshes of the net. In both of these studies the extension to three dimensions was qualitative.

Peddie attacked the three-dimensional crystal by direct summation of the magnetic fields of near-by elements at the center and at either pole of one of the equal and co-directed bar magnets. In his first paper[4] the magnet centers occupied the points of a face-centered cubic lattice (F). In a second note[5] he computed similar constants for the simple cubic lattice (S), and still later[6] extended the analysis to other than cubic lattices, but did not compute the constants for these more complicated cases. This theoretical work has been

[1] J. A. Ewing, Rep. Brit. Ass. 740–741 (1890); Proc. Roy. Soc. **A48**, 342–358 (1890); Phil. Mag. [5] **30**, 205–222 (1890).

[2] J. A. Ewing, Proc. Roy. Soc. (Edinburgh) **42**, 97–128 (1922); Proc. Roy. Soc. **A100**, 449–460 (1922); Phil. Mag. [6] **43**, 493–503 (1922).

[3] K. Honda, J. Okubo, Sci. Rep. Tohoku Imp. Univ. **5**, 153–214 (1916); **6**, 183–196 (1917); Phys. Rev. **10**, 705–742 (1917).

[4] W. Peddie, Proc. Roy. Soc. (Edinburgh) **25**, 1025–1059 (1905).

[5] W. Peddie, Proc. Roy. Soc. (Edinburgh) **28**, 643–651 (1908).

[6] W. Peddie, Proc. Roy. Soc. (Edinburgh) **32**, 216–246 (1912).

reviewed and extended by Forrest[7] who extracted from Peddie's tables the essential constants for the body-centered cubic lattice (I) and for the diamond arrangement (D). Forrest also made some computations for a few noncubic lattices. The body-centered cubic case has also been investigated by Mahajani,[8] who, however, chose equal circular current loops rather than equal bar magnets as the magnetic elements in the model crystal. Finally, Akulov[9] has computed the mutual magnetic energy of what may be called cubic lattices, (S) and (I), of magnetic quadrupoles, as dependent upon their direction of magnetization.

Whether field components or magnetic potential energies are computed the mathematical difficulty lies in the evaluation of series of the form

$$\sum_n F_n \sum_r{}' (a_0 r)^{-n-1} P_n(\cos\{\mathbf{p},\mathbf{r}\}), \qquad (1)$$

where $a_0\mathbf{r}$ is the vector from the lattice point chosen as origin to any other, $\mathbf{p}$ is a unit vector in the direction of all the magnetic axes, $\{\mathbf{p},\mathbf{r}\}$ is the angle between $\mathbf{p}$ and $\mathbf{r}$, and $P_n(\cos\theta)$ is the surface zonal harmonic of order n. The parameter a_0 is that lattice parameter in terms of which all vectors $\mathbf{r}$ must be expressed. The coefficients F_n depend upon the quantity sought and upon the nature of the magnetic element which is chosen. The presence of zonal harmonics indicates that we have already restricted ourselves to magnetic elements with full axial symmetry. The absence of magnetic charges makes $F_0=0$ and if the lattice has reflection planes through its lattice points perpendicular to $\mathbf{a}_1$, $\mathbf{a}_2$ and $\mathbf{a}_3$, the sums with respect to r are all zero unless n is even. Finally, if the lattice is cubic the sum with respect to r is zero for $n=2$ so that the first term differing from zero is $F_4\sum_r{}'(a_0r)^{-5}P_4(\cos\{\mathbf{p},\mathbf{r}\})$.

For ideal bar magnets of moment P and of length a smaller than the shortest distance between lattice points Peddie[6] gives expressions for the magnetic field components at the center and at the poles of each magnet due to all the rest of the array. In our notation[10] the component parallel to $\mathbf{p}$ takes the following forms:

At a magnet center

$$\mathbf{H}_0\cdot\mathbf{p}=P\sum_{n=2}^{n=\infty} n\,2^{-n}a^{n-2}\sum_r{}'(a_0r)^{-n-1}P_n(\cos\{\mathbf{p},\mathbf{r}\}). \qquad (2)$$

At a magnet pole

$$\mathbf{H}_a\cdot\mathbf{p}=P\sum_{n=2}^{n=\infty} n\,a^{n-2}\sum_r{}'(a_0r)^{-n-1}P_n(\cos\{\mathbf{p},\mathbf{r}\}). \qquad (3)$$

In both these series n is restricted to even integers.

Mahajani[8] derives the magnetic potential energy per magnet, obtaining, in our notation,

$$U=-P^2\sum_{n=2}^{n=\infty} a^{n-2}\sum_r{}'(a_0r)^{-n-1}P_n(\cos\{\mathbf{p},\mathbf{r}\}) \qquad (4)$$

subject to the same restriction (n even).

Mahajani also treats the case of circular Amperian current loops of radius b and magnetic moment P, obtaining the first two terms in U, which are:

$$U_2=-P^2\sum_r{}'(a_0r)^{-3}P_2(\cos\{\mathbf{p},\mathbf{r}\}), \qquad (5)$$

$$U_4=+3P^2b^2\sum_r{}'(a_0r)^{-5}P_4(\cos\{\mathbf{p},\mathbf{r}\}). \qquad (6)$$

The term U_4 is equivalent to Akulov's "quadrupole" energy per elementary magnet if we put his "quadrupole moment" equal to Pb. It would seem rather better to call Pa the quadrupole moment for the ideal bar magnet, in which case the quadrupole moment for the circular current loop has the imaginary value $Pb(-1)^{\frac{1}{2}}$ but the concept of quadrupoles is so nonphysical at best that we prefer to call $(\mathbf{H}\cdot\mathbf{p})_4$ and U_4 the quadrupole field and the quadrupole energy without closer analysis of what this may imply.

The dimensionless sum

$$S_2=\sum_r{}'r^{-3}P_2(\cos\{\mathbf{p},\mathbf{r}\}) \qquad (7)$$

has already been considered in some detail in papers[10] on dipole fields and dipole energies. The corresponding sum

$$S_4=\sum_r{}'r^{-5}P_4(\cos\{\mathbf{p},\mathbf{r}\}) \qquad (8)$$

[7] J. Forrest, Phil. Mag. [6] **50**, 1009–1018 (1925); Trans. Roy. Soc. (Edinburgh) **54**, 601–701 (1926); Phil. Mag. [7] **3**, 464–476 (1927).

[8] G. S. Mahajani, Proc. Camb. Phil. Soc. **23**, 136–143 (1926); Phil. Trans. **A228**, 63–114 (1929).

[9] N. S. Akulov, Zeits. f. Physik **57**, 249–256 (1929).

[10] L. W. McKeehan, Phys. Rev. **43**, 913, 924, 1022, 1025 (1933).

now engages our attention. We substitute

$$P_4(\cos\theta) = (1/8)(35\cos^4\theta - 30\cos^2\theta + 3), \quad (9)$$

put

$$\cos\{\mathbf{p}, \mathbf{r}\} = r^{-1}\sum_i p_i r_i \quad (10)$$

and then make use of any symmetry of the lattice to simplify the formulae for computation. The sum S_4 is absolutely convergent but converges so slowly as r increases that it turns out to be better here, as it was in computing S_2, to use the method of Ewald rather than that of Lorentz.

Cubic Arrays

In cubic arrays Eq. (8) reduces to

$$S_4 = (7R_c/8)\{5(p_1^4 + p_2^4 + p_3^4) - 3\}, \quad (11)$$

where the single coefficient R_c may be written

$$R_c = R_{11} - 3R_{23}, \quad (12)$$

with

$$R_{11} = \sum_r{}' r_1^4 r^{-9}, \quad (13)$$

$$R_{23} = \sum_r{}' r_2^2 r_3^2 r^{-9}. \quad (14)$$

A convenient auxiliary sum is

$$R_0 = \sum_r{}' r^{-5}, \quad (15)$$

because

$$3R_{11} + 6R_{23} - R_0 = 0. \quad (16)$$

Since

$$p_1^4 + p_2^4 + p_3^4 = 1 - 2(p_2^2p_3^2 + p_3^2p_1^2 + p_1^2p_2^2), \quad (17)$$

an alternative form of Eq. (11) is

$$S_4 = (7R_c/4)\{1 - 5(p_2^2p_3^2 + p_3^2p_1^2 + p_1^2p_2^2)\}. \quad (18)$$

Peddie[6] and Forrest[7] obtain by direct summation a quantity $(G-D)$, which in our notation is $-R_c/2$, $-R_c/16$ or $-R_c/512$ according to the unit of length they chose, a_0 for (S), $a_0/2$ for (I) and (F), $a_0/4$ for (D). The limiting value of r in each of these summations is 10 of their units. The tables given by Forrest[7] (pp. 676–679) contain several mistakes, and a recomputation shows that some of these also appear in Peddie's tables upon which they are based. Table I shows the changes that are necessary, and the values of R_c derived from the corrected values of $(G-D)$.

Mahajani[8] obtains for (I), the only array he considers, lower and upper limits for a quantity $(3Q-P)$, which in our notation is $-R_c/32$, by an ingenious artifice. He notes that a related

Table I.

Array	$(G-D)$* Forrest	$(G-D)$* Corrected	R_c
(S)	−3.8461	−3.55204	1.7760
(I)	0.0628	0.11101	− 1.7761
(F)	0.26622	0.26896	− 4.3034
(D)	0.11928	0.11946	−61.164

* Peddie's notation.

coefficient, $B_5 = 3^5R_0$, has already been computed to the necessary degree of precision by Jones and Ingham.[11] If we designate by a subscript the value of r with which we terminate any summation, understanding the subscript ∞ for the convergence limit, we may write Mahajani's inequalities:

$$(R_{11} - R_{23}) > (R_{11} - R_{23})_r, \quad (19)$$

$$(R_{11} - R_{23}) < (R_{11} - R_{23} - R_0)_r + (R_0). \quad (20)$$

From (16), (19) and (20) we then find

$$(R_c) < (5/3)(R_{11} - R_{23} - R_0)_r + (13/9)(R_0), \quad (21)$$

$$(R_c) > (5/3)(R_{11} - R_{23})_r - (2/9)(R_0). \quad (22)$$

In checking Mahajani's computations it appeared that the limiting value $r = 5^{\frac{1}{2}}$ which he proposed to use was not consistently adhered to in (21) and (22), and that his results were further vitiated by an inaccurate decimal equivalent for $3^{\frac{1}{2}}$, used in deriving R_0 from B_5. After making the necessary corrections the computations were extended to $r = 10^{\frac{1}{2}}$, reducing the range of uncertainty in R_c to about half its value for $r = 5^{\frac{1}{2}}$. Furthermore, values of R_c have been found for (S) and (F) as well as for (I), using additional data from Jones and Ingham.[11] The results are presented in Table II.

Akulov[9] computed two coefficients, A_0' and A' for (S), A_0'' and A'' for (I). In our notation $A_0 = (21/2)NR_c$ and $A = -(105/4)NR_c$. Akulov did not notice that the constant term in (18) is exactly 1/5 the coefficient of $(p_2^2p_3^2 + p_3^2p_1^2 + p_1^2p_2^2)$. (He gives the ratio as 0.200/2 but his own figures in the same paragraph support the correct value.) His method has been carried through much more precisely for (S), (I) and

[11] J. E. Jones and A. E. Ingham, Proc. Roy. Soc. **A107**, 636–653 (1925). The method used is essentially that of Ewald.

TABLE II.

Array	Up to $r=5^{\frac{1}{2}}$ $(3Q-P)$*		R_c
	Mahajani	Corrected	
(*I*)	>0.032	>0.043481	<−1.3914
	<0.064	<0.059864	>−1.9156

Array	Up to $r=10^{\frac{1}{2}}$ $(3Q-P)$*	R_c
(*S*)	>−0.058576	< 1.8744
	<−0.054445	> 1.7423
(*I*)	> 0.049674	<−1.5896
	< 0.057608	>−1.8434
(*F*)	> 0.122294	<−3.9134
	< 0.138719	>−4.4390

* Mahajani's notation.

(*F*). In each case the results have been checked by computation with two different values of the arbitrary parameter ϵ, *viz.*, $\epsilon=2$ and $\epsilon=3$. The formulae for computation may be put in the following form, analogous to that used in dipole computations.[10]

$$S_4 = (Q_4+R_4+R_3+R_2+R_0) + (Q_4'+Q_4''+R_4'+R_4'') \times (p_2^2p_3^2+p_3^2p_1^2+p_1^2p_2^2), \quad (23)$$

$$Q_4 = \frac{4\pi^3N}{3}\sum' f n_q (q_1^4+q_2^4+q_3^4)q^{-2} \times \exp\left(\frac{-\pi^2q^2}{\epsilon^2}\right), \quad (24)$$

$$R_4 = (\epsilon^9/12)\sum' n_r (r_1^4+r_2^4+r_3^4) g_4(\epsilon r), \quad (25)$$

$$R_3 = -(\epsilon^7/2)\sum' n_r r^2 g_3(\epsilon r), \quad (26)$$

$$R_2 = (3\epsilon^5/4)\sum' n_r g_2(\epsilon r), \quad (27)$$

$$R_0 = -6\epsilon^5/5\pi^{\frac{1}{2}}, \quad (28)$$

$$Q_4' = -2Q_4, \quad (29)$$

$$Q_4'' = 4\pi^3N\sum' f n_q q^2 \exp(-\pi^2q^2/\epsilon^2) - 3Q_4, \quad (30)$$

$$R_4' = -2R_4, \quad (31)$$

$$R_4'' = (\epsilon^9/4)\sum' n_r r^4 g_4(\epsilon r) - 3R_4. \quad (32)$$

From these, by comparison with (18), we get

$$R_c = (4/7)(Q_4+R_4+R_3+R_2+R_0) = -(4/35)(Q_4'+Q_4''+R_4'+R_4''). \quad (33)$$

Table III gives results for R_c, those newly computed being correct to five decimal places.

TABLE III.

Array	Akulov	R_c	McKeehan R_c
(*S*)	$A_0' = +18.65$	1.7757	1.77613
	$A' = -46.635$	1.7766	
(*I*)	$A_0'' = -37.295$	−1.7760	−1.77562
	$A'' = +93.24$	−1.7760	
(*F*)			−4.11336

HEXAGONAL ARRAYS

In hexagonal arrays Eq. (8) reduces to

$$S_4 = R_hP_4(\cos\{\mathbf{p}, \mathbf{a}_3\}) \quad (34)$$

or

$$S_4 = (R_h/8)(35p_3^4-30p_3^2+3). \quad (35)$$

Making the same substitutions as in our previous paper on hexagonal arrays[12] we find

$$R_h = Q_{4h}+R_{4h}+R_{3h}+R_{2h}+R_{0h} = Q_{4h}'+R_{4h}'+R_{3h}' = Q_{4h}''+R_{4h}'', \quad (36)$$

in which

$$Q_{4h} = \frac{64\pi^3N3^{\frac{1}{2}}}{81c}\sum' f n_q q_{12}^4 q^{-2}\exp\left(\frac{-\pi^2q^2}{\epsilon^2}\right); \quad (37)$$

$$R_{4h} = (3\epsilon^9/32)\sum' n_r r_{12}^4 g_4(\epsilon r); \quad (38)$$

$$R_{3h} = -(\epsilon^7/3)\sum' n_r r_{12}^2 g_3(\epsilon r); \quad (39)$$

$$R_{2h} = (\epsilon^5/3)\sum' n_r g_2(\epsilon r); \quad (40)$$

$$R_{0h} = -8\epsilon^5/15\pi^{\frac{1}{2}}; \quad (41)$$

$$Q_{4h}' = \frac{128\pi^3N3^{\frac{1}{2}}}{27c^3}\sum' f n_q q_{12}^2 q_3^2 q^{-2} \times \exp\left(\frac{-\pi^2q^2}{\epsilon^2}\right) - 2Q_{4h}; \quad (42)$$

$$R_{4h}' = \frac{3\epsilon^9c^2}{4}\sum' n_r r_{12}^2 r_3^2 g_4(\epsilon r) - 2R_{4h}; \quad (43)$$

$$R_{3h}' = -\frac{2\epsilon^7c^2}{3}\sum' n_r r_3^2 - R_{3h}; \quad (44)$$

$$Q_{4h}'' = \frac{32\pi^3N3^{\frac{1}{2}}}{27c^5}\sum' f n_q q_3^4 q^{-2} \times \exp(-\pi^2q^2/\epsilon^2) - Q_{4h}' - Q_{4h}; \quad (45)$$

[12] L. W. McKeehan, Phys. Rev. **43**, 1025 (1933).

$$R_{4h}'' = (\epsilon^9 c^4/4)\sum' n_r r_3^4 g_4(\epsilon r) - R_{4h}' - R_{4h}. \quad (46)$$

From these equations we obtain for the simple hexagonal lattice with axial ratio $c = \frac{2}{3}6^{\frac{1}{2}}$, $R_h = 2.54563$, and for hexagonal close-packing with the same axial ratio $R_h = 0.90174$. Each of these results has been computed in several ways. No previous numerical results are available for comparison. Peddie[6] gives formulae for his method of computation, but since he uses orthorhombic axes the extremely simple form of Eq. (34) does not appear in his equations, and neither he nor Forrest attempts to evaluate any of their numerous coefficients.

Variation of the Magnetic Properties of Barium with Temperature

C. T. LANE, *Sloane Physics Laboratory, Yale University*

(Received May 16, 1933)

A discontinuity in the resistivity-temperature curve for pure barium at about 370°C has led to the suggestion that two modifications of the crystal structure (α and β-barium) exist, below and above this temperature respectively. Further, the similarity of the curve to that for the ferromagnetics makes it reasonable to suppose that a discontinuity in the susceptibility-temperature curve (i.e., a Curie point) may exist. The susceptibility has been measured over a range of 400°C and such a discontinuity is found to exist at about 350°C. The experimental results are completely at variance with the current theory for paramagnetics.

INTRODUCTION

IN a recent paper, Rinck[1] reports the variation of the electrical resistivity of pure barium as a function of the temperature, and finds a sharp discontinuity in the slope of this curve at about 370°C. On the basis of this measurement he supposes two types of structure, α and β-barium, to exist, below and above this temperature, respectively. The resistance-temperature curve bears a strong resemblance to that for the ferromagnetics and it would therefore appear possible that a discontinuity in the magnetization-temperature curve should occur, similar to that occurring at the Curie point in the ferromagnetics. As no previous measurements for the susceptibility of barium above room temperature exist, this possibility has here been investigated.

PREPARATION OF THE METAL

The barium metal was obtained from Messrs. Eimer and Amend, New York, and designated by them as "C.P." For the purposes of measurement the specimens had to be in the form of small cylinders about 2 cm long and 0.3 cm in diameter. Because of the fact that barium oxidizes rapidly on exposure to the air, even at room temperature, the specimens had to be protected at all times. For the temperature measurement the specimens were prepared as follows.

The metal was melted into a small quartz tube under high vacuum, during which process the surface of the metal was covered with a hard shell due to chemical reaction with the quartz. The quartz tube was then broken off and the foreign surface matter ground off with a small carborundum wheel under ligroine. The metal cylinder was then introduced into a second, very thin-walled, quartz tube and evacuated. It was found the metal specimens so produced had a very dull appearance, quite unmetallic looking. It was apparent that the ligroine used to protect the specimens before evacuation had attacked the metallic surface. To remedy this the following artifice was used. Pure argon gas (at *ca.* 1 mm pressure) was introduced into the tube, and the latter made several times longer than the metal cylinder and of such a diameter that the barium specimen could slide inside it. The end of the tube containing the metal was now placed in an electric furnace and held at a temperature of about 500°C for some minutes. It was found that the metal apparently slowly evaporated depositing the surface contamination on the walls of the quartz, in the immediate vicinity of the metal. The barium was now slid to the other end of the tube and the quartz sealed off as near the specimen as possible. This final specimen was silvery in appearance, and provided the temperature was not raised much above 400°C no evidence of further evaporation or chemical change could be detected. At no stage in the process was iron allowed to come in contact with the metal. Earlier attempts at preparation of suitable specimens without all these precautions gave erratic values of susceptibility.

[1] E. Rinck, Comptes Rendus **193**, 1328–1330 (1931).

Method of Measurement

The Weiss translation method with permanent magnet dynamometer in the form described by Foex and Forrer[2] was adopted. Only slight modifications were introduced, notably the use of Balsa wood for the beam and the sensitive mirror system described previously by Montgomery.[3] The apparatus was set up in a constant temperature room and all observations made through a window outside this room. Temperatures were recorded by means of a chromel-alumel thermocouple which was calibrated against a standard platinum, platinum-rhodium couple.

The holder for the specimen for the measurement at room temperature consisted of a quartz tube, very nearly the same size as the metal, sealed at one end and having a small amber plug at the other. The specimen was wetted with ligroine and quickly introduced into the holder, the thin surface film of ligroine protected the metal from oxidation and was so thin that its magnetic properties were negligible. The susceptibility was measured in terms of distilled water ($\chi=-0.72\times10^{-6}$) and gold ($\chi=-0.145\times10^{-6}$) the values agreeing within one percent. Corrections for the susceptibility of the air were applied, the product of mass susceptibility and density being taken as $+0.029\times10^{-6}$. In the temperature measurement no correction was necessary for the quartz container as the susceptibility of quartz is independent of temperature.[2] Finally the susceptibility was measured at various field strengths over a range of about five kilogauss as a test on the presence of any ferromagnetic impurity.

Results

In Table I are given the results for the susceptibility of barium at various temperatures and these values are plotted in Fig. 1. It will be seen that a very definite discontinuity in the temperature-magnetization curve occurs at about 350°C which, allowing for specimen differences, agrees well with Rinck's estimate. Beyond this point the susceptibility is somewhat smaller as was predicted. Each point on the curve is the mean of at least three and usually of more than three determinations. The values were found to be perfectly reproducible, that is to say it was found to be immaterial whether one started at 20°C and went up or started at 400°C and came down. The possibility of chemical change was thus excluded.

Table I. *Variation of susceptibility with temperature.*

Temperature	Mass suscept.	Temperature	Mass suscept.
20°C	$+0.147\times10^{-6}$	312°C	$+0.332\times10^{-6}$
76	0.162	326	0.345
110	0.172	336	0.356
145	0.188	343	0.358
185	0.212	350	0.359
224	0.234	360	0.372
246	0.258	372	0.383
270	0.280	384	0.396
288	0.298	393	0.406
300	0.316	400	0.415

It is pertinent to inquire whether the effect might not be due to a ferromagnetic impurity having its Curie point in the vicinity of 350°C.[4] That this is not the case may be seen from Table II. In the fourth column, under the heading "mass susceptibility estimated," are given the calculated values of the susceptibility on the assumption that the change in the vicinity of 350°C is entirely due to ferromagnetic impurity.

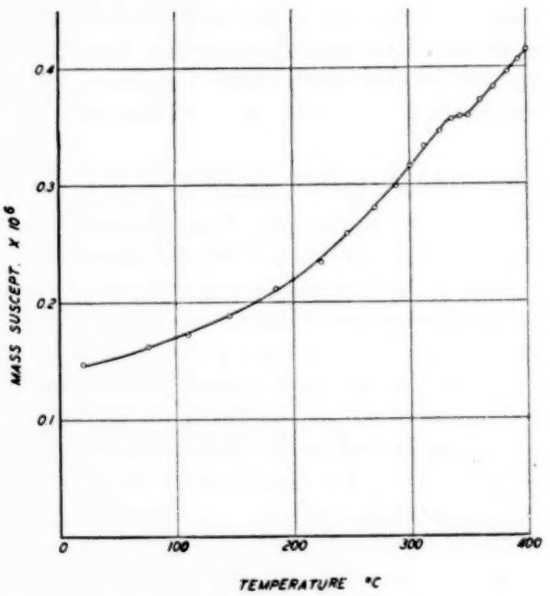

Fig. 1. Mass susceptibility of barium as a function of temperature.

[2] G. Foex, R. Forrer, J. de Physique [6] **7**, 180–187 (1926).

[3] C. G. Montgomery, Phys. Rev. [2] **36**, 498–505 (1930).

[4] The Curie point of pure nickel is about 359°C.

TABLE II. *Variation of susceptibility with field (H) at 20°C.*

Magnet current (amp.)	H	Mass susceptibility observed	Mass susceptibility estimated
2.5	3300	$+0.153\times10^{-6}$	0.171
3.0	3960	0.152	
3.5	4570	0.150	
4.0	5080	0.146	
5.0	5840	0.145	
6.0	6300	0.148	
7.0	6700	0.146	
8.0	7000	0.147	
9.0	7300	0.147	0.147
14.0	8150	0.150	0.145

By extrapolating the part of the temperature curve below about 335°C it is evident that the change in susceptibility amounts to at least $\Delta\chi=0.02\times10^{-6}$ and is probably more. Knowing the field strength at which the temperature measurements are made (7300 gauss) we may thus calculate σ in the Honda relation $\chi_{obs.}=\chi_{\infty}+\sigma/H$ and hence estimate the susceptibility at various field strengths.

By extrapolating the observed values to infinite field we find $\chi=+0.145\times10^{-6}$, or in other words the actual value of σ is 29.5, while the value which would be necessary to cause the effect observed, if due to ferromagnetic impurity, is 146, say five times as great. Hence even in the unlikely event that all the ferromagnetic impurities present have Curie points in the vicinity of 350°C, their amount is in nowise sufficient to cause the observed change.

These measurements were all carried out on two specimens with good agreement. The accuracy of the determination of the susceptibility at room temperature is about one percent, that of the relative temperature measurements being slightly better.

The present theory of paramagnetism is quite unable to account for the results observed here, namely an increase in the paramagnetic susceptibility with increasing temperature. If we choose to regard the phenomenon as due to a decrease of a diamagnetic component, the behavior is still anomalous since diamagnetism is a property which should be, theoretically, independent of temperature. Until allowance for the effect exchange phenomena have on magnetic properties is made we can hardly hope for a satsfactory explanation of the known magnetic properties of metals.

Finally it gives me great pleasure to thank Professor L. W. McKeehan, who suggested the problem, for his interest and advice throughout its progress. I am also greatly indebted to the Royal Commission for the Exhibition of 1851 (London, England) for a fellowship which made this work possible.

On Irregularities in Magnetization

K. J. SIXTUS, *General Electric Company, Schenectady, N. Y.*

(Received March 25, 1933)

Line patterns of iron oxide deposited from a suspension, similar to those observed by F. Bitter on large crystals of iron and nickel, have been studied on cold-drawn, polycrystalline nickel-iron wires under uniform applied stress and in a magnetic field. The patterns consisted of parallel lines but they differed from the highly regular patterns published by Bitter, in that the spacing between adjacent lines varied considerably and in that they appeared very consistently in the same places even after changes in magnitude and direction of the applied field. The spacing of the lines lay within the range 0.7 to 10×10^{-3} cm. Both experiments on a wire under tension and the agreement of results on a twisted wire with conclusions from R. Becker's theory prove that the lines form perpendicular to the direction of induction in the material. No further evidence regarding the origin of the pattern could be found.

1. *Previous Evidence*

The first account of a new kind of irregularity found in the magnetization of ferromagnetics was given by F. Bitter.[1] When a suspension of red magnetic iron oxide in ethyl acetate was spread on the surface of crystals of nickel, iron, silicon-iron and cobalt, the particles arranged themselves under certain conditions in rather regular patterns. Bitter has obtained two different kinds of line patterns, for which Figs. 1 and 2 in his first publication are representative. The pattern found on an iron-silicon alloy in a large field (Fig. 1 in Bitter's paper) consisted of short sections of lines which were nearly straight, were in general parallel to each other with varying distances, and were perpendicular to the field. The second kind of pattern was obtained on the same sample in smaller fields (Bitter's Fig. 2) and showed a system of strictly parallel lines with equal spacings, the lines forming angles of less than 90° with the field direction. There is evidence that the second kind of pattern is determined by the crystal lattice because the lines were found to have three possible directions in iron, four in nickel and only one in cobalt. This fact suggested that they were somehow related to the directions of easy magnetization and therefore to the direction of magnetization itself. In the first kind of pattern which appeared at high fields, the lines formed perpendicular to the field direction and here again it is possible to assume that the magnetization determines their direction.

The present investigation of the line patterns was started under the following consideration. The magnetic symmetry present in single crystals can be approximated in polycrystalline material by the application of stress. Thus in a nickel-iron wire of low nickel content, e.g., 15 percent, tension causes the elementary magnetic vectors to line up parallel to the axis in the absence of an external field, thus establishing the wire axis as direction of easy magnetization. This magnetic symmetry is similar to that of a cobalt crystal along its (0001) axis. In addition, one has the advantage over single crystals that the direction of easy magnetization can be varied at will by changing the amount of tension and torsion applied to the wire.

2. *Experimental Procedure*

In the first experiments a wire (0.038 cm in diameter) of 15 percent Ni, 85 percent Fe content was tested with a suspension of Fe_2O_3 in

[1] F. Bitter, Phys. Rev. **38**, 1903 (1931) and **41**, 507 (1932). After the preparation of this paper, three articles on the same subject have appeared. N. Akulov and M. Degtiar [Ann. d. Physik **15**, 750 (1932)] and R. Becker and H. F. W. Freundlich [Zeits. f. Physik **80**, 292 (1933)] have observed the lines on large crystals. The photographs in both publications allow, in accord with our results, the interpretation that the lines form perpendicular to the magnetization and the latter one shows also the reproducibility of the pattern after a field change. F. Zwicky [Phys. Rev. **43**, 270 (1933)] attempts to interpret Bitter's observations. His theory in its present form, however, seems to be too general to apply to our results.

ethyl acetate as recommended by Bitter.[2] The oxide powder used almost exclusively was prepared by slight heating in air of the black oxide (Fe_3O_4) which is ordinarily used as polishing powder. An electromagnet supplied the magnetic field. The wire was inserted through holes in the pole pieces except in the few cases where it made large angles with the field direction. When the wire was put under a tension of 85 kg/mm^2, its hysteresis loop was very nearly a rectangle with a coercive force of 5.8 oersteds and a remanence which was within a few percent of the saturation value. The wire was brought into the remanence state, the oxide suspension was applied and the surface was watched through a microscope with a $100\times$ magnification. Before every new test the oxide had to be wiped off and another drop of the suspension applied.

3. *Effect of the Applied Field*

No regular pattern could be obtained without field. Only after the field had been increased to 50 oersteds was one able to discern short lines formed by the oxide which were of irregular width, were very nearly parallel to each other, and lay at right angles to the wire axis. At 90 oersteds a distinct pattern appeared and this happened also at 250 oersteds where the smallest distance observed between lines was 1.5×10^{-3} cm, but where also heavy lines formed with greater spacing. A photograph of a section of the wire surface with rather wide lines is shown in Fig. 1. In this and the following figure the lines do not show up as distinctly as they appeared in visual inspection through the microscope. This is because of the inherent difficulty of obtaining a satisfactory photographic reproduction of a round surface. At 1200 oersteds the powder showed a tendency to coagulate but in some places one could distinguish very fine lines of about 0.7×10^{-3} cm spacing and approximately 5×10^{-3} cm long. In many cases the lines had a length of about 0.020 cm and thus crossed a large number of the thread-like crystals of which the wire consisted and which were less than 0.001 cm in diameter. The pattern resembles the one identified above as the first type more than the second one in that its lines, being very nearly parallel, have irregular spacings. The resemblance, however, does not extend to the behavior of the lines. Whereas Bitter's lines of the first type formed perpendicular to the applied field, it will be shown later that this was not necessarily the case with the present patterns.

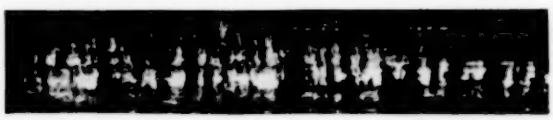

FIG. 1. Powder lines (black) on a cold drawn nickel-iron wire under a tension of 85 kg/mm in a field of 280 oersteds. (40×.)

Two points in these results are particularly striking: the first one is that the pattern can be seen even when the material is practically saturated, and that it is only the tendency of the strongly magnetized powder to form clusters which makes the recognition of the lines increasingly difficult in large fields. If the lines are caused by local changes in direction of the induction vector, either through a small angle—which seems extremely unlikely because of their regularity—or through 180°, as one might conclude from a nuclear concept of ferromagnetic behavior such as Bloch's—they should disappear at complete saturation. A more detailed study of the patterns as complete saturation is approached might solve this problem and might, at the same time, reveal important facts about their origin.

The second surprising result is that, whereas the lines were observed in an applied field, they did not appear in zero field although the difference in induction was extremely small, that is, about one percent. This can be explained by the fact that the powder must itself be magnetized in order to reveal the inhomogeneities in the magnetization of the underlying surface. The surface density of pole strength alone is too small in the present case to magnetize the powder sufficiently, and the attractive force of the surface poles for the small induced poles on the powder particles is overcome by convection currents in the evaporating liquid and by friction against the metal. The high demagnetizing factor associated with the spherical shape of the particles reduces any remanent magnetization to too minute a value to produce the necessary

[2] I am indebted to Dr. F. Bitter for sending me samples of iron oxide.

magnetic attraction. Bitter has observed patterns on single crystals without an applied field.[3] We must assume that in his case the surface poles were strong enough to magnetize the powder appreciably.

4. *Direction of the Lines*

Next, the effect of the direction of the magnetizing field on the orientation of the pattern was studied. The wire, under tension, was placed between the magnet poles at an angle of 65° with the field. Here again lines formed perpendicular to the axis in fields greater than 50 oersteds. In a field of about 1000 oersteds, however, the powder was attracted strongly to the wire sides facing the pole pieces and only occasionally could a pattern be found under these conditions. These observations obtain significance in connection with the following tests: In fields of the order of a few hundred oersteds at any angle to the wire axis, the direction of magnetization for minimum energy is still very nearly axial. This was tested in a special experiment where the wire, magnetized longitudinally, was subjected to a transverse field. No ballistic voltage was induced in a search coil around the wire upon the application of transverse fields up to 1000 oersteds. A small rotation of the induction vector, however, must have occurred, resulting in the development of poles on the sides of the wire facing the pole pieces, rendered visible by the collection of powder. Since the powder responds already to very weak poles, as judged from the appearance of lines in a nearly saturated wire, this deviation from axiality was probably small, so that it escaped notice in the test referred to above. When the wire made an angle of 90° with the field, no lines could be found. In that case the magnetization of the powder particles had no component in the direction of magnetization in the wire, which is evidently the reason for the failure to obtain the effect.

We conclude from these experiments that the pattern is independent of the direction of the applied field, being fixed rather by the state of magnetization of the material, the lines probably lying at right angles to the magnetization. This view was strengthened by experiments in which

[3] Reference 1, Fig. 10.

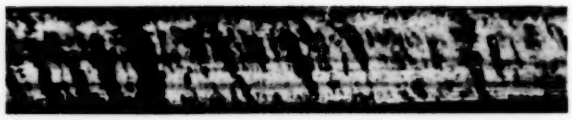

FIG. 2. Powder lines on the same wire as in Fig. 1 with a torsion of 2 turns in a field of 115 oersteds. (40×.)

the wire was twisted. Fig. 2 shows that in this case the lines formed short sections of helices. Their pitch decreased as the applied field was increased. The behavior of the magnetization vector under these conditions falls within the scope of R. Becker's theory[4, 5] which relates the magnetic state of ferromagnetics to their state of strain. This theory will be applied in Section 6 to calculate the direction of magnetization for comparison with the direction of the powder lines.

Under these circumstances it is obvious that the effects reported cannot arise from any factor fixed in the material, such as structural inhomogeneities, strains, inclusions, cracks, fluctuations in the concentration of Ni and fluctuations in grain orientation.

The necessity of a certain degree of uniformity in the direction of induction may be seen from results obtained with a wire without applied stress. Here with applied field parallel to the wire axis the pattern first appeared only between 100 and 200 oersteds, as compared to 50 in the wire under high stress. The induction in the unstressed wire at 200 oersteds was, however, lower than in the stressed wire at 50 oersteds. In the unstressed wire the lower field limit was determined by the uniformity of induction; in the stressed wire by the magnetization of the powder, as pointed out before.

5. *Special Observations*

The problem of reproducibility of the lines was then investigated with a wire under tension. Bitter, working with single crystals, observed that after removal and reapplication of the field the lines had changed their position. We found, however, that quite irrespective of the magnetic history, the lines always tended to form at the same places. Thus, after a reversal of field

[4] R. Becker, Zeits. f. Physik **62**, 253 (1930).

[5] R. Becker and M. Kersten, Zeits. f. Physik **64**, 660 (1930).

direction, a number of adjacent lines, whose position was defined by a scale in the eyepiece of the microscope, were found at the same places. Even a change in stress from 89 to 0 kg/mm² did not affect the positions as the following comparison shows. The positions of three neighboring heavy lines were at

89 kg/mm², 140 oersteds: 57–61, 64–68, 70–74

0 kg/mm², 250 oersteds: 58–60, 65–68, 71–74

where the figures are scale readings with 1 scale div. $=0.74\times10^{-3}$ cm. Even after 2×10^{-3} cm of the surface of the wire had been etched away, the lines were consistently found in the same positions. It is, of course, understood that in all these tests the powder was removed and a new layer applied after the field and tension changes described had been made. On the other hand, the transition from tension to torsion caused shifts, disappearances and new appearances, although in some cases outstanding lines reappeared in nearly the same places.

In case any interaction of the powder particles with each other played an important part in the production of the pattern, we should expect that powders of different permeabilities would show different patterns. Samples of black iron oxide (Fe_3O_4) and of the red oxide had permeabilities—as measured in a glass tube filled with the powder—of 2.1 and 1.2, respectively, these values being nearly constant throughout the range of fields used in the investigation (0 to 800 oersteds). The lines, however, appeared in exactly the same places for both powders, although the black one showed a greater tendency to form clusters on account of its greater permeability.

Other nickel iron alloys have also been tried under tension or torsion. In 20 and 55 percent NiFe, patterns could be obtained with both tension and torsion, although they were rather faint for the latter alloy. No effect could be observed on permalloy, whether it was hard drawn or soft permalloy which had been stretched plastically. In nickel no effect could be found under torsion.

6. *Comparison of the Direction of Magnetization with the Direction of the Powder Lines*

The direction of induction in a wire under stress as a function of applied field can be found by a treatment similar to that used for nickel by Becker and Kersten.[5] We start with the "modified dipole formula"[6] which gives an expression for the energy of a crystal lattice as found from symmetry considerations. The three constants in this equation are evaluated by introducing the magnetostriction λ, which is assumed to be equal in all crystal directions. In addition, the volume change accompanying magnetization is assumed to be zero. Both assumptions, though not experimentally confirmed for the 15 percent NiFe alloy seem to be justified for the following reasons. Sixtus and Tonks[7] have found that tension increases the magnetization parallel to the direction of tension quite independently of the crystal orientation. From this we conclude that the magnetostriction, being the reverse of this elastic effect, is positive in all crystal directions. The fact that the magnetostriction may have different values along the main axes which deviate from the assumed average value does not seriously affect the correctness of the derivation as long as the anisotropy remains small. This has been discussed by R. Becker.[8] The conservation of volume in magnetization appears plausible from observations on other ferromagnetics where this condition has always been found to be very nearly fulfilled.

The formula for U_{dip} is then, except for a change in sign, identical with Becker and Kersten's Eq. (6):

$$U_{dip}=\lambda G\{A_{11}+A_{22}+A_{33}-3(A_{11}\alpha^2+A_{22}\beta^2+A_{33}\gamma^2)-6(A_{12}\alpha\beta+A_{23}\beta\gamma+A_{31}\gamma\alpha)\}. \quad (1)$$

Here G denotes the modulus of rigidity, A_{ik} the strain components, and $\alpha\beta\gamma$ the cosines of the angles between the magnetization vector I and the axes of our system of coordinates.

We choose a plane system with y axis parallel to the wire axis and the x axis tangent to the wire circumference. The strain components for the case of combined tension and torsion, the latter treated as simple shear, are for a point on the

[6] Reference 5, Eq. (4).

[7] K. Sixtus and L. Tonks, Phys. Rev. **42**, 419 (1932).

[8] R. Becker, Wiss. Veröff. a.d. Siemenskonz **11** (2), 1 (1932).

wire surface

$$A_{22}=\sigma/E, \quad A_{11}=A_{33}=-(\rho/E)\sigma,$$
$$A_{12}=s/2, \quad A_{23}=A_{31}=0,$$

where σ is the tension, E denotes Young's modulus, ρ Poisson's ratio and s the shear. By making these substitutions in Eq. (1) and adding the magnetic energy $-HI_s\cos(H, I)=-HI_s\beta$ (I_s is the intensity of magnetization at saturation) we obtain the total energy

$$U=(\lambda\sigma/2)(1-3\beta^2)-3s\lambda G\alpha\beta-HI_s\beta, \quad (2)$$

using the substitution $E=2G(1+\rho)$.

I_s takes that direction in the xy plane which makes U a minimum. This direction, defined by φ, the angle between it and the y axis is found by putting $dU/d\beta=0$ and substituting $\cos\varphi$ for β. The relation between φ and H thus comes out to be

$$H=(3\lambda/I_s)[sG(\cos 2\varphi/\sin\varphi)-\sigma\cos\varphi]. \quad (3)$$

Incidentally, the special case of this equation for $H=0$ is given in Eq. (3) of a paper by L. Tonks and K. Sixtus[9] where it was derived in a different manner.

In Fig. 3 both experimental results and theoretical curves based on Eq. (3) have been plotted for two cases: I for a torsion of 2 turns and no tension, II for a torsion of 2 turns and a tension of 62 kg/mm² as function of the magnetizing field. The experimental points were obtained by adjusting a scale in the eyepiece of the microscope parallel to the powder lines. The angle between them and the circumference of the wire was then indicated by a pointer fastened to the eyepiece. The angle formed by individual lines differed not more than a few degrees from the average plotted in Fig. 3. No points could be determined at low field values where no lines appeared on account of the insufficient magnetization of the powder.

In substituting numerical values in Eq. (3), in order to draw the theoretical lines, I_s is taken to be 1700 c.g.s. and G, computed from E and a value of ρ of 0.3 is equal to 5.95×10^3 kg/mm². The shear s per turn is for the present wire (diameter 0.038 cm, length 40 cm) 3×10^{-3} at the wire surface. We meet, however, with the

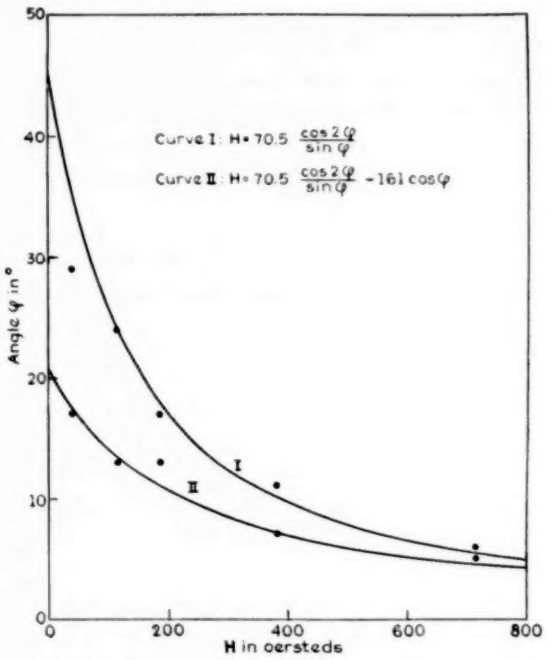

FIG. 3. Angle between powder lines and wire circumference found experimentally (dots) and angle between induction and wire axis derived theoretically (lines) as a function of field strength. I. Torsion $T=2$ turns. II. Torsion $T=2$ turns, tension $\sigma=62$ kg/mm.

difficulty that no reliable values are available for the saturation magnetization of the 15 percent alloy. The *International Critical Tables*, referring to measurements by Honda and Kido, give only the values 12.71 and 13.45×10^{-6} for an 18.5 percent and 9.2 percent NiFe alloy respectively at a field of 550 oersteds. Rather than adopt an uncertain value of λ to calculate the relation between direction of induction and field strength, it seemed better to assume that the powder lines lie perpendicular to the induction and to find what value of λ, if any, would give agreement throughout the range of field strength between φ as derived theoretically and the observed angle between powder lines and wire circumference. Actually the value $\lambda=11.5\times10^{-6}$ was found to be satisfactory, the agreement with the experimental points being shown by the curves of Fig. 3. This value of λ is lower than those for other similar materials under slightly different conditions (unsaturated), but it comes close enough to them to constitute a practical proof for our original assumption by which it was derived. The difference may well arise from the neglect of the

[9] L. Tonks and K. Sixtus, Phys. Rev. **43**, 70 (1933).

inherent longitudinal stress in the surface of the wire.

Since Becker's theory has been proved for reversible processes by several experimental investigations, the present agreement between theoretical and experimental results establishes definitely one property of the powder lines, namely that they lie in a direction perpendicular to the direction of induction. We cannot, of course, draw the same conclusion for Bitter's highly regular patterns, although it seems very likely that the same is true of them. Knowledge about the origin of the patterns and how closely the two types may be related has still to be obtained.

In the light of this result, the deviations from parallelism evident in Fig. 2 and also in Fig. 1 can now be discussed. In some cases they are obviously due to powder accumulating in a line connecting the ends of two "regular" lines, of which one lies nearly in the continuation of the other. In other cases, however, this explanation does not apply and we may assume large scale variations in internal strain, which are accompanied by variations in the direction of induction and accordingly of the powder lines. If this interpretation is correct, a quantitative analysis of the line spreading would yield the direction and amount of internal strains.

In conclusion, the author wants to express his gratitude to Dr. I. Langmuir and Dr. L. Tonks for stimulating discussions on the subject.

LETTERS TO THE EDITOR

Prompt publication of brief reports of important discoveries in physics may be secured by addressing them to this department. Closing dates for this department are, for the first issue of the month, the twentieth of the preceding month; for the second issue, the fifth of the month. The Board of Editors does not hold itself responsible for the opinions expressed by the correspondents.

Cosmic-Ray Nuclear Disintegrations

Cosmic-ray nuclear disintegrations associated with what are usually termed Hoffman's Stösse have been studied in an iron vessel 120 cm high, 90 cm in diameter, with wall thickness about 17 mm. The vessel was provided with similar independent electrodes in the top and bottom halves, and these halves could be separated by a slab of metal of any desired thickness. The purpose was to study the spurts of ionization in the two halves in the absence of the slab, and then observe it again with the slab, and so deduce from the indications in the two halves information as to the number and character of the nuclear disintegrations occurring in slabs of different materials, and the absorbability of the products of disintegration in the materials.

Each insulated system was connected to an independent FP54 Pliotron operating a short period galvanometer. Suitable means for compensation of average ionization current and of fluctuations of applied potential were employed.

In order to provide further evidence as to the reality of the indications, experiments were performed in which a Geiger-Mueller counter system, consisting of three sets of counters placed in different positions around the vessel, was used, and arranged so as to record through the amplifier only if a ray went through each simultaneously. The two galvanometers recording the spurts of ions reflected vertical lines onto the horizontal slit of the photographic recording apparatus, so that the motions of the lines drew curves on the moving paper. When the counters discharged they lighted a lamp which also illuminated the slit, producing on development a shadow whose starting edge indicated the instant at which the counter discharges took place.

Fig. 1 represents records of several of the nuclear disintegrations observed. It will be seen that in most of the examples given simultaneous spurts were observed in the top and bottom halves. The simultaneous discharge of the counters is indicated in three of the examples shown by the lower edge of the shadow *S*. These counter records taken with apparatus entirely dissociated from the ionization apparatus, and produced by effects outside of the vessel, demonstrate conclusively, by their correspondence with the spurts of ionization, the reality of those spurts, and relieve them of any suspicion of being caused by accidental phenomena, vibrations and so forth.

At the lower end of each trace is given the number of millions of ions corresponding to the spurt of ions observed on that curve. If one knew the average distribution of the secondary rays which participated in producing any of the above spurts, and if he should assume a number for the ionization per centimeter of path by the rays, he could calculate the number of rays involved in the spurt. The greatest distance which any ray can travel in one of the halves of the vessel is about 150 cm. The gas in the vessel

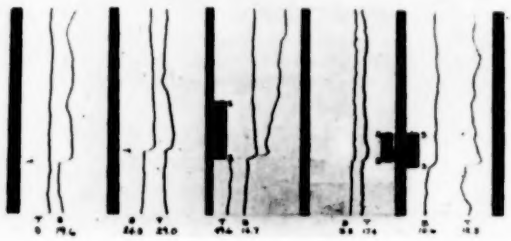

FIG. 1. Values in millions of ions at 100 lb./sq. in. of nitrogen. *T*, top half of chamber; *B*, bottom half of chamber.

was nitrogen at pressures of the order 100 lb. per square inch. Hence, if using the ion spurt corresponding to 49.6×10^6 ions recorded in Fig. 1, we divide by 100/14, the pressure in atmospheres, by 150 cm, the maximum path length, and by 50 ions/cm, which is the order of magnitude of the ions produced per centimeter of path by an electron in nitrogen at atmospheric pressure, we shall obtain the minimum number of rays which can be associated with this nuclear disintegration if these rays are assumed to be of the positive or negative electron type with energies corresponding to those usually associated with cosmic-ray phenomena. The number in question comes out as approximately 1000. It of course varies with the spurt considered. However, for all spurts examined it is large. There of course remains the somewhat unlikely possibility of the ionization being caused by a few particles of very much greater ionization per centimeter of path than that corresponding to electrons. As evidence against this, however we have the counter data.

Each of the 3 counters had an area of about 250 sq. cm.

An examination of the statistics of the problem shows that if in an appreciable fraction of ionic spurts, say 20 percent as observed, the counters also record, then the number of rays is probably not considerably less than what would correspond to an average of one ray through each counter set. Taking into account the average distances involved, we are led to the conclusion that the nuclear disintegrations observed corresponded to at least 100 secondaries, and may of course represent many more. The possibility of there being more secondaries than would correspond to the total number of electrons and protons in the disintegrated atom naturally raises interesting considerations regarding the mechanism of the processes accompanying the disintegration.

W. F. G. SWANN
C. G. MONTGOMERY

Bartol Research Foundation of
The Franklin Institute,
Swarthmore, Pennsylvania,
June 1, 1933.

Scattering of Molecular Rays in Gases

Knauer[1] has recently investigated the scattering of molecular rays in gases. By the aid of high speed pumps the author has found it possible to produce a more intense beam so that scattering might be investigated with higher resolving power.

A beam is formed by three successive slits and the distribution of the scattered molecules or atoms studied by the aid of a Pirani gauge. Two slits placed before the gauge permit molecules to enter it only when they are scattered from a definite position in the beam.

Fig. 1 (curves *A* and *B*) shows the scattering curves which have been obtained for hydrogen molecules and helium atoms. The temperature of the source of the beam and scattering chamber was 20°C. The scattered intensity is expressed in arbitrary units, being simply the galvanometer deflection multiplied by sin θ to correct for the variation in the length of the beam from which scattered molecules may enter the gauge.

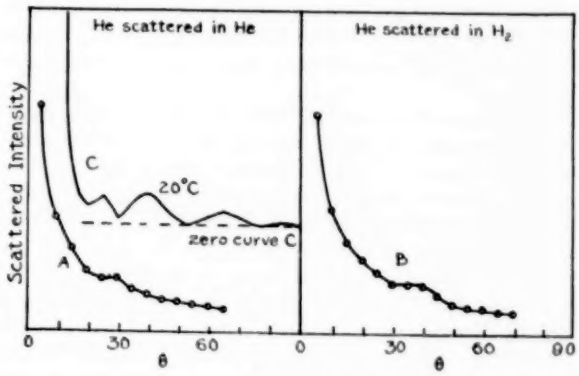

FIG. 1. Curve *A*, He scattered in He; curve *B*, H_2 scattered in H_2; curve *C*, results of Massey and Mohr for He scattered in He.

Massey and Mohr[2] have computed the scattered intensity for helium atoms having a relative kinetic energy corresponding to 20°C and −185°C. The results which they have obtained offer a qualitative explanation of the helium scattering curve. Curve *C* (Fig. 1) is reproduced from their article after being multiplied by sin 2θ and divided by sin θ to obtain the scattering per unit solid angle in a coordinate system in which one atom is initially at rest. One peak occurs at 25° and another at 40°. From a qualitative point of view three effects are immediately obvious which would tend to merge these two peaks into the one observed at 30°. The first is the finite resolving power of the apparatus, second the Maxwellian distribution of velocities in the beam and third the fact that the scattering molecules are not at rest but are moving in random directions with a Maxwellian distribution of velocities.

The intensity of the region of 65° is too small to determine definitely whether a peak exists there.

A complete report will appear in a short time.

R. M. ZABEL*

Massachusetts Institute of Technology,
June 3, 1933.

* National Research Fellow

[1] Knauer, Zeits. f. Physik **80**, 80 (1933).

[2] Massey and Mohr, Nature **130**, 277 (1932).

On the Production of the Positive Electron

The experimental discovery of the positive electron gives us a striking confirmation of Dirac's theory of the electron, and of his most recent attempts to give a consistent interpretation of the formalism of that theory. As is well known, and quite apart from the difficulties connected with the existence and stability of the electron itself, the theory in its original form led to very grave difficulties in all problems involving lengths of the order of the Compton wavelength, in that it predicted the occurrence of electrons of negative kinetic energy, in gross conflict with experience. Dirac has pointed out that we might obtain a consistent theory by assuming that it is only the absence of electrons of negative kinetic energy that has a physical meaning; in this way one could avoid the occurrence of the critical transitions, and yet understand the validity of many correct predictions of the theory, such as the formula for the relativistic fine structure, and the Thomson and Klein-Nishina scattering formulae: only the physical interpretation of the formulism was changed, and involved in many cases the appearance pairs of electrons and "antielectrons"

—particles of electronic mass and of positive charge numerically equal to that of the electron. It was this aspect of the theory which remained dubious; and the discovery of the positive electron appears to settle that doubt.

Perhaps the simplest example of the production of pairs is the case of an externally maintained electrostatic field in which differences of potential greater than 2 mc^2 occur. Here one may see in a particularly clear way that the production of pairs is a typical quantum effect, depending upon the finite wave-length of the electron waves, and disappearing, as the correspondence principle requires, when $h \to 0$. For all macroscopic fields such an effect is negligible; and for the fields within nuclei, where alone the pairs might be expected to be of primary importance, we know that Dirac's theory, together with the whole notion of the electron as a particle, becomes inapplicable. It is for this reason that the anti-electrons could so long escape detection.

In the case of a Coulomb field the theory shows that to detect the pairs we should have to use radiation (electrons or gamma-rays) of energy greater than 2 mc^2 (strictly greater than $mc^2[1+(1+\alpha^2Z^2/(1-\alpha^2Z^2)^{\frac{1}{2}})^{-\frac{1}{2}}]$ where Ze is the charge producing the field). Thus, if we allow gamma-rays of energy γ to fall upon a nucleus, we should expect pairs to appear; the kinetic energy of the pairs would be $\gamma - 2\ mc^2$; and the effect might be interpreted as a photo-electric absorption of the gamma-ray by the pair; in the process the nucleus necessarily takes up a small recoil momentum. The recent experiments of Anderson and Neddermeyer with filtered gamma-rays of Th C″ show that in fact pairs are produced when the radiation passes through lead; and this very strongly supports the tentative suggestion made by Blackett and Occhialini that that part of the absorption of these rays in lead which cannot be accounted for by the scattering and photo-effect of the atomic electrons is to be ascribed to the creation of pairs near the nucleus. This hypothesis, even without calculation, finds much support in the evidence, for the number of pairs observed by Anderson and Neddermeyer is of the right order to account for the excess absorption of the gamma-rays. Further Gray and Tarrant[1] have found that a part, but not all, of the excess energy absorbed is re-radiated; the reradiated gamma-rays consist, wholly for the light elements, and for the greater part in lead, of quanta of energy 5×10^5 volts. This is what we should expect from the pairs, which should lose practically all of their kinetic energy in passing through matter, and in which the anti-electron near the end of its range should combine with an electron with the radiation of two quanta of about a half-million volts.

We have applied the theory to this simple model, in which gamma-rays of high energy may be absorbed by the production of pairs in the Coulomb field of nuclei. When the energy of the gamma-rays is only a little greater than the threshold energy, and the kinetic energy of the pair is small, so that relativistic effects for electron and positive may reasonably be neglected, the calculations can easily be made strictly. The important term in the effective absorption cross section per nucleus (of charge Z) for gamma-rays of energy γ is

$$\sigma = (\pi/3\ (2)^{\frac{1}{2}})\alpha^4Z^2(e^4/m^2c^4)g^{\frac{3}{2}}e^{-2\pi\alpha Z(2g)^{-\frac{1}{2}}}; \quad \text{with}$$

$$g = \gamma/mc^2 - 2. \quad (1)$$

The positives tend to take most of the available kinetic energy, and the distribution in the direction of ejection of the particles about the direction of the incident gamma-rays is given by the cosine-square law.

For higher energies of the gamma-rays, we have made an approximate calculation, in which we have found the wave functions for the pair to the first order only in the perturbing field of the nucleus. For $\gamma \to \infty$ we find asymptotically

$$\sigma = (\pi^2/6 - 2/3)\alpha Z^2e^4/m^2c^4. \quad (2)$$

Here the relative probability of a distribution of energy between positive (ϵ_+) and electron (ϵ_-) is given by

$$\epsilon_+^2 + \epsilon_-^2 \qquad (\epsilon_+ \gg mc^2; \quad \epsilon_- \gg mc^2). \quad (3)$$

Both particles tend to come off within a small angle of the original beam. The probability of ejection falls off rapidly for angles $\gg mc^2/\epsilon_+$, mc^2/ϵ_- for the two particles.

From (2) we see that the excess absorption of hard radiation should be proportional to Z^2, in good agreement with the experiments with Th C″ gamma-rays. Further, even the asymptotic formula (2) gives reasonable values for the absolute magnitude of the excess absorption. Numerical calculation for the case of Th C″, $\gamma \leqq 2.6\times10^6$ v (with the use of the same approximate wave functions), gives an excess absorption of about 25 percent of the Klein-Nishina absorption of these rays in lead, and 15 percent in tin, in excellent agreement with experiment. We see too from a comparison of (1) and (2) that the absorption due to the production of pairs rises very rapidly as the energy of the gamma-rays is increased; at half the energy of the Th C″ rays the absorption is only one five-hundredth as great. The small effect for gamma-rays near the threshold arises in part from the small number of states available, and in part from the repulsion of the low energy positive by the nuclear field. In this way we can understand that the excess absorption and the reradiated gamma-rays were not observed with incident gamma-rays of energy much lower than 2×10^6 volts. Thus the theory gives a reasonable account of the dependence of the excess absorption on the gamma-ray energy and on the atomic number and of the absolute magnitude of the absorption. The origin of the radiation of $\sim 10^6$ volts which Gray and Tarrant found re-radiated from heavy element is not altogether clear. It is possible that this arises by the annihilation of a positive in a process in which only one quantum is radiated, and an electron or nucleus takes up a small recoil momentum. The relative importance of such processes would increase with the atomic number, as is observed.

According to the theory the gamma-rays from a radioactive nucleus should occasionally be "internally converted" by the production of a pair near the nucleus. The internal conversion coefficient is of the order α^3Z^2, and is

[1] Gray and Tarrant, Proc. Roy. Soc. **A136**, 662 (1932).

about 2×10^{-4} for the quadripole gamma-ray of Th C'', $\gamma \leqq 2.6\times10^{6}$ volts.

The application of (2) to the absorption of cosmic rays is in some respects illuminating. For as the energy of the gamma-ray is increased, the absorption by the production of pairs becomes relatively more important than the absorption by Compton effect. This would account for Anderson's observation that among high energy particles the numbers of positives and negatives are roughly equal; and it would increase the energy of the gamma-rays as estimated from their absorption coefficients. Further (2) gives a limiting penetration, which is of the same order for water as that observed for the hardest cosmic rays. Nevertheless (3) is here in definite disagreement with experiment, in that a penetration in water twice as great as that predicted by (2) has been observed by Regener, and further in that (2) predicts serious deviations from the mass absorption law which are certainly not found experimentally. It appears that deviations from the Coulomb law for the nuclear fields could not sensibly affect our result; and one is tempted to see in this discrepancy a failure of the theory when applied to radiation whose wave-length is of the order of the critical distance e^2/mc^2 which marks the limit of applicability of classical electron theory. But we must emphasize that (2) was derived by the use of approximations which may be unsound; just in the range of high energies and large atomic numbers their validity appears doubtful; and we believe that no conclusions may justly be drawn until this purely analytical point is settled. Even for light elements the use of (2) for γ greater than 10^8 volts appears to us questionable.

On the present simple theory there is no place for the simultaneous production of large numbers of pairs. The fast electrons and positives, however, will themselves tend to produce further pairs; and although this point too wants much closer investigation, it is possible that one may so be able to account for the multiple tracks observed.

We want to express our profound thanks to Professor Bohr, who has helped us to understand the essential consistency of the theory which we have here applied.

J. R. OPPENHEIMER
M. S. PLESSET*

California Institute of Technology,
Pasadena, California,
June 9, 1933

* National Research Fellow

The Emission of Alpha-Particles from Various Targets Bombarded by Deutons of High Speed

Using a sample of hydrogen containing 50 percent of the heavy isotope, H^2, in our apparatus for the multiple acceleration of ions we have given to the ions H^1H^{2+} energies of 2,000,000 volts. These ions striking any target immediately yield 660,000 volt-protons and 1,330,000 volt H^2 nuclei which we call deutons. We have directed these particles against various targets.

It was of particular interest to study elements of the nuclear type $4n+2$ in order to ascertain whether these would yield nuclei of type $4n$ and α-particles. As a matter of fact the two targets which were most striking because of the range and number of emitted α-particles were NH_4NO_3 and LiF, which contained the nuclei N^{14} and Li^6. Experience with other targets containing O, H and F shows that most of the effects observed were due to N and Li. N yielded about 100 α-particles per 10^9 deutons all apparently homogeneous with a range of 6.8 cm. The minimum deuton energy at which we observed this disintegration was 600,000 volts. The energy of the α-particles obtained in this disintegration is only about one-half of that which should be set free in the process $N^{14}+H^2\rightarrow C^{12}+He^4$.

With Li a large number of α-particles of range 8.2 cm were obtained which are very likely due to the accompanying protons. In addition there are about one-tenth as many with the great range of 14.5 cm corresponding to an energy of 12,500,000 volts. No other known natural or artificial disintegration has yielded particles of so great energy. If we assume the process $Li^6+H^2\rightarrow 2He^4$ and take for He the mass 4.0022 and for H^2 and Li^6 the most recent values of Bainbridge, which he has kindly communicated to us, the values 2.0136 and 6.0145, respectively, and take account of the kinetic energy of the deuton (1,300,000 volts), we find 23,400,000 volts as the total energy set free. If this energy is equally divided between the two α-particles, each would have 11,700,000 volts, whereas, from the observed range we find 12,500,000 volts. This calculation of the energy from the range is a wide extrapolation, with the use of the 3/2 power voltage range relation, and the agreement between the observed and calculated values is well within the limits of uncertainty because of this and other causes. An alternative, but less likely hypothesis, that the process involves Li^7 with the emission of a neutron, happens to agree equally well with the observations if the mass of the neutron has the low value (about unity) that we discuss later.

With the Be target α-particles were obtained of the same range (3.3 cm) as those obtained in this laboratory in similar experiments with high speed protons. But the number of disintegrations per deuton was at least 100 times as great as the number per proton. The identity of the two ranges strongly suggests that the bombarding particle merely causes the disintegration of the unstable Be nucleus; in other words, that we have disintegration without capture. This is a process which has already been suggested by Bainbridge[1] for the disintegration of Be by α-particles. If we take Bainbridge's value for the mass of Be, 9.0155, our value for the kinetic energy of the α-particles and Chadwick's[2] for the kinetic energy of the neutron, the mass of the neutron would come out as a little less than unity, which tends to confirm the estimate of the mass of the neutron (following communication) which we have obtained from quite different experiments.

Of the remaining targets studied, Al and Mg gave a small

[1] Bainbridge, Phys. Rev. **43**, 367 (1933).
[2] Chadwick, Proc. Roy. Soc. **A136**, 692 (1932).

number of α-particles of about 6 cm range when the deuton had an energy of at least 1,200,000 volts. B_2O_3 also yielded α-particles which may however have been produced by the protons rather than the deutons. CaF_2 and NaCl gave a small number of particles of 3.8 and 2.8 cm range, respectively, but these also require further investigation. The remaining targets SiO_2, $NaPO_3$, C, CuS, $Ca(ClO_3)_2$, Au, Pt, brass and mica gave no detectable α-particles.

We are indebted to Dr. M. C. Henderson, who constructed the linear amplifier used in these experiments and who has kindly helped us in many other ways. We are also indebted to the Research Corporation and the Chemical Foundation for their support.

GILBERT N. LEWIS
M. STANLEY LIVINGSTON
ERNEST O. LAWRENCE
Radiation Laboratory, Department of Physics,
Department of Chemistry,
University of California,
June 10, 1933.

The Emission of Protons from Various Targets Bombarded by Deutons of High Speed

Deutons (nuclei of H^2) with energies ranging from 600,000 to 1,330,000 volts have been directed against the following targets: carbon, gold, platinum, lithium fluoride, silicon dioxide, sodium phosphate, calcium chlorate, copper sulphide and brass (the backing of the other targets). In addition to the emission of alpha-particles, which we have already reported in the preceding communication, we have observed the emission of protons in large numbers, with various ranges up to more than forty centimeters.

Every target, including gold and platinum which could hardly be expected to suffer nuclear disintegration, yielded protons of about 18 cm range in air. We have been unable to account for this group of protons common to all targets except on the hypothesis that the deuton itself is breaking up, presumably into a proton and a neutron. This assumption implies a lower value for the mass of the neutron than that of Chadwick[1] whose value, however, rests on the assumption that in the disintegration of B^{11} by α-particles, to form N^{14} and a neutron, there is no γ-radiation.

To examine this hypothesis of the instability of the deuton we have observed the relation between the range of the emitted protons and the energy of the bombarding deutons. In the case of gold we observed that when the deuton energy was increased from 1,000,000 to 1,330,000 volts the maximum range of the protons increased approximately from 16.7 cm to 17.9 cm, corresponding to an increased energy of 160,000 volts. This is in accord with the assumption that the proton and neutron fly apart with equal kinetic energies. Realizing that all of these assumptions may be modified by later work, we may nevertheless make a tentative calculation of the mass of the neutron. From the masses of H^1 and H^2 and from the measured energies of the deuton and the emitted proton, the mass of the neutron appears very close to unity. In the case of carbon the change in the energy of the proton was found to be approximately equal to the change in the energy of the deuton which suggests, if our hypothesis is at all correct, that in addition to the dissociation of the deuton there is a change in the carbon nucleus itself.

Aside from this group of protons common to all targets we have observed large numbers of protons from silica and sodium phosphate with ranges in the neighborhood of 12 cm and which were not obtained with the other targets. The investigations have not yet been carried below this range. On the other hand, sodium phosphate and lithium fluoride yielded protons of very high energy. In the former case two long range groups were observed, one of 26 cm and one of 35 cm. Lithium fluoride was not so carefully investigated but protons with ranges as great as 40 cm were observed.

A study of the relation between the number of emitted protons and the energy of the deuton shows that in all cases the emission of protons becomes unobservable when the deuton energy falls below 800,000, and at least in the case of the group common to all targets, there seems to be a very sharp threshold.

We are again indebted to Dr. M. C. Henderson who constructed the linear amplifier used in these experiments and who has kindly helped us in many other ways. We are also indebted to the Research Corporation and the Chemical Foundation for their support.

ERNEST O. LAWRENCE
M. STANLEY LIVINGSTON
GILBERT N. LEWIS
Radiation Laboratory, Department of Physics,
Department of Chemistry,
University of California,
June 10, 1933.

[1] Chadwick, Proc. Roy. Soc. **A136**, 692 (1932).

The Masses of the Lithium Isotopes

The mass of Li^6 referred to O^{16} was measured as 6.0145 $\pm$0.0003 from five spectra by comparison with H_3^2 by the "doublet" method. The mass of Li^7 was measured from the same spectra as 7.0146$\pm$0.0006. The lithium ions were obtained from a heated spiral of flat tungsten strip coated with spodumene. Simultaneously a discharge was run in hydrogen containing a high concentration of the heavy isotope. The hydrogen had been put at the disposal of the writer through the kindness of Professor G. N. Lewis.

Fig. 1 illustrates two $Li^{6+}-H_3^{2+}$ doublets.[1] The upper spectrum is one of the five used in the mass determinations. The mass of H^2 had previously been accurately determined

in reference to that of helium.[2] The mass of Li^{7+} was measured in reference to that of H_3^{2+} by a less direct and less accurate method than was possible in the case of Li^6. If the mass-scale were strictly linear the mass of Li^7 could be obtained by direct extrapolation. Because of the di-

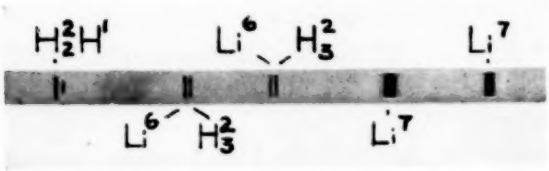

FIG. 1. Mass-spectra of Li^6 and Li^7.

vergence of the mass-scale from absolute linearity it is necessary to apply a small negative correction to the mass secured on the basis of a linear mass-scale. This correction is easily found and was known from the dispersion data secured from earlier plates. The probable error introduced by this corrected extrapolation may conservatively be taken as ± 0.0003 mass units and it has been included in the probable error given in the first paragraph.

The mass ratio of the isotopes of lithium secured in this investigation does not agree with the value from the band spectrum analysis[3] but it is in good accord with the ratio from Costa's earlier mass-spectrograph measurements.[4]

The author is indebted to Dr. W. F. G. Swann for his interest and helpful discussions. The writer wishes to express his appreciation of the generous gift by Professor G. N. Lewis of the fractionated hydrogen used in this work.

KENNETH T. BAINBRIDGE

Bartol Research Foundation of
The Franklin Institute,
Swarthmore, Pennsylvania,
June 14, 1933.

[1] These particular spectra cannot be used for the determination of the relative abundance of the lithium isotopes owing to the conditions of voltage existent while the spectra were taken. The fiducial line appears next to $H_2^2H^1$.

[2] K. T. Bainbridge, Phys. Rev. **44**, 57 (1933).

[3] Andrew McKellar, Phys. Rev. **43**, 215 (1933). F. A. Jenkins and Andrew McKellar, Bull. Am. Phys. Soc. **8**, No. 4, 23 (1933).

[4] J. L. Costa, Ann. de Physique **4**, 425 (1925).

Comparison of the Masses of H^2 and Helium

The mass of H^2 has been measured from twelve spectra as 2.01363 ± 0.00004 referred to helium[1] as 4.00216 and 2.01363 ± 0.00008 referred to O^{16} when the probable error in the helium-oxygen ratio is taken into account.

Fig. 1 is a contact print of eight of the spectra used in this comparison of the mass of H^2 with that of helium. The

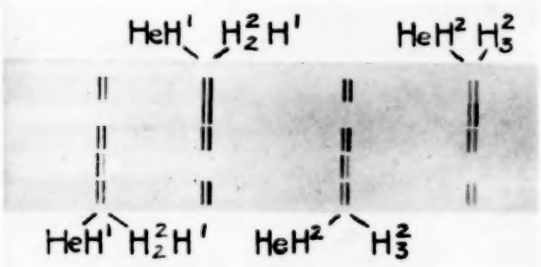

FIG. 1. Mass-spectra for the comparison of the masses of H^2 and He.

individual spectra are indicated, as in some cases two spectra were taken at the same position of the plate. Each spectrum gives two determinations of the mass of H^2 one from the comparison of He H^{1+} with H_2^2 H^{1+} and another from the comparison of He H^{2+} with H_2^{2+}.

The measured positions of the HeH^1 and HeH^2 molecular ions provided the dispersion measurements for these spectra. The mass of H^1 was taken as 1.007775 and the mass of He as 4.00216, as their ratio had been determined from a previous investigation.[2] An error of 1 part in 1000 in the dispersion determination could only introduce an error of 1 part in 200,000 in the determination of the mass of H_2^2 H^{1+} or an error of 1 part in 240,000 in the mass of H_3^{2+}.

This sensitiveness to possible errors in the dispersion constants is an ordinary advantage inherent in the measurement of close doublets. In addition it can be shown that the use of two related doublets, as in the present determination, greatly simplifies the detection and elimination of small systematic errors. Also corrections for nonlinearity of the mass scale appear only in the fifth decimal place if a single mass determination of H^2 is derived from the average of the two values obtained from the "five" doublet and from the "six" doublet. The probable error in the evaluation of the mass of H^2 from twelve spectra was calculated on the basis of twelve average determinations, not twenty-four single values. Moreover it can be shown that the mass of H^2 is evaluated in terms of He alone and the mass determination of H^2 is insensitive to whatever value is selected for H^1 in the range ± 0.1 percent from the figure 1.007775. Similarly, in obtaining the dispersion from the separation of the HeH^1 and HeH^2 lines, the final mass determination of H^2 is not sensitive to the value of H^2 used to obtain the mass of HeH^2.

The writer is greatly indebted to Professor G. N. Lewis who very generously gave the writer some "heavy water" containing $H^2 : H^1$ in the approximate abundance range of 1 : 2 to 2 : 3.

KENNETH T. BAINBRIDGE

Bartol Research Foundation of
The Franklin Institute,
Swarthmore, Pennsylvania,
June 14, 1933.

[1] F. W. Aston, Proc. Roy. Soc. **A115**, 487 (1927).

[2] K. T. Bainbridge, Phys. Rev. **43**, 103 (1933).

A Suggested Dependence of Nuclear Moments on Atomic Number

It is the purpose of this letter to point out *that for nuclei of odd mass number the magnitude of nuclear magnetic and mechanical moments appears to depend somewhat upon whether, Z, the atomic number, is even or odd.* All of the data in Goudsmit's[1] recent paper (entitled *Nuclear Magnetic Moments*) point to such a dependence. In his table[1] there are five nuclei for which Z is even; their magnetic moments vary from $+0.60$ down to -0.67. The fifteen nuclei with Z odd have magnetic moments ranging from $+0.9$ up to $+5.4$, while for eleven of these the values are greater than $+2.0$. Thus for these nuclei there is a definite difference, all the nuclei with Z even having small positive or negative magnetic moments, while nuclei with Z odd have magnetic moments which are all positive, and somewhat larger and more variable in magnitude.

This correlation suggested by Goudsmit's data[1] is supported by our own experimental results.[2] We have studied the neighboring pairs of nuclei Cb^{93} and Mo^{95}, also Ta^{181} and W^{183} which differ by one unit in Z, and by two units in mass number. We have found in each case the member of the pair with Z odd to have a very considerably larger magnetic moment than that with Z even.

For nuclei of odd mass number we have compiled a rather complete table of the experimentally determined I values. This table shows that I also depends on whether Z is even or odd. Nuclei with Z even have small I values, generally $\frac{1}{2}$ or $\frac{3}{2}\cdot h/2\pi$, whereas those with Z odd show much more variation, ranging from $\frac{1}{2}$ to at least $9/2$, with quite a number of nuclei[2] having $I \geq 5/2$.

Since nuclear magnetic moments depend directly upon the value of I, then the smaller I values, found for nuclei with Z even, will in part account for the differences in magnetic moments to which reference has been made above. If, however, we compare the magnetic moments of nuclei having the same I value (virtually comparing nuclear g-factors) we find that nuclei with Z odd definitely have the larger magnetic moments; e.g., for $I=\frac{1}{2}$ the magnetic moments are,[1] for Z odd; Al^{27}, $+2.1$; Tl^{203} and Tl^{205}, $+1.8$; whereas for Z even; Cd^{111} and Cd^{113}, -0.67; Hg^{199}, $+0.55$; and Pb^{207}, $+0.60$.

A more complete discussion of the general field of nuclear moments will be published shortly.

Note: Since this letter was written a very interesting paper by Fermi and Segrè (Zeits. f. Physik **82**, 729 (1933)) on nuclear magnetic moments has appeared. His results are in excellent agreement with those of Goudsmit and they therefore lend considerable additional support to the generalizations suggested in this letter.

NORMAN S. GRACE*

Department of Physics,
University of California,
June 19, 1933.

* Commonwealth Fellow.

[1] Goudsmit, Phys. Rev. **43**, 636 (1933).

[2] Grace and Ballard, and Grace and More, Bull. Am. Phys. Soc. **8**, No. 3, papers 2 and 3; Grace and McMillan, Bull. Am. Phys. Soc. **8**, No. 4, paper 54; Grace and White, Phys. Rev. **43**, 1039 (1933); and unpublished data.

Fine Structure of H^2 Alpha

Through the courtesy of Professor G. N. Lewis we were supplied with an amount of water containing equal parts of the two hydrogen isotopes for purposes of spectroscopic investigation. A large discharge tube of the modified Wood type entirely immersed in liquid air was used. The spectrum was photographed through an etalon interferometer with the first order of a 30 foot grating spectrograph for auxiliary dispersion. The lines $H^1\alpha$ and $H^2\alpha$ were widely separated, each showing its own system of interference fringes. With the interferometer separation used, namely 7.8 mm the fringe system of one main component of the fine structure was displaced with reference to that of the other main component by almost exactly one-half of a fringe. In the case of both isotopes the presence of a third component ($n=3\rightarrow 2$, $j=\frac{1}{2}\rightarrow\frac{1}{2}$) at the indicated position is distinctly shown by dissymmetries in the microphotometer tracings. This effect is noticeably more evident in the case of the heavier isotope (see Fig. 1). A preliminary measure of the doublet separation corrected for the effect of the weaker components indicates strongly a value, corresponding on the basis of the present theory, to $1/\alpha=138$. This is distinctly greater than the value given by Birge[1] from other data. This discrepancy does not necessarily imply erroneous values for e and h but may arise from an incompleteness of the theory of fine structure. The similarity of the interference fringe systems for the two isotopes affords a very accurate method of determining the difference in wave-length between $H^1\alpha$ and $H^2\alpha$. From this value m, the mass of the electron, can be computed and combined

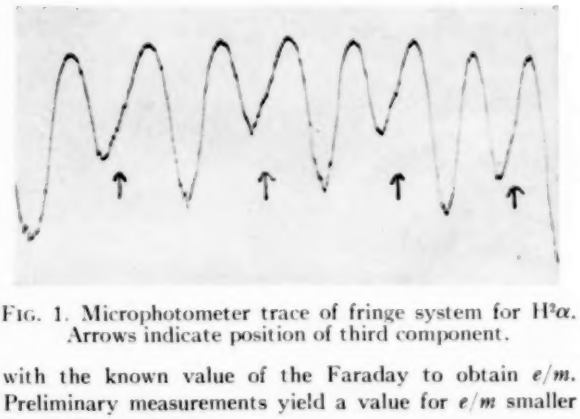

FIG. 1. Microphotometer trace of fringe system for $H^2\alpha$. Arrows indicate position of third component.

with the known value of the Faraday to obtain e/m. Preliminary measurements yield a value for e/m smaller than 1.758×10^7 e.m.u.

The authors wish to express their sincere appreciation of the generosity of Professor Lewis who suffered his own investigations to be somewhat delayed that H_2^2O might be furnished for the present study.

FRANK H. SPEDDING
C. D. SHANE
NORMAN S. GRACE

Departments of Chemistry,
Astronomy and Physics,
University of California,
June 19, 1933.

[1] Birge, Phys. Rev. **40**, 228 (1932); **40**, 319 (1932).

Failure to Detect Radioactivity in Beryllium with the Linear Amplifier

We have attempted to confirm the pressure of radioactivity in beryllium, as observed in the ionization-chamber-electrometer measurements of Langer and Raitt,[1] by using a linear amplifier that will detect individual alpha-particles; but we have obtained negative results. In the present experiments an ionization chamber resembling that used by Wynn-Williams and others, 20 mm in diameter and 4.5 mm deep, with only a coarse wire-grid as first electrode, was connected to a Wynn-Williams linear amplifier. The output of the amplifier operated a loudspeaker, an oscilloscope, and a Thyratron counter. Standardization with polonium showed that the amplifier recorded each alpha-ray whose path in the chamber was 2 mm or greater in length. Qualitative tests showed the amplifier responsive to the alpha-particles emitted from the surface of a granite rock containing 10^{-12} g radium per g of rock.

A flat boss 20 mm in diameter was ground on a face of a lenticular block of beryllium, and this fresh beryllium surface was mounted 1 mm from the entrance to the ionization chamber. All alpha-particles emitted from the beryllium block with a range of 3 mm or greater should therefore have been recorded. Langer and Raitt postulate that each decaying atom of Be^9 emits 2 alpha-particles and a neutron and they ascribe a decay constant of 10^{-21} sec.$^{-1}$ and an alpha-particle range of 10 mm to beryllium. The Be alpha-particles should therefore have a range of about 5.2μ in Be, if the Bragg-Kleeman rule is assumed to hold. Thus there should escape from the Be boss used in our experiments some 2.9 alpha-particles per minute having a range greater than 3 mm of air, or 1.9 per minute having a range greater than 5.5 mm of air. The background count of the amplifier was about 0.5 per minute, hence less than one tenth of the expected beryllium activity could have been detected.

The experiments have been repeated four times during the past six weeks, always with negative results within the probable error. The last set of measurements will be given in some detail. Actually, the time of occurrence of each count was recorded, and analyses of these data, in the light of the Bateman criteria, demonstrated the true random character of the counting.

Table I shows the results of four measurements: first, unscreened beryllium; second, beryllium screened by aluminum foil of 1.5 cm air stopping power; third, unscreened beryllium; fourth, beryllium screened by aluminum foil of 3.5 cm air stopping power. The aluminum foil was fresh stock, and samples of it were tested in an ionization chamber and found to be free from radioactive contamination. The probable errors given were obtained from analysis of the data, using Peter's formula. These observations show the absence of alpha-ray emission from the beryllium block, well within the probable error, which is about 1/30 of the reported activity.

TABLE I.

	Run	Total counts	Duration	Counting rate
I	Be	24	45 min	0.53±0.10
II	Be+1.5 cm Al	48	73	0.66±0.10
III	Be	59	90	0.66±0.09
IV	Be+3.5 cm Al	42	76	0.55±0.09

Naturally, the results reported above do not prove that beryllium is wholly nonradioactive, but they do indicate that if beryllium is active it either emits very short (*ca.* 3 mm) alpha-particles, or has a decay constant which is much smaller than has been suggested by Langer and Raitt. Geological evidence, as Lord Rayleigh points out[2] is not in agreement with the second alternative, and mass defect considerations do not suggest a very short range alpha particle. The present experiments are therefore regarded as suggesting that beryllium is stable.

ROBLEY D. EVANS*
M. C. HENDERSON

Physics Department,
University of California,
June 19, 1933.

* National Research Fellow.

[1] Langer and Raitt, Phys. Rev. **43**, 585 (1933).

[2] Lord Rayleigh, Nature **131**, 724 (1933).

Extension of Fowler's Theory of Photoelectric Sensitivity as a Function of Temperature

Fowler's highly successful application of the Fermi-Dirac statistics to photoelectric emission, in explaining the temperature variation of the apparent threshold, is valid for frequencies close to the threshold. The analysis starts with the following expression (in Fowler's notation) for the number of "available" electrons (with normal kinetic energies exceeding a particular value $\epsilon' = \chi_0 - h\nu$),

$$N_B = (4\pi kTm^2/h^3)\int_{\epsilon'}^{\infty} \log\,[1+\exp\,(\epsilon^* - \tfrac{1}{2}mu^2)/kT]du$$
$$= (2\pi kTm^2/h^3)(2kT/m)^{\frac{1}{2}}\int_0^{\infty}[y+(\chi_0-h\nu)/kT]^{-\frac{1}{2}} \times \log\,\{1+\exp\,[-y+(h\nu-\chi)/kT]\}dy,$$

where

$$y = (\epsilon - \chi_0 + h\nu)/kT, \qquad \epsilon = \tfrac{1}{2}mu^2, \qquad \epsilon^* = \chi_0 - h\nu_0.$$

Fowler's ensuing treatment is restricted to cases where the frequency lies near the threshold by the assumption (a) that, before integration, y may be neglected in comparison with $(\chi_0 - h\nu)/kT$ in the denominator, and (b) that, in the final working expression, $\chi_0 - h\nu$ is approximately constant under these conditions.

It was thought desirable to investigate the extent to which these approximations are valid for frequencies removed from the threshold. A more general expression for the number of available electrons may be obtained somewhat more readily by integrating with respect to the normal velocity component, u, instead of the kinetic energy. Thus

$$N_B = (4\pi m^2 kT/h^3)\int_{u'}^{\infty} \log\,(1+Ae^{-au^2})du,$$

where

$$\tfrac{1}{2}mu'^2=\chi_0-h\nu, \qquad a=m/2kT, \qquad \log A(\text{Fermi})=\epsilon^*/kT.$$

If u^* is defined by $Ae^{-au^2}=1$, two cases arise as usual, namely $u'>u^*$ and $u'<u^*$, wherein the logarithm may be expanded in powers of Ae^{-au^2} and its reciprocal, respectively, with the result that probability integrals occur for which series approximations may be written at once. The results are:

$u'>u^*$ $(h\nu<h\nu_0)$:

$$N_B=[(2m)^{\frac{1}{2}}\pi k^2T^2/h^3\epsilon^{*\frac{1}{2}}]\{s_2(e^x-e^{2x}/4+e^{3x}/9-\cdots)-\tfrac{1}{2}\gamma s_3(e^x-e^{2x}/8+e^{3x}/27-\cdots)+\cdots\}, \quad (1)$$

$u'<u^*$ $(h\nu>h\nu_0)$:

$$N_B=[(2m)^{\frac{1}{2}}\pi k^2T^2/h^3\epsilon^{*\frac{1}{2}}]\{s_1\chi^2/2+\pi^2/6-s_2(e^{-x}-e^{-2x}/4+\cdots)-\tfrac{1}{2}\gamma s_3(e^{-x}-e^{-2x}/8+\cdots)+\cdots\}, \quad (2)$$

where

$$x=(\epsilon^*-\epsilon')kT=h(\nu-\nu_0)kT,$$
$$\gamma=kT/\epsilon^*=kT/(\chi_0-h\nu_0),$$
$$s_1=1+\delta/3+3\delta^2/16+\delta^3/8+\cdots,$$
$$s_2=1+\delta/2+3\delta^2/8+5\delta^3/16+\cdots,$$
$$s_3=1+3\delta/2+15\delta^2/8+35\delta^3/16+\cdots,^1$$
$$\delta=(\epsilon^*-\epsilon')/\epsilon^*.$$

The two expressions are given to the first approximation in $\gamma(=kT/\epsilon^*)$ which is always small (of the order of 0.04 at most). Eqs. (1) and (2) differ from Fowler's (a) in the additional γ-term, and (b) in the introduction of the series in δ, which when multiplied by $1/(\chi_0-h\nu_0)^{\frac{1}{2}}$ replace the factor $1/(\chi_0-h\nu)^{\frac{1}{2}}$ and provide the desired correction for frequencies away from the threshold.

Using Eqs. (1) and (2) in further development after Fowler's method, on the assumption that the photoelectric current $I\propto N_B$:

$$I=A'T^2(\chi_0-h\nu_0)^{-\frac{1}{2}}f'(x),$$

where

$$f'(x)=s_2(e^x-e^{2x}/4+e^{3x}/9+\cdots)-\tfrac{1}{2}\gamma s_3(e^x-e^{2x}/8+e^{3x}/27-\cdots)+\cdots, \qquad x\leq 0$$
$$=s_1x^2/2+\pi^2/6-s_2(e^{-x}-e^{-2x}/4+\cdots)-\tfrac{1}{2}\gamma s_3(e^{-x}-e^{-2x}/8+\cdots)+\cdots, \qquad x\geq 0.$$

$$\log I/T^2=B'+F'(x),$$

where

$$F'(x)=\log f'(x),$$

and $B'=\log A'-\frac{1}{2}\log(\chi_0-h\nu_0)$, whose last term is strictly constant.

The function $F'(x)$ is seen to be dependent upon δ and γ as well as upon their ratio $x(=\delta/\gamma)$, and thus its universal character is gone to the extent of this higher approximation. When $\delta=0$ (at the threshold frequency, hence $x=0$) $F'(x)$ reduces to Fowler's $F(x)$ except for the added term in γ. In extreme cases (T large and ϵ^* small) this might amount to 2 percent of $f(x)$ or a difference, $F'-F=-0.01$. The deviations of $F'(x)$ from $F(x)$ depend upon the value of δ. Practical limitations on current measurement prevent δ from becoming more negative than -0.1. Such would be the case for Cs where $\lambda_0=6600$A, $\epsilon^*=1.53$ e.v. (assuming one free electron per atom) and incident light of $\lambda=7170$A. Then $F'-F$ would vary from -0.01 at $\delta=0$ to $\log(s_2+\frac{1}{2}\gamma s_3)=-0.016$ at $\delta=-0.1$.

On the short wave-length side of the threshold δ may become 0.2 for Ni illuminated with 2050A light, or 0.4 for Cs illuminated with 5000A light. In the case of Ni, $F'-F$ varies from -0.01 at $\delta=0$ to 0.03 at $\delta=0.2$, while for Cs, $F'-F$ varies from -0.01 to 0.07 at $\delta=0.4$, the upper limit being almost independent of temperature in each case. By examining Eqs. (1) and (2) it is seen that for values of x greater than 5, the γ term is negligible and $F'-F=\log s_1$, a function of δ only. So there is a slight change of shape in Fowler's theoretical curve to which experimental curves are shifted, depending upon the distance from the threshold.

If DuBridge's method[2] of plotting isochromatic instead of isothermal curves is used, for each curve there will be a constant δ and an almost constant difference $F'-F$ which produces a negligible change of shape and hence is absorbed in the arbitrary vertical shift. This method then introduces less error for frequencies far from the threshold.

If at any time the exact value of the proportionality constant between photoelectric current and the number of available electrons becomes of value, it will be given more accurately by this extension of Fowler's analysis.

A. T. WATERMAN
C. L. HENSHAW

Sloane Physics Laboratory,
Yale University,
June 16, 1933.

[1] These series converge for $\delta<1$.

[2] DuBridge, Phys. Rev. **39**, 108 (1932).

Nuclear Spin and Magnetic Moment of Sodium from Hyperfine Structure

Until recently attempts to determine the nuclear spin of sodium had led to inconsistent results. Recently Rabi and Cohen[1] from a Stern-Gerlach field deflection method and Joffe and Urey[2] from alternating intensities in band spectra have reported the nuclear spin of sodium to be 3/2. The writers have made measurements of the relative intensities of the hfs components of the sodium D lines which also yield 3/2 for the nuclear spin. In this research a liquid air cooled Schüler tube with argon as a foreign gas was used as a source. The hfs was resolved by means of a glass Fabry-Perot interferometer with spacers ranging

[1] Rabi and Cohen, Phys. Rev. **43**, 582 (1933).

[2] Joffe and Urey, Phys. Rev. **43**, 761 (1933).

from 14 mm to 25 mm. As has been reported by Schüler[3] each D line was found to consist of two components the separation between which is approximately the splitting in the $3\,^2S_{\frac{1}{2}}$ level since the splitting in the upper levels ($3\,^2P_{\frac{3}{2}}$ and $3\,^2P_{\frac{1}{2}}$) are too small to be resolved. A print of the Fabry-Perot pattern of the D lines is shown in Fig. 1. The j value for the lowest state is $\frac{1}{2}$, so that the

FIG. 1.

number of resolvable components in both $D_2(\lambda 5890)$ and $D_1(\lambda 5896)$ is $(2j+1)=2$ independent of the value of the nuclear spin. In order to determine the spin it was thus necessary to resort to intensity measurements of the hfs components.

The relative intensity of the components as given out by the source was determined photographically by comparing them with intensity marks put on the plate by means of a tungsten filament lamp. In doing this considerable care was taken to determine and correct for the influence of the diffuse background which is always present in the pattern formed by the Fabry-Perot interferometer.

In order to interpret the results of these measurements it was necessary to determine the effect of absorption in the source. This was done by measuring the relative intensity of D_2 and D_1 and by making use of formulas and tables given by Ladenburg and Levy.[4] For any value of the ratio D_2/D_1 could be calculated the relative intensities of the hfs components given out by the source, for any assumed value of the nuclear spin. By comparing the measured ratios with those calculated for the same value of D_2/D_1 but for various values of the spin, the nuclear spin could be determined. The data from one of the plates are given in Table I. D_{2a} and D_{2b} are the components of D_2 and D_{1a} and D_{1b} those of D_1. These and the other data obtained are consistent only with a nuclear spin of $3/2$.

By careful measurements on the separations between the components of D_2 and D_1 a determination of the total hfs splittings in the $3\,^2P_{\frac{1}{2},\frac{3}{2}}$ levels, which are too small to be resolved directly, has been made. Because of the hfs of the $3\,^2P_{\frac{3}{2}}$ and $3\,^2P_{\frac{1}{2}}$ levels the separation between the components of D_2 and D_1 is not quite the same. After having determined the nuclear spin and by using the theoretical relation between the interval factors of the $3\,^2P_{\frac{3}{2}}$ and $3\,^2P_{\frac{1}{2}}$ levels, it is possible to compute the ratios of the splittings of these levels to the resultant difference in the separations between the resolvable components of the D_2 and D_1 lines. The results of the measurements are

TABLE I.

	$\frac{D_{2a}}{D_{2b}}$	$\frac{D_{1a}}{D_{1b}}$	$\frac{D_{2b}}{D_{1a}}$	$\frac{D_{2a}+D_{2b}}{D_{1a}+D_{1b}}$
Average measured ratios	1.62	1.59	1.19	1.92
Calculated ratios	1.90	1.95	1.00	for $i=1$
	1.59	1.63	1.19	$i=\frac{3}{2}$
	1.45	1.48	1.31	$i=2$

$$\Delta\nu(D_2)=0.0555\pm0.001\ \text{cm}^{-1},$$

$$\Delta\nu(D_1)=0.0612\pm0.001\ \text{cm}^{-1},$$

$$\Delta\nu(D_1)-\Delta\nu(D_2)=0.0057\ \text{cm}^{-1}.$$

The writers feel that the accuracy in this difference is better than that in either interval because in the method employed it is not likely that one interval is overestimated and the other underestimated. The difference obtained above is consistent with a total splitting of 8.3×10^{-3} cm^{-1} for the $3\,^2P_{\frac{1}{2}}$ level and $3/5\times8.3\times10^{-3}=5.0\times10^{-3}$ cm^{-1} for the $3\,^2P_{\frac{3}{2}}$ level. This splitting obtained for the $3\,^2P_{\frac{3}{2}}$ level is in fair agreement with results obtained by Heydenburg and Ellett[5] for this same level from polarization of resonance radiation. From this information it may be concluded that the magnetic moment of the sodium nucleus is approximately 2.6/1840 Bohr magnetons.

C. M. VAN ATTA
L. P. GRANATH

Department of Physics,
New York University,
University Heights,
June 16, 1933.

[3] Schüler, Naturwiss. **16**, 512 (1928).

[4] Ladenburg and Levy, Zeits. f. Physik **65**, 189 (1930).

[5] Heydenburg and Ellett, Bull. Am. Phys. Soc. **8**, 23 (1933). (Paper presented at the Chicago meeting of the Physical Society, June, 1933.)

The Isotopes of Calcium by the Magneto-Optic Method

We have checked a large number of the minima reported by Allison[1] to an accuracy of 0.02 units. In addition to the two isotopes which Allison reports for calcium, we always find a faint third minimum. Thus in a dilute HCl solution which shows no minima in the calcium region, we find, upon the addition of a trace of calcium chloride, minima located at 18.45, 18.59, and 18.66, expressed in terms of Allison's units. The values reported by Allison are 18.44 and 18.66. From the position of the third minimum we believe it is due to the presence of Ca^{41}.

WENDELL M. LATIMER
HERBERT A. YOUNG

Department of Chemistry,
University of California,
June 17, 1933.

[1] F. Allison, J. Am. Chem. Soc. **52**, 3798 (1930).